TRANSPORTATION RESEARCH RECORD 1007

Nondestructive Pavement Evaluation and Overlay Design

TRB
TRANSPORTATION RESEARCH BOARD
NATIONAL RESEARCH COUNCIL
WASHINGTON, D.C. 1985

Transportation Research Record 1007
Price $9.60
Editor: Scott C. Herman
Compositor: Phyllis D. Barber
Layout: Harlow Bickford

modes
1 highway transportation
4 air transportation

subject areas
24 pavement design and performance
40 maintenance
62 soil foundations

Transportation Research Board publications are available by ordering directly from TRB. They may also be obtained on a regular basis through organizational or individual affiliation with TRB; affiliates or library subscribers are eligible for substantial discounts. For further information, write to the Transportation Research Board, National Research Council, 2101 Constitution Avenue, N.W., Washington, D.C. 20418.

Printed in the United States of America

Library of Congress Cataloging in Publication Data
National Research Council. Transportation Research Board.
Nondestructive pavement evaluation and overlay design.

(Transportation research record; 1007)
1. Pavements–Testing–Addresses, essays, lectures. 2. Nondestructive testing–Addresses, essays, lectures. 3. Pavements–Design and construction–Addresses, essays, lectures. I. National Research Council (U.S.). Transportation Research Board. II. Series.
TE7.H5 no. 1007 380.5 s 85-14165
[TE250] [625.8'028'7]
ISBN 0-309-03817-0 ISSN 0361-1981

Sponsorship of Transportation Research Record 1007

GROUP 2–DESIGN AND CONSTRUCTION OF TRANSPORTATION FACILITIES
Robert C. Deen, University of Kentucky, chairman

Pavement Management Section
W. Ronald Hudson, University of Texas at Austin, chairman

Committee on Pavement Rehabilitation
Gordon W. Beecroft, Oregon Department of Transportation, chairman
James F. Shook, The Asphalt Institute, secretary
Edward Aikman, Ralph W. Allen, Martin L. Cawley, W. G. Davison, Paul J. Diethelm, Denis E. Donnelly, Wade L. Gramling, Joseph B. Hannon, W. J. Head, James W. Hill, Walter P. Kilareski, Joe P. Mahoney, Richard W. May, Gene R. Morris, Louis G. O'Brien, Robert G. Packard, John C. Potter, Lawrence L. Smith, Richard L. Stewart, R. N. Stubstad, Reuben S. Thomas, Harvey J. Treybig, Loren M. Womack

Lawrence F. Spaine, Transportation Research Board staff

The organizational units, officers, and members are as of December 31, 1984.

1207

Contents

Addresses of Authors

Abd El Halim, A. O., Department of Civil Engineering, Carleton University, Ottawa, Ontario K1S 5B6, Canada
Carmichael, R. Frank, ARE, Inc.–Engineering Consultants, 2600 Dellana Lane, Austin, Tex. 78746
Cesarini, Maurizio, Autostrade S.p.A., Via Bergamini, 50, Rome 00159, Italy
Fornaci, Massimo G., Autostrade S.p.A., Via Bergamini, 50, Rome 00159, Italy
Hudson, W. R., Department of Civil Engineering, University of Texas at Austin, Austin, Tex. 78712
Lybas, John M., Department of Civil Engineering, University of Florida, Gainesville, Fla. 32611
Lytton, Robert L., Department of Civil Engineering, Texas A&M University, College Station, Tex. 77843
Malgarini, Mauro, Autostrade S.p.A., Via Bergamini, 50, Rome 00159, Italy
Marchionna, Aurelio, Department of Hydraulics, Transportation and Roads, University of Rome, Via Eudossiana, 18, Rome 00184, Italy
McCullough, B. F., Department of Civil Engineering, University of Texas at Austin, Austin, Tex. 78712
Meyer, A. H., Center for Transportation Research, University of Texas at Austin, Austin, Tex. 78712
Ruth, Byron E., Department of Civil Engineering, University of Florida, Gainesville, Fla. 32611
Seeds, Stephen B., ARE, Inc.–Engineering Consultants, 2600 Dellana Lane, Austin, Tex. 78746
Sharma, Jay, Pavement Consulting, Inc., 9800 Roosevelt Way, N.E., Suite 2, Seattle, Wash. 98115; formerly with Seattle Engineering International, Inc.
Smith, Roger E., ERES Consultants, Inc., P.O. Box 1003, Champaign, Ill. 61820
Stokoe, K. H., II, Department of Civil Engineering, University of Texas at Austin, Austin, Tex. 78712
Terrel, Ronald L., Pavement Technologies, Inc., 15042 N.E. 40th Street, Suite 201, Redmond, Wash. 98052
Tholen, Olle, KUAB Konsult och Utveckling AB, Stora Industriomradet, 795 00 Rattvik, Sweden
Tia, Mang, Department of Civil Engineering, University of Florida, Gainesville, Fla. 32611
Uddin, Waheed, ARE, Inc.–Engineering Consultants, 2600 Dellana Lane, Austin, Tex. 78746; formerly with University of Texas at Austin

Operating Characteristics and User Satisfaction of Commercially Available NDT Equipment

ROGER E. SMITH and ROBERT L. LYTTON

ABSTRACT

The results of a recent study conducted for FHWA are presented herein. The objective of the study was to develop a ready reference that describes available nondestructive testing (NDT) devices and methods for use in designing the thickness of asphalt concrete overlays for flexible pavements. The report was developed to serve as a guide to practicing highway engineers who are considering the purchase of new equipment or developing (or modifying) overlay design procedures for flexible pavements. A conscientious effort was made to determine and evaluate factors that agencies noted as important decision criteria in selecting NDT devices. The analysis was limited to equipment currently available from commercial sources. Equipment characteristics were provided by the manufacturers. To determine user feelings concerning the NDT equipment, a questionnaire was sent to selected agencies and available literature was reviewed. Summary tables of equipment characteristics and operating capabilities are provided. Selected overlay design procedures that use NDT input were described in the report; however, in this paper only basic equipment characteristics and user comments concerning the equipment are discussed.

In this paper the results of a recent study conducted for FHWA (1) are described. The objective of the study was to develop a ready reference that describes available nondestructive testing (NDT) devices and methods for use in designing the thickness of asphalt concrete overlays for flexible pavements. In the following sections basic equipment characteristics and user comments concerning the equipment are presented.

DESCRIPTION OF NDT EQUIPMENT

Four general classes of NDT equipment are routinely used to collect deflection data (1): static deflection equipment, automated beam deflection equipment, steady-state dynamic deflection equipment, and impulse deflection equipment. The basic characteristics and costs of each of the commonly used commercially available NDT devices are given in Table 1.

Static Deflection Equipment

Devices that measure the deflection response of a pavement to slowly applied loads are generally classed as static deflection equipment. The most commonly used equipment in this class are Benkelman beam devices. Other equipment that has been used includes plate bearing test equipment and curvature meter (2).

The Benkelman beam was originally a 12-ft (3.65-m) beam pivoted at the third point. This provides an 8-ft (2.44-m) probe with the extreme tip resting on the pavement and supported at the near third point by a pivot point. The rear end is a 4-ft (1.22-m) cantilever beam that moves upward when the pavement deflects downward. A dial indicator rests on the rear end and measures this movement.

This type of device requires a loaded truck to create the deflection to be measured. It has been used for many years, and much of the early work in deflection-based overlay design for flexible pavements was based on this device (3,4). The deflection measurements are made by using one of two more or less standard procedures: AASHTO T256-77, "Standard Recommended Practice for Pavement Deflection Measurements" (5); and the Asphalt Institute's rebound deflection testing procedure (6).

Generally, only the maximum deflection is measured with beams. The major technical problems associated with the beams include ensuring that the front supports are not in the deflection basin, and the difficulty or inability in determining the shape and size of the deflection basin.

Automated Beam Deflection Equipment

Commercially available equipment that automates the Benkelman beam process is the La Croix Deflectograph. It has been used widely in Europe and other parts of the world; however, it has not been used widely in the United States. The traveling deflectometer is a similar device that was built for the California Department of Transportation and has been in use by that agency for several years.

The La Croix Deflectograph consists of a two-axle, six-tire truck with deflection-measuring beams connected to a placement frame and necessary displacement measurement and recording equipment. The beam probes (one for each dual wheel set) are mounted on a common frame mounted below the truck and pivot. The frame with both beams is placed on the road surface in front of the oncoming dual wheels. As the wheel approaches the beam tip, the beam rotates about the pivot and the rotation is measured by inductive displacement transducers. This measurement continues until the wheels pass the beam tip. During this period the beam remains in the same location as the vehicle approaches it. The beams and frame are then lifted from the pavement surface, moved forward, and repositioned to begin a new cycle. The system can be set up to record the deflection basins as the vehicle approaches the beams.

TABLE 1 Characteristics of Commercially Available NDT Devices

Device Name	Principle of Operation	Load Actuator System	Minimum Load (lb)	Maximum Load (lb)	Static Weight on Plate (lb)	Type of Local Transmission
Benkelman beam (AASHTO)	Deflection beam	Loaded truck axle	NA	NA	NA	Truck wheels
Deflection beam (British)	Deflection beam	Loaded truck axle	NA	NA	NA	Truck wheels
La Croix Deflectograph	Mechanized deflection beam	Moving truck loaded with blocks or water	Empty truck weight	Loaded truck wheel weight (9,000)	NA	Truck wheels
Dynaflect	Steady-state vibratory	Counter rotating masses	1,000	1,000	2,100	Two 16-in.-diameter urethane-coated steel wheels
Road rater						
Model 400 B	Steady-state vibratory	Hydraulic rotating masses	500	2,800	2,400	Two 4 x 7-in. pads with 5.5-in. center gap[c]
Model 2000	Steady-state vibratory	Hydraulic rotating masses	1,000	5,500	3,800	Circular plate 18 in. diameter[e]
Model 2008	Steady-state vibratory	Hydraulic rotating masses	1,000	8,000	5,800	Circular plate 18 in. diameter
Falling weight deflectometer						
KUAB 50	Impact	Two dropping masses	1,500	12,000	?	Sectionalized circular plate 11.8 in. diameter[f]
KUAB 150	Impact	Two dropping masses	1,500	35,000	?	Sectionalized circular plate 11.8 in. diameter[f]
Dynatest model 8000 falling weight deflectometer	Impact	Dropping masses	1,500	24,000	?	Circular plate 11.8 in. diameter

Note: 1 in. = 25.4 mm, 1 lb = 4.45 N, 1 lb = 0.45 kg, NA = not applicable.

[a]Costs $71,000 without truck, but requires 1 to 3 man-months to install on purchasers' vehicle.

[b]One in each wheelpath.

[c]Circular plates are available.

The load on the rear axles can be varied from 12,000 to 26,000 lb (5 442 to 11 791 kg). The vehicle can move at 1.25 to 2.5 mph (2 to 4 km/h) while collecting data at 12- to 20-ft (3.5- to 6-m) intervals.

The technical problems of automated beam equipment are similar to any beam equipment. If the deflection basin is large, the point used for reference may be in the basin. In addition, it is difficult to determine deflection at a given point. It cannot be used to determine load transfer across a joint or crack. Also, the large amount of data collected by this equipment requires automated collection and analysis.

Steady-State Dynamic Deflection Equipment

Any device that produces a sinusoidal vibration in the pavement with a dynamic force generator is classed in this group. The most commonly used commercially available devices are the Dynaflect and various models of the road rater. These devices place a static load on the pavement surface. A steady-state sinusoidal vibration is then induced in the pavement with a dynamic force generator. The magnitude of the peak-to-peak dynamic force (high to low) must be less than twice the static force to ensure that the device does not bounce off the pavement surface. This means there must always be some amount of dead weight or static force applied. As the dynamic peak-to-peak loading is increased, this preload must also be increased. Some researchers are concerned that this preload changes the stress state of the existing pavement and may cause the pavement to exhibit an altered response to the load. Therefore an inertial reference is used, and the magnitude of the deflection change can be compared directly with the magnitude of the dynamic force.

Dynaflect

The Dynaflect was one of the first pieces of commercially available steady-state dynamic deflection devices. It is a trailer-mounted device that can be towed by a standard automobile.

A static weight of 2,000 to 2,100 lb (907 to 952 kg) is applied to the pavement through a pair of rigid steel wheels. The dynamic force generator uses a pair of unbalanced flywheels, which rotate in opposite directions at a speed of 8 cycles per second to produce a 1,000-lb (4.45-kN) peak-to-peak force. The deflection is measured by using five velocity transducers (geophones). The transducers are suspended from a placing bar normally placed in the center of the loaded area and at 1-ft (305-mm) intervals. The testing frequency and deflection measurements of all five transducers register on the standard digital control unit simultaneously. This unit also controls the equipment operation. An optional data terminal is available that controls the operation, prints the data on paper tape, and records the data on magnetic cassettes.

The normal sequence of operation is to move the device to the test point and hydraulically lower the loading wheels and transducers to the pavement surface by using the remote control unit. A test is run and the data are recorded. At this point the operator has the option of raising both the sensors and the loading wheel or only the sensors. If the next test point is nearby, the sensors can be raised, and the device can be moved to the next site at speeds up to 6 mph (9.7 km/h) on the loading wheels.

Technical limitations of the device include: peak-to-peak loading is limited to 1,000 lb (4.45 kN), load cannot be varied, frequency of loading cannot be changed, the deflection directly under the load cannot be measured, and it is difficult to determine the contact area.

Road Rater

The road rater is the second series of steady-state dynamic deflection equipment commercially available. There are three production models: 400 B, 2000, and 2008. They vary primarily in the magnitude of the

Method of Recording Data	Type of Carriage	Type of Prime Mover	Basic Cost ($)	Contact Area (in.^{2})	Vibratory Frequency and Range (Hz)	Deflection Measuring System	No. of Deflection Sensors	Normal Spacing of Sensors	Load Measuring System
Manual	NA	NA	1,000	NA	NA	Dial indicator	1	NA	None
Manual	NA	NA	1,500	NA	NA	Dial indicator	1	NA	None
Manual, printer, or automated	Truck	None	166,500[a]	NA	NA	Inductive displacement transducers	2[b]	NA	None
Manual, printer, or automated	Trailer	Tow vehicle	22,185	~32	8	Velocity transducers	5	Center and at 1-ft intervals	None
Manual, printer, or automated	Trailer[d]	Tow vehicle	30,580	56	5-70	Velocity transducers	4	Center and at 1-ft intervals	Load call
Manual, printer, or automated	Trailer	Tow vehicle	40,800	254	5-70	Velocity transducers	4	Center and at 1-ft intervals	Load cell
Manual, printer, or automated	Trailer	Tow vehicle	64,000	254	5-70	Velocity transducers	4	Center and at 1-ft intervals	Load cell
Manual, printer, or automated	Trailer	Tow vehicle	70,000	109	NA	Seismic deflection transducers	5	Center and 0.6 to 8.0 ft	Load cell
Manual, printer, or automated	Trailer	Tow vehicle	85,000	109	NA	Seismic deflection transducers	5	Center and 0.6 to 8.0 ft	Load cell
Manual, printer, or automated	Trailer	Tow vehicle	86,500	109	NA	Velocity transducers	7	Center and 0.6 to 7.4 ft	Load cell

[d] Earlier versions of the model 400 were mounted on vehicles.

[e] Plates of other diameters are available.

[f] Solid plates and plates of other dimensions are available.

load they apply. These models are all trailer mounted, although the 400 B can be mounted in the cargo bay of a van. The static weights are created by the weight of the force actuator system and hydraulic pressure against the trailer. The load is applied to the pavement surface through a steel loading plate. The standard loading plates are 4 x 7-in. (101.7 x 177.8-mm) steel pads with a 5.5-in. (140-mm) center gap for the model 400 B and an 18-in.-diameter (457.2-mm) circular plate for models 2000 and 2008; however, other sizes and shapes of loading plates are available for all models. The dynamic force generator uses a lead-filled steel mass that is accelerated up and down by a servo-controlled hydraulic actuator.

The deflection is measured by using four velocity transducers that are lowered onto the pavement at the same time the loading plate is lowered. One sensor is located in the center of the loaded area, and the remaining three sensors are attached to an arm trailing the plate, normally at 1-ft (0.3-m) intervals from the center.

Both the amplitude and frequency can be changed. This allows different dynamic peak-to-peak loadings of 500 to 3,000 lb (2.2 to 13.3 kN) for the model 400 B; 1,000 to 5,500 lb (4.4 to 28.9 kN) for the model 2000; and 1,000 to 8,000 lb (4.4 to 42.1 kN) for the model 2008. The force is measured with a strain-gauge-type force transducer in all models. The loading frequency can be varied continuously from 5 to 70 cycles per second at 0.1-cycle-per-second increments.

The signals from the transducers are all registered simultaneously with the force and frequency on liquid crystal meters of the standard control box. This unit also controls the complete operation of the device, including setting or changing the force and frequency. An optional automated system that uses a Hewlett Packard model 85 computer (HP-85) is available for the equipment, which will control the complete operation, print the results on paper tape, and record the data on a magnetic cassette.

The normal sequence of operation is to move the device to the test point and hydraulically lower the test plate and deflection sensors to the surface by using the remote control system next to the driver. A test is run at selected loads and frequencies, the loading plate and sensors are lifted from the surface, and the device is ready to move to the next test site.

Technical limitations of this equipment include the limited load levels for some models, the need for a heavy static preload for the heavier devices, and the nonuniform loading configurations.

Impulse Deflection Equipment

Equipment that delivers a transient force impulse to the pavement surface is included in this group. The equipment uses a weight that is lifted to a given height on a guide system and is then dropped. The falling weight strikes a plate, which transmits the force to the pavement. By varying the mass of the falling weight or the drop height or both, the impulse force can be varied.

In addition to the advantages listed for the dynamic deflection devices, loadings in the range of actual wheel loadings can be obtained. The impulse equipment has a relatively small preload compared with the actual loadings. The resulting deflection closely simulates deflections caused by a moving wheel load.

Some dynamic deflection equipment such as the FHWA thumper and road rater can be used to generate an impulse-type loading by placing a static load on the pavement and reacting against that load with half-sine wave deflection impulse. However, preload problems still persist for the road rater devices.

Dynatest Falling Weight Deflectometer

The most widely used falling weight deflectometer (FWD) in the United States is the Dynatest model

8000 Falling Weight Deflectometer System. It is trailer mounted and can be towed by a standard-sized automobile.

The impulse force is created by dropping weights from different heights. By varying the drop heights and drop weights, a force range of 1,500 to 24,000 lb (7 to 105 kN) can be developed. The weights are raised hydraulically and released by an electronic signal. The weights drop onto a rubber buffer system (different for each weight configuration) to provide a load pulse in approximately a half-sine wave form. The load is transmitted to the pavement through an 11.8-in.-diameter (300-mm) loading plate. The impulse load is measured by using a strain-gauge-type load transducer (load cell).

The deflection is measured by using up to seven velocity transducers with one in the center of the loading plate and the remainder mounted on a bar that is lowered automatically with the loading plate. The information from the transducers and load cell are fed into an HP-85 computer, which records the information on paper tape and a magnetic cassette. The HP-85 also controls the complete operation. The display, printed results, and stored results can be in either metric or standard units.

The normal sequence of operation is to move the device to the test point and hydraulically lower the loading plate and transducers to the pavement. A test sequence is then completed by using the desired number of drops at each height selected. The loading plate and sensors are then hydraulically lifted, and the device is ready to move to the next site.

KUAB Falling Weight Deflectometer

The KUAB is mounted in an enclosed trailer that can be towed by a standard-sized automobile. The impulse force is created by dropping a set of two weights from different heights. By varying the drop heights and weights, the impulse force can be varied from 2,698 to 35,000 lb (12 to 150 kN). The two-mass falling weight system is used to create a smoother rise of the force pulse on pavements with both stiff and soft subgrade support.

A rise time from no load to peak load is developed in approximately 28 microseconds, which approximates the load development time of a vehicle traveling at approximately 44 mph (70 km/h). The load is transmitted to the pavement through an 11.8-in.-diameter (300-mm) loading plate. On smooth pavements a solid plate is recommended. On uneven surfaces a segmented steel plate with hydraulic load distribution is used.

A load cell is used to measure the load generation of the equipment. The deflection is measured by using five absolute seismic displacement transducers (seismometers) that are lowered automatically with the loading plate. One sensor is placed through the middle of the loading plate; the remaining sensors can be placed from 7.9 to 100 in. (200 to 2500 mm) from the center of the plate. The signals from the seismic displacement transducers and load cell are fed into an HP-85 computer. The HP-85 also controls the complete operation of the device.

The normal sequence of operation is the same as for the Dynatest FWD. The trailer is completely encased, including the bottom, in a protective cover. The bottom cover is automatically opened for the test. The test system is supported by a three-leg guide system that is lowered to the road for the test sequence.

Phoenix Falling Weight Deflectometer

The Phoenix FWD is also trailer mounted. The mast and weight are mounted by a pivot so they can be transported in a horizontal position for long distances, but they can also be placed upright for testing and travel in the test area.

A single weight can be dropped from different heights to develop impact loads of 2,248 to 11,240 lb (10 to 50 kN). The load is transferred to the pavement through an 11.8-in.-diameter (300-mm) plate. The deflection is measured by using three deflection sensors. One is located in the center of the loading plate, and the others are located at 11.8 and 29.5 in. (300 and 749 mm) from the center.

These sensors are set automatically by the equipment as the plate is lowered. The force is calculated based on drop height. The deflection measurements are recorded on an HP-85 computer, which also controls the operation of the equipment.

The primary advantages of the impulse deflection equipment are that the created deflection basins closely match those created by a moving wheel load of similar magnitude, and that the magnitude of the force can be quickly and easily changed to evaluate the stress sensitivity of the pavement materials being tested.

USER COMMENTS ON EQUIPMENT

Several factors were reviewed to determine which factors should be considered when making a decision to purchase an NDT device. Information included availability, cost, characteristics, principle of operation, estimated maintenance cost, estimated cost of operation, estimated cost of data reduction, ease of use, and traffic control requirements. Information on data bank availability and data acquisition systems was also collected.

To get input from actual equipment users, a review was made of printed information and a questionnaire was sent to a select group of users. Nine state agencies were selected primarily on the basis of available information that indicated that the state had been active in the use or development (or both) of deflection-based overlay design procedures for flexible pavements. In addition, agencies were selected to cover all types of NDT equipment as much as possible. Agencies that use more than one type of equipment were also given precedence over those that use only one device. The states contacted were Arizona, California, Florida, Illinois, Kentucky, Minnesota, Pennsylvania, Texas, and Virginia.

The U.S. Army Corps of Engineers Waterways Experiment Station was contacted because of its work in evaluating several devices (7). Great Britain and South Africa were contacted because of their use of the La Croix Deflectograph.

Some of the equipment used by states replying to the questionnaire are older models that are no longer available from the manufacturer. Their performance may not represent the performance of the newer models that are currently available and described earlier. In particular, the road raters used by Kentucky and Pennsylvania, along with the FWD used by Arizona, are no longer production models. This will be so noted when appropriate.

The responses from each of the agencies contacted are given in Table 2.

DATA SUMMARY OF USER COMMENTS

Selected data for the deflection beams, Dynaflect, FWDs, road raters, and automated beam equipment are presented in tabular format in the basic report. The data from each user agency are presented along with the means and standard deviations for each selected item (the mean and standard deviation may have lim-

ited use with the small number of data points). All readers are cautioned against reading only the summarized totals. Much of the variation that appears is caused by the difference between users rather than equipment. For instance, one could infer from the tables that the average daily traffic control costs are higher for the Dynaflect than for the road rater. However, if the data in Table 2 are studied, it will be noted that every agency that used more than one automated device reported the same traffic control costs for both devices. As a result, it can be surmised that there is no significant difference in traffic control costs attributable to different automated NDT devices.

Time in Service

The time in service of the NDT equipment varied from less than 1 year to more than 20 years. Benkelman beams have been in service the longest. The Dynatest FWDs have been in service the least amount of time (no KUAB or Phoenix FWDs were reported in service in the United States). The mechanized beams, Dynaflects, and road raters vary in service time from 5 to 17 years. No La Croix Deflectographs are currently used in the United States.

The time in service, as well as the number of agencies owning a particular device, may be a function of how long the device has been available. No

TABLE 2 Summary of Agency Responses to Questionnaire

Agency	Type & Model of Equipment	Length of Time Used (years)	Number of Personnel in Operating Crew	Professional Qualifications of Crew		
				Engineer	Technician	Driver
Arizona (AZ-D)	Dynaflect	12	2		X	
(AZ-F)	Falling Weight Deflectometer	3	2		X	
California (CA-TD)	Travelling Deflctometer	16	2		X	X
(CA-D)	Dynaflect	17	1		X	
Florida (FL-F)	Falling Weight Deflectometer	1	2		X	
(FL-D)	Dynaflect	16	2		X	
Illinois (IL-D)	Road Rater 200-8X	6	2		X	
(IL-BB)	Benkelman Beam	20-	3		X	X
Kentucky (KY-R)	Road Rater 200	12	1-2	X	X	
Minnesota (MN-F)		1	1-2		X	
(MN-R)		5	1		X	
Pennsylvania (PA-R)	Road Rater 400	10-12	1		X	
Texas (TX-D)	Dynaflect 100-8A	18	2		X	
Virginia (VA-D)	Dynaflect	16	1		X	
VA-BB)	Benkelman Beam	20-	3		X	X
Great Britian (GB-DF)	Deflectogragh	16	2		X	X
(GB-BB)	Benkelman Beam	20-	3		X	X
South Africa (SA-DF)	Deflectograph	10	2		X	X
WES (WE-RR)	Road Rater 2008	5	1		X	
(WE-F)	Falling Weight Deflectometer	2	2		X	

R = ROAD RATER
D = DYNAFLECT
F = FALLING WEIGHT DEFLECTOMETER
TD = TRAVELLING DEFLECTOMETER
BB = BENKELMAN BEAM
DF = LaCROIX DEFLECTOGRAPH

Agency	Purpose of Collecting Data					Number of Test Points per Day	Number of Load Levels per Point	Number of Man-Hours per Test Day
	Overlay Design	Layer Mat'l Properties	Load Limits	Condition Evaluation	Pavement Management			
AZ-D	YES	YES	NO	YES	NO	75	1	16
AZ-F	NO	YES	NO	YES	NO	75	2	16
CA-TD	YES	NO	NO	YES	NO	1500-2000	1	16
CA-D	YES	NO	NO	YES	NO	420	1	8
FL-F	NO	NO	NO	YES	YES	100-200	1-3	16
FL-D	NO	NO	NO	NO	NO	200-400		20
IL-R	YES	YES	NO	YES	YES	150-200	1	12-16
IL-BB	YES	YES	NO	YES	YES	100	1	18-24
KY-R	YES	NO	NO	YES	YES	300-400	1	8-16
MN-F	YES	YES	NO	NO	NC	200-300	1-4	8-16
MN-R	YES	NO	YES	NO	NO	360	1	8
PA-R	YES	NO	YES	NO	NO	150-400	1	8
TX-D	YES	YES	YES	YES	YES	150-400	1	16
VA-D	YES	NO	YES	YES	YES	100	1	24
VA-BB	YES	NO	YES	YES	YES	50	1	24
GB-DF	NO	NO	NO	YES	YES	2500-4000	1	24-32
GB-BB	NO	NO	NO	YES	NO	100	1	16
SA-DF	YES	NO	NO	YES	YES	3000	1	8
WE-R	YES	YES	YES	NO	YES	200	2	16
WE-F	YES	YES	YES	NO	YES	200	2	

TABLE 2 continued

Agency	Automatic	Keyborad Entry	Manual Data Sheets	Equipment Produced Printout	Data Storage Medium: Magnetic Tape	Cassette/ Diskette	Data Sheets	Equipment Produced Printout	Cost to Prepare & Analyze One Day's Data	Supporting Data Needed: Layer Thicknesses	Layer Stiffnesses	Marshall Stability	Flow	Hveem Stability	Base Properties	Subbase Properties	Subgrade Properties
AZ-D			X		X				$25	YES					*	*	*
AZ-F			X		X				$25	YES					*	*	*
CA-TD			X				X		$200	YES							
CA-D			X				X		$200	YES							
FL-F	X			X	X			X	8-16 hrs.								
FL-D				X				X									
IL-R			X				X		$500-$600	YES	NO	NO	NO	NO	NO	NO	YES
IL-BB			X				X		$250-$300	YES	NO	NO	NO	NO	NO	NO	YES
KY-R	X		X			X	X		$300	YES	NO	NO	NO	NO	NO	NO	NO
MN-F	X			X	X	X				YES	YES	YES	YES	NO	NO	YES	YES
MN-R	X			X	X	X				YES	NO	NO	NO	NO	YES	YES	YES
PA-R			X		X				$100	NO	NO	NO	NO	NO	NO	NO	NO
TX-D	X		X			X	X		$50	YES	NO	NO	NO	NO	NO	NO	NO
VA-D			X				X		$75	YES	NO	NO	NO	NO	YES	YES	YES
VA-BB			X				X		$75	YES	NO	NO	NO	NO	YES	YES	YES
GB-DF			X	X					$145-$725	YES	NO	NO	NO	NO	NO	NO	YES
GB-BB									$15-$50	YES	NO	NO	NO	NO	NO	NO	YES
SA-DF				X			X	X	$200	NO	NO	NO	NO	NO	NO	NO	NO
WE-R				X				X	$500	YES	NO	NO	NO	NO	T	T	T
WE-F				X				X	$500	YES	NO	NO	NO	NO	T	T	T

Agency	Enviromental Corrections: Temperature	Moisture	Seasonal	Enviromental Testing Restrictions: Season	Temperature	Average Annual Maintenance Cost	Traffic Control Methods: Warning Signs	Barricades	Mobile Lane Closure	Mobile Barricades	Flashing Lights	Flagmen	Traffic Control Cost Per Test Day
AZ-D	NO	NO	NO	YES		$5000	YES	NO	YES	YES	YES	YES	$750
AZ-F	NO	NO	NO	YES		$5000	YES	NO	YES	YES	YES	YES	$750
CA-TD	NO	NO	NO	YES		$3000	YES	NO	YES	NO	YES	YES	$600
CA-D	NO	NO	NO	YES			YES	NO	YES	NO	YES	YES	$600
FL-F	YES	YES	YES				YES	YES	YES	NO	YES	NO	$140
FL-D	NO	NO	NO	YES	NO		YES	NO	NO	NO	NO	YES	$140
IL-R	YES	NO	YES	NO	NO		YES	YES	YES	NO	YES	YES	$200
IL-BB	YES	NO	YES	NO	YES	$1600	YES	YES	YES	NO	YES	YES	$250-300
KY-R	YES	YES	YES	NO	YES	$100	NO	NO	YES	NO	YES	YES	$100
MN-F							YES	NO	YES	NO	YES	NO	*
MN-R	YES	NO	YES	YES	YES		YES	NO	YES	NO	YES	NO	*
PA-R	YES	NO	YES	NO	NO	$5600		NO	NO	NO	YES	YES	$200
TX-D	NO	NO	NO	NO	YER	$850	YES	YES	--	--	YES	YES	$100-$500
VA-D	YES	NO	NO	NO	YES	$875	YES	YES	YES	YES	YES	YES	$250
VA-BB	YES	NO	NO	NO	YES		YES	YES	YES	YES	YES	YES	$250
GB-DF	YES			YES	YES	$2900-4350	YES	NO	YES	--	--	--	--
GB-BB	YES			YES	YES	$15-70	YES	NO	YES	--	--	--	--
SA-DF	NO	NO		N/A			**	NO	YES	NO	YES	NO	
WE-R	YES	NO	YES	N/A	YES	$1000	NO	NO	YES	YES	YES	NO	$200
WE-F	YES	NO	YES	N/A	YES	$1500	NO	NO	YES	YES	YES	NO	$200

* Exact cost unknown, however, no difference in traffic control for FWD and Road Rater.
** Escort Vehicles
Included in total cost

particular inference should be made from these two statistics as far as reliability or usefulness is concerned.

Crew Size

All agencies reporting on the Benkelman beam indicated that they used a three-person crew. All agencies reporting on the mechanized beams indicated a two-person crew. All other devices had a one- or two-person crew.

It appears that the crew of three for the Benkelman beam and crew of two for the deflectograph are valid requirements. The number of personnel required for the crew of the current generation of Dynaflect, FWDs, and road raters will depend on the data recording and control system and testing requirements. The Dynaflect and road rater standard equipment require recording the data from a digital readout by hand. These devices can be more efficiently operated with an additional person to record the data.

Both of these can be equipped with an optional data recording system, and an automated data recording system is standard equipment on FWDs. In this mode they can be operated efficiently by a single operator. However, if the equipment must be accurately sited over a specific point, a second person may still be needed, although the Dynatest FWD has been sited with remote video. This is not normally a requirement in routine testing of flexible pavements.

Some concern was mentioned in the literature to indicate that a crew of two was necessary with automated equipment. A second operator was used to relieve the first operator because of operator fatigue (8).

Professional Qualification of Crew

All agencies indicated that they normally used experienced engineering technicians as the operating crew. Some agencies indicated that they used an engineer on the crew when they conducted research studies or other nonroutine testing. Those reporting on the Benkelman beam and deflectograph and traveling deflectometer indicated they also used a truck driver. Operator training requirements varied substantially. The range was from 1 day to 3 months; however, the equipment operation training portion of this time was normally 1 to 3 days. The remainder of the time was devoted to training the operator in selecting the proper testing locations and conditions. The majority of the long training periods was devoted to on-the-job training.

Number of Test Points Per Day

The lowest number of points tested per day was reported for the Benkelman beam. The range was 50 to 100 points per day. The traveling deflectometer and La Croix Deflectograph had the largest number at 1,750 to 3,250 points per day. The La Croix manufacturer stated that 12,000 measurements a day for 12.4 to 18.6 miles (20 to 30 km) could be achieved.

The range for the other devices was from 75 to 420 points per day. It is interesting to note that the Dynaflect had both those values reported. It was expected that the Dynaflect would have the largest number of points per day because it can test at only one load level and one frequency. Arizona and Virginia reported the lowest number of test points per day (75 and 100, respectively) for the Dynaflect. The low production rate appears to be caused by their test procedure and travel time between test points. There is no relation between the number of persons in the operating crew and the number of test points per day. For the Dynaflect, 200 to 300 points a day would appear reasonable with some lost time for travel to the test site, calibration, setup, and tear-down. If the travel time to and between sites is short, then a total of 300 to 400 points a day is possible.

The road rater would appear to have a similar range of test points per day when only one load and one frequency are used at each test site. Although the model 400 appears to have a slightly higher number of points per day than others, it must be realized that these models are no longer available. With the models available, there should be no difference in test rates among the 400 B, 2000, and 2008 models.

The Dynatest FWD has a slightly lower number of test points per day reported. However, all reporting agencies indicated that they ran more than one load level at each site. Therefore, the number of tests would be at least double the number of points. Approximately 200 points a day should be reasonable for moderate travel time to and between sites with two drop heights.

It should be noted that agencies that use equipment with more load-level capabilities tend to use more test time per test point because they often run more than one load level at a test point. As with vibratory devices, which are normally run at a steady load level and frequency for a short period to reach a steady pavement response (9), some of the agencies that use the FWD reported using a "seating load" on flexible pavements before testing. Either of these operations takes a small amount of additional time, about 15 to 30 sec per site. More accurate data comparing NDT devices in a controlled situation are required to develop a more accurate assessment of this parameter. It appears that the agencies that use more than one load level are sacrificing speed to collect more information at each site.

Cost Per Test Point

The cost to collect one day's data, or cost per test point, was an item that was considered. However, the different manners in which state agencies handle costs such as overhead made it almost impossible to get meaningful cost data. It was decided to use manhours instead of cost data as often as possible.

Maintenance Costs

The average annual maintenance costs of the various pieces of equipment were evaluated. This information was not reported on 8 of the 18 replies. Obviously, the Benkelman beam should, and did, have the lowest maintenance cost. However, the cost does not include the maintenance cost of the loaded truck required for the testing. The deflectograph and the traveling deflectometer have the highest maintenance cost at more than $3,000, which reflects the cost of maintaining both the vehicle and a rather complicated electrical and mechanical system.

Average annual maintenance costs vary considerably for the other equipment. Most of the reporting agencies indicated that the maintenance costs reported were estimates. Some agencies, such as in Pennsylvania where the model 400 road rater is used, included vehicle maintenance, fuel, and depreciation costs with the NDT device because the road rater is mounted on the vehicle. Other agencies, such as

Texas, were careful to avoid reporting tow vehicle costs. The mean maintenance cost for each device was between $2,000 and $3,500 per year. However, because of the large variation and small sample, no finding of significant difference can be substantiated. Of the two agencies that reported on the maintenance costs of two devices, Arizona indicated no difference in the maintenance costs of the Dynaflect and the FWD, whereas the U.S. Army Waterways Experiment Station indicated that the maintenance cost for the model 2000 road rater was slightly less than for the FWD. It should be noted that both of these FWD devices are older models that are no longer in production, but the costs indicate that major differences are not apparent. From the information available, it cannot be stated that there is a significant difference in the average annual maintenance costs among the Dynaflect, road raters, or Dynatest FWD. More accurate long-term data are needed to address this point.

Traffic Control Costs

The traffic control costs do not reflect a significant cost difference based on equipment type. Of the agencies that reported on more than one piece of equipment, only Illinois indicated a difference. Because the Benkelman beam testing required more time in one location with a stopped truck, Illinois was required to use more controls for the beam than were used for the road rater. All other agencies reported the same costs for both devices. This would indicate that the differences in cost are caused by the local agency's policies rather than equipment type. Except for the Benkelman beam, data do not provide evidence to indicate that a significant difference in traffic control cost exists among the equipment types. A good description of one state's traffic control procedure for NDT testing is given elsewhere (10).

Data Recording Method

Five of the twelve reporting agencies indicated that their only data recording method was manual. Four agencies reported that they had automated data recording systems, and three more reported that they had machine-generated printouts. All of the commercially available devices, including the Benkelman beam, can be provided with an equipment-generated paper recording. The Dynaflect, road raters, deflectographs, and FWDs can be provided with automatic magnetic cassette data recording systems. Some of the equipment manufacturers also provide programs to sort data to help break pavements into uniform sections based on deflections.

Data Storage

The data collected from NDT devices are stored in computerized data bases by four of the agencies reporting. All other agencies store the data on the medium on which they collected it (i.e., data sheets, cassettes, and equipment-produced printouts).

Towing Vehicle

The cost of the towing vehicle should be practically the same for all trailer-mounted devices. The model 2000 and model 2008 road raters are the heaviest devices and may require a vehicle with a larger towing capability. The general recommendations from the various agencies and reports include a vehicle with a diesel engine and automatic transmission because of the length of time the vehicle engine idles during testing and the number of frequent starts and stops. The vehicle should be equipped with heavy-duty suspension and an appropriate tow package to pull the trailer-mounted devices. Air conditioning is recommended to reduce operator fatigue; Minnesota recorded temperatures of 120° F (49° C) with doors open in the unairconditioned cab of a tow vehicle (8). High-intensity warning lights are recommended for safety. A distance measurement indicator for the vehicle and a pavement temperature sensing device that can make quick accurate readings, such as an infrared thermometer, are also recommended.

The Dynaflect, Dynatest FWD, and KUAB FWD operate on the vehicle's electrical system; therefore heavy-duty, 100-amp charging systems are required for the tow vehicles used with them. Vehicles with bucket seats appear to work best for the systems that use the computer controlling and recording system. This allows a stand to be mounted between the two front seats on which the computer can be mounted. This mount should provide a stable support during testing and traveling. It should also allow the computers to be easily removed for more secure storage when the equipment is not in use.

PREVIOUS STUDIES

Several studies of various models of the NDT equipment had been conducted previously; these were reviewed for this study. Summaries of the most pertinent studies and comments are included in the FHWA report (1). Although some reports discussed use of NDT equipment for other than flexible pavements, only the information pertinent to flexible pavements is discussed here.

One of the most comprehensive studies was the one by the U.S. Army Corps of Engineers Waterways Experiment Station (WES) (7), conducted between April 1978 and July 1979. In that study the Benkelman beam, the Dynaflect, an early model of the Dynatest FWD, a model 400 road rater (vehicle mounted), a model 510 road rater, a model 2008 road rater, and a WES 16-kip vibrator were all evaluated.

Several characteristics were analyzed in the study. These included ease of operation, speed of operation, manpower requirements, initial costs, operating costs, transportability by cargo aircraft, accuracy and reproducibility of deflection measurements, accuracy and reproducibility of force and frequency measurements, accuracy and reproducibility of force, velocity and deflection signals, and depth of significant influence.

University of Tennessee

The most recent work available was completed by Moore and Highter (11) of the University of Tennessee. This report, published in February 1983, was prepared for the Tennessee Department of Transportation. The researchers basically considered the Dynaflect, road rater, and Dynatest FWD in their study. They sent questionnaires to all agencies that they knew owned one or more of these three devices. They visited four agencies for personal interviews.

The three devices were evaluated based on "economic considerations, operational characteristics, technical merits and other factors pertaining to the applicability of each device for pavement evaluations and for determining overlay design parameters for use in the State of Tennessee" (11). The evaluation considered all devices equally equipped with automatic control and data recording systems.

Moore was gracious enough to share the raw data from his questionnaires with the authors of this paper. Most of this information is discussed in the preceding section; however, some more detailed information on user satisfaction and reasons for purchasing equipment are presented in the basic report (1).

University of Illinois

Two reports (10,12) published as a part of IHR Project 508, Load Response Characteristics of Flexible Pavements, considered the Benkelman beam, an early model 2008 road rater, and a Dynatest FWD. The study compared the equipment primarily in terms of pavement response to load, with responses measured under moving wheel loads. Moving wheel-load-induced deflections were measured with accelerometers implanted in the pavement section. The electrical responses were double integrated to determine deflection. The vehicle speed was measured by using timed responses of photocells at known distances.

The data from these reports indicate that the surface response produced by the FWD more closely simulates a pavement response under a moving truck than does the road rater or Benkelman beam. The road rater tends to produce a stiffened response in the pavement system, which indicates a stronger pavement than actually is present under moving wheel loads because of the static preload and steady-state harmonic loading without rest. Benkelman beam deflections are "quasi-static" loads that tend to overpredict deflections compared with those of moving wheel loads.

CONCLUSIONS

The following conclusions were made based on the data presented in the report:

1. Static load, automated beam, steady-state dynamic, and impulse NDT devices are all commercially available to U.S. agencies.
2. Deflection beams, dynamic deflection devices, FWDs, and automated beam devices can be used to measure maximum deflection.
3. The Dynaflect, road raters, Dynatest FWD, and KUAB FWD are equipped to more quickly and efficiently measure deflection basin parameters than the static and automated beam devices.
4. All automated beam, dynamic, and FWD devices have been equipped with automated equipment to record measured parameters and control the test cycles to facilitate rapid measurements.
5. Automated beam, FWD, and road rater model 2008 devices can develop loads at or near normal design loads.
6. Load as well as deflection can be easily measured by road raters, Dynaflect FWDs, and KUAB FWDs.
7. Devices that can produce several load levels up to or near design loads can be used to determine the stress sensitivity of the pavement system.
8. Steady-state dynamic devices that use a relatively heavy static preload change the stress state in the pavement before the testing.
9. All available NDT devices lack the capability for simple lateral movement to assist in precise load placement.
10. There are significant advantages for using an NDT load that equals that of a heavily loaded truck wheel load (e.g., 9,000 lb). The response of the pavement to this heavy load can be accurately measured and directly used for structural evaluations and overlay design without questionable correlations or stress sensitivity assumptions.
11. Automated NDT devices that have more than one load level and have load levels at or near design loads are more expensive than devices with relatively light loads. However, they provide additional information about the pavement section.

RECOMMENDATIONS

1. The location of deflection sensors on equipment such as the Dynaflect, road raters, and FWDs should be standardized.
2. Consideration should be given to standardizing the size and shape of loading plates (at least for the equipment with load levels approaching design levels). For equipment with load levels significantly less than design loads, development of loading plate size and shape to develop a minimum surface contact pressure should be considered.
3. The tire size and inflation pressure for trucks used as the loading vehicle for Benkelman beam testing should be standardized.
4. Load as well as deflection should be measured by NDT equipment.

ACKNOWLEDGMENTS

The work discussed in this paper was sponsored by the Office of Research and Development, FHWA. The contracting officer's technical representative was Richard M. May. The assistance of the several states contacted and the equipment manufacturers is gratefully acknowledged. Sincere appreciation is expressed to A. Moore of the University of Tennessee for sharing his report and raw data.

Discussion

Goran Ullberg*

The Swedish National Road Administration has used FWDs for the past 13 years, and since 1976 has used the KUAB 50 FWD. Measurements are currently made by the Bearing Capacity Group, VFY, Härnösand. Such measurements are made on a routine basis; some figures from this work should be of interest to the readers because they probably reflect what a new user can expect to produce, after some "running-in time," with efficient equipment and efficient planning.

During 1984 more than 50,000 test points were measured. The distance between the points was 50 m, and the average capacity during 1984 was 264 points per day. Note that transportation time, time to find and mark out the test sites, "social visits" to the local road administrations, and so forth are included in the measuring time. Because measurements were made in an area the same size and shape as California, transportation time was significant; in some cases it took more than one day to transport the equipment to the site and back. During the main season--the spring--when the number of sites was sufficient for

*Regional Road Administration, Box 186, S-871 01 Härnösand, Sweden

more efficient transportation planning, the average capacity was 310 points per day. One peak force level (50 kN) was used in each point. Using three peak force levels in each point reduced the capacity by about 15 percent. The average crew size was 1 person.

In regard to the costs mentioned in the paper--cost to analyze one day's data, average annual maintenance cost, and average daily traffic control costs--in Sweden, they were substantially lower in all three cases. Although such a cost comparison would be interesting, detailed reports are not given here because it may not be possible to make a meaningful comparison of such costs between countries.

Authors' Closure

We appreciate the additional operating information provided by Ullberg. The operating rate for a single force level presented by Ullberg is similar to the rate for the Dynaflect, which is a single load level test.

The test rates described in the basic report represent the testing program employed by the using agency as well as equipment operating capabilities. Ullberg's information further emphasizes the problem of comparing performance among different using agencies. All other agencies reporting on the FWD indicated that they used more than one load level.

REFERENCES

1. R.E. Smith and R.L. Lytton. Synthesis Study of Nondestructive Testing Devices for Use in Overlay Thickness Design of Flexible Pavements. Report FHWA/RD-83/097. FHWA, U.S. Department of Transportation, 1983.
2. R.L. Lytton, W.M. Moore, and J.P. Mahoney. Pavement Evaluation Equipment. FHWA, U.S. Department of Transportation, 1975.
3. The AASHO Road Test--Report 5: Pavement Research. Special Report 61E. HRB, National Research Council, Washington, D.C., 1962, 352 pp.
4. R.W. Bushey et al. Structural Overlays for Pavement Rehabilitation. Report CA-DOT-TL-3128-3-74-12. California Department of Transportation, Sacramento, 1974.
5. Standard Recommended Practice for Pavement Deflection Measurements. AASHTO Designation T 256-77. In Standard Specification for Transportation Materials and Methods of Sampling and Testing, Part II, AASHTO, Washington, D.C., 1982.
6. Asphalt Overlays for Highway and Street Rehabilitation. Manual Series 17. The Asphalt Institute, College Park, Md., 1983.
7. A.J. Bush III. Nondestructive Testing for Light Aircraft Pavements--Phase 1: Evaluation of Nondestructive Testing Devices. U.S. Army Corps of Engineers Waterways Experiment Station, Vicksburg, Miss., 1980.
8. E.O. Lukanen. Evaluation of the Model 2000 Road Rater. Investigation 201, Final Report. Minnesota Department of Transportation, St. Paul, and FHWA, U.S. Department of Transportation, 1981.
9. R.W. May. Interpreting Dynamic Surface Deflections in the Granular Base Layer of the Pavement Structure. FHWA, U.S. Department of Transportation, 1981.
10. M.S. Hoffman and M.R. Thompson. Nondestructive Testing of Flexible Pavements, Field Testing Program Summary. Illinois Department of Transportation and the Department of Civil Engineering, University of Illinois, Urbana-Champaign, 1981.
11. A.B. Moore and W.H. Highter. Pavement Design Using Rapid Methods of Collecting and Analyzing Deflection Data--Phase I: Equipment Evaluation. University of Tennessee, Knoxville, 1983.
12. M.S. Hoffman and M.R. Thompson. Mechanistic Interpretation of Nondestructive Pavement Testing Deflections. Department of Civil Engineering, University of Illinois, Urbana-Champaign, 1981.

Use of Nondestructive Testing in the Design of Overlays for Flexible Pavements

ROBERT L. LYTTON and ROGER E. SMITH

ABSTRACT

The results of a recent study conducted for FHWA are described in this paper. The objective of the study was to develop a ready reference that describes available nondestructive testing (NDT) devices and methods for use in designing the thickness of asphalt concrete overlays for flexible pavements. The report was developed to serve as a guide to practicing highway engineers who are considering the purchase of new equipment or developing (or modifying) overlay design procedures for flexible pavements. Selected overlay design procedures that use NDT input are reviewed. Important components related to the use of NDT data with overlay design procedures are discussed. The following items and their relation to overlay design of flexible pavements using deflection data are discussed in depth: seasonal influences on deflections, location of test points on the pavement surface, frequency of testing, need for cores and laboratory testing, type of NDT measurements (i.e., maximum deflection, basin characterization), additional field measurements that are required, corrections to NDT measurements for temperature and so forth, pavement properties calculated or inferred from the NDT measurements, method used to distinguish between different design sections, relationships that are used to convert NDT measurements to design parameters, relationships that relate design parameters to the useful life of the pavement, and the NDT devices that are available for use.

In this paper the results of a recent study conducted for FHWA (1) are described. The objective of the study was to develop a ready reference that describes available nondestructive testing (NDT) devices and methods for use in designing the thickness of asphalt concrete overlays for flexible pavements. Selected overlay design procedures that use NDT input are reviewed, and important components related to the use of NDT data with overlay design procedures are discussed.

OVERLAY DESIGN PROCEDURE

The data in Table 1 summarize the major features of the overlay design procedures. The common features in overlay design procedures that use NDT include the following:

1. Season in which testing is performed for design purposes;
2. Location on the pavement where tests are made;
3. Frequency of testing along the pavement;
4. Need for taking cores and performing laboratory tests;
5. NDT device(s) that are or may be used;
6. Measurements that are made with the NDT devices;
7. Other measurements that are made in addition to NDT;
8. Corrections that are made either to the NDT measurements or to the calculated pavement properties;
9. Properties of the pavement or layers that are calculated or inferred from the NDT measurements;
10. Methods that are used to distinguish between sections of pavement that require different thicknesses of overlay;
11. Empirical relations that are used to convert the NDT measurements to those that are used in design, such as (a) correlations between the deflections measured with an NDT device and those produced by a design load, (b) correlations between layer material properties that correspond to the load level applied by the NDT device and the same material properties at design load level, or (c) correlations between an NDT deflection and a design strain at a critical point in the pavement structure; and
12. Empirical design relations that convert the measurement at design load into the number of load applications that the pavement can support.

Each of these 12 aspects of an overlay design procedure is discussed in the following sections.

Testing Season

The recommended testing season is normally the "critical period" for a pavement based on the time when deflections and stresses are the largest. There are some exceptions to this. The FHWA-Resource International, Inc. (RII) method (3,4) uses the annual average condition, the Utah method (13) uses the fall, and the Kentucky method (9) uses either a soaked California bearing ratio (CBR) laboratory test or the minimum in-place subgrade modulus.

Test Location and Frequency

NDT tests are usually made on the pavement in the outer wheelpath or in areas that show major distress. Test sections around 1,000 ft (305 m) long are selected. Tests are made every 50 to 500 ft (15 to 152 m). The closer spacings are normally used in areas with high severity distress or rapid changes in topography. The usual spacing is 100 to 200 ft (30 to 60 m). For reflection cracking purposes,

TABLE 1 Major Features of Selected Overlay Design Procedures

Overlay Design Procedure	NDT Device		Type of Overlay Design Method	NDT Measurements	Corrections		Calculated or Inferred Pavement Properties
	Primary	Alternative			NDT Measurements	Pavement Properties	
FHWA-Austin Research Engineers, Inc. (*2*)	Dynaflect		Mechanistic	Deflection basin design; deflection based on selected reliability			Subgrade modulus
FHWA-Resource International, Inc. (*3,4*)	Dynaflect	Road rater, FWD (trailer and van)	Mechanistic	Deflection basin (4 deflections)		Surface course modulus for temperature; stress level of base, subbase, and subgrade moduli	Moduli of layers in a 3- or 4-layer pavement
Asphalt Institute (*5*)	Benkelman beam		Deflection	Deflection (97th percentile)	Temperature, season		"Effective modulus" of pavement
Shell Oil (*6*)	FWD		Mechanistic	Deflection basin		Surface course modulus for temperature	Layer elastic modulus
California (*7,8*)	Traveling deflectometer	Benkelman beam, Dynaflect, road rater, Dehlen curvature meter, FWD	Deflection	Deflection (80th percentile)	Temperature less tan 50°F		
Kentucky (*9*)	Dynaflect		Structure deficiency	Deflection basin; maximum deflection (50th-90th percentile)	Load level, temperature, load frequency, AC modulus, air voids, asphalt content		Subgrade modulus; effective AC thickness; effective base course thickness
Louisiana (*10*)	Road rater		Deflection	Maximum deflection (95th percentile)	Temperature, moisture		Subgrade stiffness; spreadability; effective pavement thickness
Pennsylvania (*11*)	Road rater	Dynaflect	Deflection	Deflection basin (90th percentile)	Temperature, season		
Texas (*12*)	Dynaflect		Deflection	Deflection basin			Surface curvature index (SCI)
Utah (*13*)	Dynaflect		Deflection	Deflection basin; maximum deflection (80th percentile)	Temperature		SCI; base curvature index (BCI); qualitative condition of surface, base, and subgrade
Virginia (*14*)	Dynaflect		Deflection	Deflection basin; maximum deflection			Spreadability; subgrade modulus; effective pavement thickness
University of Illinois (*15,16*)	FWD		Mechanistic	Deflection; maximum deflection (84th-97th percentile)		Temperature, stress level	Basin area; AC modulus; break point modulus of subgrade
FHWA-Waterways Experiment Station (*17*) (Lytton critique)	FWD		Structure deficiency	Deflections at joints, cracks, and centers			Joint or crack load, shear, and moment transfer efficiency
NCHRP-Texas Transportation Institute (*18*)	FWD		Deflection	Deflections at joints, cracks, and centers			Joint or crack load, shear, and moment transfer efficiency

Note: FWD = falling weight deflectometer, AC = asphalt concrete, ESAL = equivalent single-axle load, and CBR = California bearing ratio.

deflections on the loaded and unloaded side of a crack or joint should be made, as well as deflections in the center of an intact section.

Required Coring and Laboratory Testing

The two overlay design methods that require laboratory testing of samples are the FHWA-Austin Research Engineers (ARE) method (2) and the Kentucky method (9). The FHWA-ARE method requires tests of the asphaltic concrete, base course, subbase, and subgrade, with the latter three in a triaxial apparatus at different levels of confining pressure. The resilient modulus of the asphaltic concrete is determined at the mean annual temperature. The Kentucky method determines a soaked CBR value for the subgrade sample and multiplies it by 1,500 to get an approximate subgrade modulus.

NDT Devices Used

Each overlay design procedure has a principal NDT device and may have several alternates. The use of any alternate device usually requires a correlation between the deflections measured by each device. However, there are fundamental difficulties with this approach. As noted in the reports by Majidzadeh and Ilves (3) and Southgate et al. (9), the correlation between the deflections measured by two different devices changes with the thickness and modulus of

Section Delineation Criteria	Empirical Relations: Required Correlation	Empirical Relations: Design Assumption	Test Season	Test Location	Test Frequency (ft)	Core Required	Laboratory Testing
Statistically different maximum deflection; severity of alligator cracking	Layer moduli	Fatigue rutting from AASHO Road Test	"Worst" season; high deflection			ACZ base, subbase, and subgrade	Resilient modulus; triaxial tests
Statistical difference, required overlay thickness	Layer moduli	Fatigue from AASHO Road Test	Annual average condition	Outer wheelpath	50-150		
Statistically different maximum deflection	Deflection	Design deflection versus 18-kip ESAL/day	"Critical" period				
Statistically different maximum deflection	Layer moduli; correlation between subgrade and base modulus	Fatigue: strain versus number of design loads					
Difference >0.01 in 80 percent deflection	Deflection	Tolerable deflection versus design traffic; percent deflection reduction versus overlay thickness	Spring to early summer	Outer wheelpath (1,000-ft sections)	50		
Significant difference in 90th percentile deflection, subgrade modulus, or AC thickness	Road rater deflection versus subgrade modulus	Total pavement thickness versus 18-kip ESAL for various CBRs; percent of AC in pavement structure	Soaked subgrade CBR or time to weakest subgrade			Subgrade	Soaked CBR test
Statistically different maximum deflection	Deflection; Dynaflect versus Benkelman beam	Tolerable deflection versus 18-kip ESALs; percent deflection reduction versus overlay thickness		Wheelpath with most distress (0.2-mile-long section)	264		
	Temperature adjustment versus surface temperature; deflection; road rater versus Benkelman beam	Road rater deflection versus 18-kip ESAL design life	Spring	Outer wheelpath areas of greater distress (1,000-ft sections)	100		
Statistically different maximum deflection	Deflection; Dynaflect versus Benkelman beam	Loss of serviceability index related to SCI and number of 18-kip ESALs					
Statistically different maximum deflection	Deflection; Dynaflect versus Benkelman beam	Maximum deflection versus number of 18-kip ESALs	Fall	Closer spacing around heavy cracking			
Statistically different maximum deflection	Deflection; Dynaflect versus Benkelman beam	Maximum deflections versus number of 18-kip ESALs			≤500		
Coefficient of variation of maximum deflection >20 percent	Strain versus deflection; road rater versus FWD	Fatigue: strain versus number of 18-kip ESALs	Spring	Outer wheelpath	100-200		
	Equivalent pavement section	Bonding condition versus exponent					
	Deflection	Joint or crack deflections versus number of 18-kip ESALS					

each pavement layer and the modulus of the subgrade. Thus there is no unique multiplier that relates the deflections measured by one NDT device to those of another. The multipliers that have been found in field correlations must be regarded as applying only to those pavements on which the correlation was made.

Even when the primary device is used, care must be exercised to ensure that the equipment has the configuration (loading plate size and shape, sensor locations, and so forth) for which the overlay design procedure was developed. In addition, the equipment must be operated in the same manner (load level, frequency, and so forth).

The primary devices used include the Dynaflect, road rater, falling weight deflectometer (FWD), California traveling deflectometer, and Benkelman beam. The alternate devices include Dynaflect, road rater, FWD, Benkelman beam, and Dehlen curvature meter. Further discussion of correlations is continued later.

As an alternative to correlating deflections from different NDT devices, the FHWA-RII method (3) provides for a separate analysis for each NDT device to determine the moduli of each layer in the pavement.

NDT Measurements

NDT measurements that are made are either a single deflection, a deflection basin, or deflections on the loaded and unloaded side of a joint or crack.

Other Measurements

In addition to NDT measurements, the following measurements are also made: date and time of test, air temperature, pavement surface temperature, thickness of asphalt layer, mean air temperature over previous 5-day period from a nearby weather station, and thickness of all layers from construction drawings. The air temperature should be measured every hour on bright, sunny days and as far apart as 3 or 4 hr on cloudy days with relatively stable air temperature. The temperature measurements are used in making temperature corrections using methods such as the one developed by Southgate and Deen (19).

Correction to NDT Measurements

Measured deflections are corrected to a standard condition that is used for design purposes. The most extensive set of corrections that are made to measured deflections is applied in Kentucky (9), where there are correction methods for load level, temperature, loading frequency, modulus, voids, and asphalt content of the asphaltic concrete surface layer. The normal corrections are for temperature and season.

Most areas of the country experience significant changes in surface temperature and subgrade moisture content. Therefore a temperature increase tends to "soften" asphalt concrete, whereas a temperature decrease tends to "stiffen" asphalt concrete. This in turn affects the deflection measured by NDT devices. A typical correction procedure requires measurement of the pavement surface temperature and determination of the mean 5-day air temperature to estimate the mean pavement temperature. This temperature is then used to determine a multiplier used to adjust maximum deflection from the determined mean to an equivalent maximum deflection at a standard temperature. All corrected deflections can then be compared (5,19).

Some areas of the country experience significant seasonal variations in subgrade strength because of moisture changes and frost action. Figure 1 (5) shows the type of variation that could be experienced. Of course subgrade materials also affect this variation, and Figure 2 shows the effect of materials on season variation. Each agency must develop this relationship and adjust deflections to a standard adjusted deflection, measure deflections at a standard time, or determine that no significant variation exists. Seasonal adjustment factors should account for differences in subgrade materials as well. Thus different adjustment factors may be required for different subgrade types.

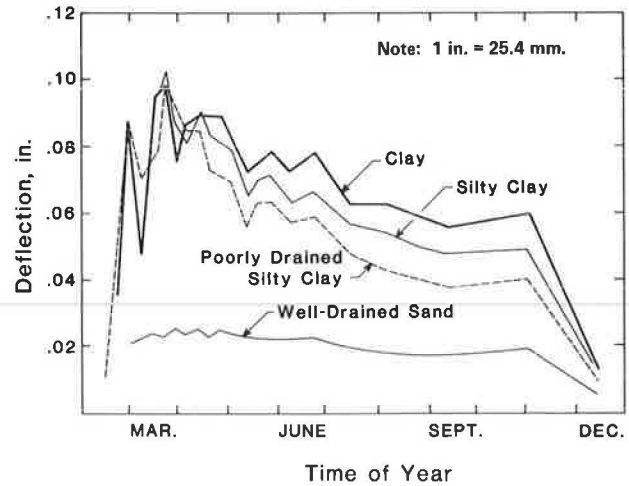

FIGURE 2 Effects of subgrade materials on seasonal influence on deflections.

California (8) makes no corrections except for temperatures less than 50° F (10° C). Louisiana has a method (10) of correcting for moisture beneath the pavement by using the spreadability-versus-maximum-deflection chart. Some procedures, namely the FHWA-RII (3), University of Illinois (15), and the FHWA-ARE (2) methods, prefer to calculate the moduli of pavement layers directly from the NDT deflection measurements and then correct the moduli for temperature, stress level, and season. The FHWA-ARE method corrects only the subgrade modulus for stress level.

The FHWA-RII method assumes that all pavements are composed of three or four layers and corrects each layer modulus for temperature or stress level. The stress level corresponds to the level that is imposed by the design load. The Shell method (6) corrects the modulus of the surface course for temperature by using a stiffness modulus chart that was developed for FWD loading conditions.

Calculated or Inferred Pavement Properties

The pavement properties calculated or inferred from deflection measurements range from qualitative ratings of the pavement layers [Utah (13)] to layer moduli [(FHWA-RII (2)]. The pavement properties can be separated into five categories:

1. Qualitative ratings,

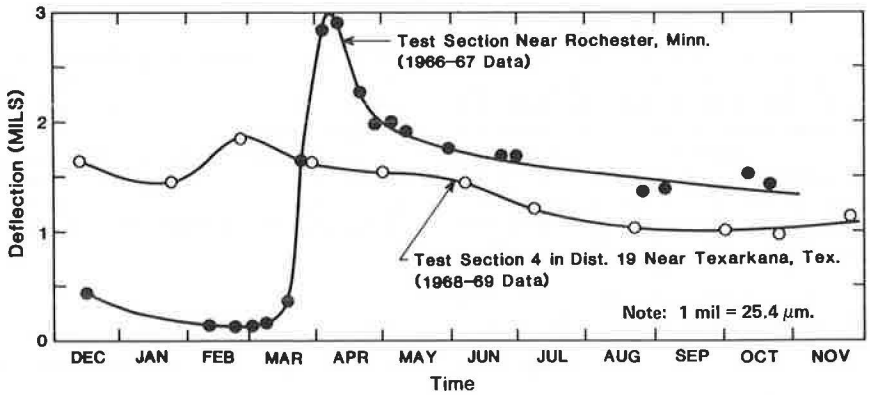

FIGURE 1 Effects of seasonal influence on deflection in different climatic areas (5).

2. Representative deflections,
3. Representative basin properties,
4. Representative pavement structural properties, and
5. Layer moduli.

The pavement section is normally represented by elastic layers (Figure 3 contains four) of known thickness (except for the lowest layer, which is assumed to have infinite depth) and characterized by Young's moduli (E) and Poisson's ratios (m). When a load of known intensity is applied over a known area, deflections are created at some distance from the center of the loaded area. It is normally assumed that the load is distributed through the pavement system by a truncated zone (represented by the dashed line in Figure 3).

Based on this concept, deflection d_4 at a distance r_4 from the center of load can only be due to the "elastic" compression of layer 4 because layers 1, 2, and 3 are outside the influence cone created by the load. Likewise, deflection d_3 at distance r_3 is due to the compression of layers 3 and 4; the deflection at distance r_2 is due to compression in layers 2, 3, and 4; and deflection d_1 is due to compression in all layers.

This can be used, at least conceptually, to determine the influence of the various layers in the pavement structure. This general approach is used to back-calculate properties of pavement layers.

More subjective analyses consider just the curvature and maximum deflection to determine general behavior. This concept is shown in Figure 4 from the Utah overlay design procedure (13), which uses representative deflection and basin properties to arrive at qualitative descriptions of the condition of the surface, base, and subgrade. The Dynaflect maximum deflection (DMD), the surface curvature index (SCI), and the base curvature index (BCI) are all used to arrive at these ratings. The dividing lines between good and poor are 1.25 mils (DMD), 0.48 mil (SCI), and 0.11 mil (BCI). One mil is 0.001 in. (0.0254 mm).

Representative deflections are usually those that are larger than a selected percentile between 50 and 97 percent, as estimated by using a normal distribution. These percentiles apply to deflections that are measured at a crack or joint or between them.

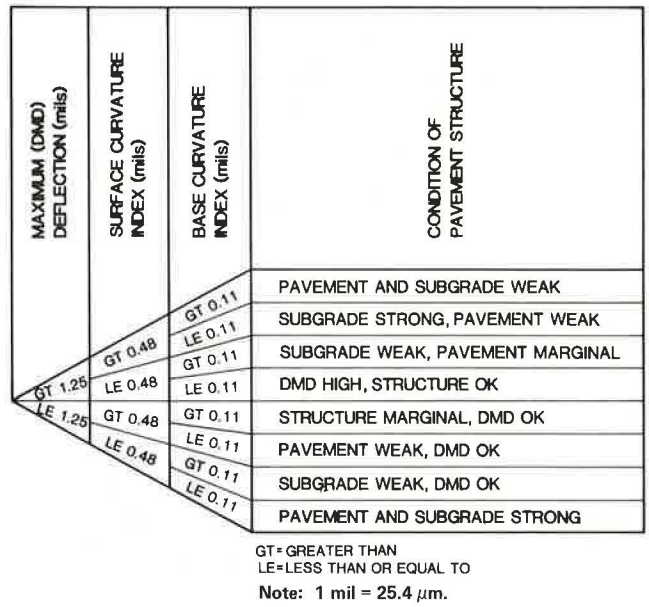

FIGURE 4 Use of deflection basin parameters to analyze pavement structural layers (13).

Representative basin properties include spreadability, SCI, BCI, and area. These are normally used with maximum deflection to determine structural properties (representative or moduli) of pavement layers.

Representative structural properties of a pavement include the effective thickness of the pavement as in the Virginia (14) and Louisiana (10) methods, effective thickness of asphaltic concrete and base course as in the Kentucky method (9), and effective modulus in the Asphalt Institute method (5). Joint and crack load, shear, and deflection transfer efficiencies are calculated from deflections on the loaded and unloaded sides of cracks in the existing pavement.

Layer moduli that are calculated from deflection measurements usually include the subgrade modulus. However, in the FHWA-RII method (3), all layer mod-

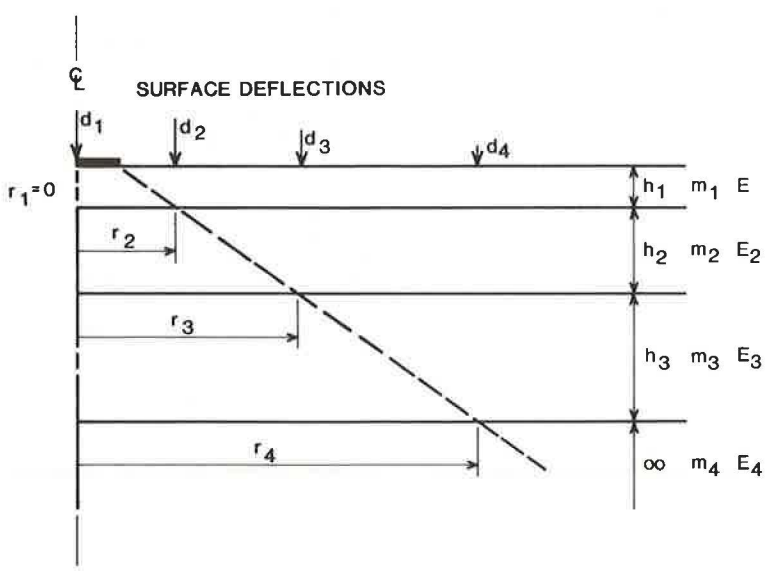

FIGURE 3 Four-layer elastic representation of a pavement system.

uli are calculated for a three- or four-layer pavement. The Shell procedure (6) assumes a correlation between the subgrade and base course moduli and then determines the surface course modulus in an assumed three-layer pavement. The University of Illinois procedure (15) assumes a modulus of the aggregate base course and determines the modulus of the asphaltic concrete and the break-point modulus of the subgrade, thus taking into account some of the stress sensitivity in these layers.

Methods of Delineating Common Pavement Sections

There are two methods used to delineate common sections of pavement to receive a uniform overlay treatment: one differentiates sections based on deflections and visual condition, and the other distinguishes sections based on the required overlay thickness. In the first method statistical tests are made by using a mean and standard deviation of deflections of sections that are suspected of being different. In the second, used only by the FHWA-RII method (3), required overlay thicknesses are calculated for each deflection basin, and then statistical tests are made by using the mean and standard deviations of the overlay thicknesses. In both methods a change in overlay thickness is made only if there is a significant difference either in the design deflection or in the design overlay thickness between two sections that are believed to be different. The design deflection is the one that is larger than 50 to 97 percent of all other deflections in a section, based on the reliability selected by the highway agency. The percentile for the design overlay thickness is thought to be between 67 and 75 percent, although there is not enough experience with the FHWA-RII method to say for certain. Currently, the selection of the design percentile is left to the design engineer.

Empirical Relations Between NDT Measurements and Design Quantities

There are three types of correlations between NDT measurements and design quantities:

1. Correlations between deflections produced by an NDT device and those produced by a design load,
2. Correlations between material properties at the load level produced by the NDT device and those same material properties at the design load level, and
3. Correlations between an NDT deflection and a design strain at a critical point in the pavement.

Correlations between deflections measured by different devices are most common in these overlay design procedures, and they are usually relations between the Benkelman beam maximum deflection and that produced by the principal NDT device used in pavement evaluation. In Louisiana (10), Texas (12), and Utah (13) the correlation is with the Dynaflect, and in general the multiplier is usually found to be between 20 and 30. In Texas the correlation was not between maximum deflections but between SCI values. In Pennsylvania (11) the correlation is between the maximum deflection of the road rater and that of the Benkelman beam. In California (8) correlations are available between the traveling deflectometer and several other NDT devices, including Dynaflect, road rater, and Dehlen curvature meter. Indiscriminate use of correlations can lead to significant error. Further discussion is presented later.

Correlations between material properties at different load levels are usually done with the aid of stress-strain curves of the material at different stress levels. This is the case with the subgrade in the FHWA-ARE (2) and the University of Illinois (15) methods and with the base, subbase, and subgrade in the FHWA-RII method (3).

Correlations between an NDT deflection and a design Asphalt Concrete (AC) strain are used in the University of Illinois method.

Empirical Design Life Relations

Every overlay design procedure has an empirical relation between the number of design load applications that a pavement can carry and a deflection, pavement thickness, or a calculated strain at a critical point in the pavement structure. In fact, overlay design procedures are fit into three categories based on which value is used to specify the design life of the overlay:

1. Deflection (based on deflections),
2. Structural deficiency (based on thickness), or
3. Mechanistic (based on a calculated strain).

Deflection overlay design procedures are used by the Asphalt Institute (5); the states of California (8), Louisiana (10), Pennsylvania (11), Texas (12), Utah (13), and Virginia (14); and the new NCHRP-Texas Transportation Institute (TTI) design procedure (18). Texas is unique in relating pavement design life to the SCI rather than to maximum deflection.

Structural deficiency overlay design procedures are used by Kentucky (9) and by the FAA (17).

Mechanistic overlay design procedures are used in the FHWA-ARE (2), FHWA-RII (3), Shell (6), and University of Illinois (15) methods, all of which use a fatigue relation that relates the strain at the bottom of the AC layer to the number of design load applications. In addition, the FHWA-ARE method considers rutting and provides a stress-check procedure for reflection cracking.

In all cases the design life relation is empirical in that it must be based on field observations. The design strain is calculated for the design level of load, and in all cases the stress sensitivity of the material in at least some of the pavement layers is taken into account in making this calculation.

Some of the commonly used NDT devices, such as Dynaflect or road rater, apply loads that are much smaller than the design loads. The moduli that are back-calculated from the deflections measured by devices with small loadings do not correspond to the moduli used in calculating the design strain. This means, in practice, that the moduli from the lightly loaded NDT devices must be adjusted to account for stress sensitivity. This adjustment is not a constant, but depends on the pavement section and the materials in the pavements. Methods for doing this explicitly are included in the FHWA-ARE procedure (2) for the subgrade and in the FHWA-RII procedure (3) for all layers beneath the surface course. The Shell (6) and University of Illinois (15) methods use the FWD, which is capable of applying a design load level to an existing pavement.

DESIGN ASSUMPTIONS AND REQUIRED CORRELATIONS FOR OVERLAY DESIGN

The foregoing review of overlay design procedures indicates that all design methods that use NDT are based on at least one design assumption and one

related NDT empirical correlation. The design assumptions that have been used or might be used are presented in the following list. The number of design loads [18,000 lb (80 kN) equivalent single-axle loads (ESALs)] in the useful life of an overlay is related to one or more of the following:

1. The deflection it experiences under that design load,
2. The amount of bending (SCI) it experiences under the design load,
3. The effective thickness of the pavement above the subgrade,
4. The tensile strain at the bottom of the asphaltic concrete layer under a design load,
5. The compressive strain either in the subgrade or in the asphaltic concrete overlay material under a design load,
6. The distressed condition of the underlying pavement and the thickness of the overlay, and
7. The differential deflection across cracks or joints in the underlying pavement due to the application of the design load and the thickness of the overlay.

Obviously, still other design assumptions could be made. In every case, however, the relation described in the design assumption must be based on field observations.

The use of an NDT device in an overlay design procedure requires that a related correlation must be developed between the results of the NDT measurement and the design quantity that is assumed to control the useful life of the pavement. Typical required correlations include

1. Deflections under the design load correlated with deflections under the NDT device,
2. Bending (SCI) under the design load correlated with the bending (SCI) under the NDT device,
3. Strain under the design load correlated with the deflection or strain under the NDT device, and
4. Layer modulus under the design load correlated with the layer modulus under the NDT device.

It should be noted that the first and second correlations would not be needed if the NDT device produced deflections and bending equivalent to those produced by design loads. The third and fourth correlations are used with mechanistic design procedures. In principle, any NDT device can be used with any design procedure, provided that the required correlation can be found. As a caution, it is noted that the design assumption must also be demonstrated by field observations to be valid for the pavement where it is to be applied. In general, those NDT devices that simulate design loads and produce equivalent deflections will be the most simple to use, thereby resulting in less error because of correlations.

EVALUATION OF CURRENT OVERLAY DESIGN PROCEDURES FOR COMPATIBILITY WITH AVAILABLE NDT DEVICES

Each of the required correlations discussed in the previous section relates NDT measurements to the design quantity that appears in the design assumption of an overlay design procedure. For the equipment to be compatible with the design procedure, this correlation must be possible. The NDT devices were separated into four categories: static deflection, automated beam deflection, steady-state dynamic deflection, and impulse deflection.

The static deflection devices include the plate bearing test, the curvature meter, the Benkelman beam, and the deflection beam. For both beams it is possible to develop, either by observation or analysis, all four of the required correlations (i.e., deflection, curvature, strain, or layer modulus). For the curvature meter, the only required correlation it can develop is for curvature. For the plate bearing test, it is possible to develop, either by observation or analysis, all of the required correlations, except for curvature.

The automated beam deflection devices include the La Croix Deflectograph and the California traveling deflectometer. It would be simpler to develop a required correlation for deflection or strain with these devices than for curvature or layer modulus. Theoretically, the required correlation for layer modulus could be developed by using some form of mechanistic analysis because the La Croix can be used to measure basin responses.

The steady-state dynamic deflection devices include the Dynaflect and the road rater models 400 B, 2000, and 2008. In each of these, deflections are measured at a number of points on the pavement surface, which makes it possible to determine deflections and curvatures directly and to calculate strains and layer moduli. Therefore, the required correlations can, in principle, be developed with each of these devices.

The impulse deflection devices include the Dynatest, KUAB, and Phoenix FWDs and the wave propagation devices currently being developed at the University of Texas and at the University of New Mexico for the U.S. Air Force. Because all FWDs measure deflections at several points on the pavement surface, it is possible, in principle, to develop all four required correlations with them. In addition, these devices produce impulse loads equal to design loads. The deflections produced by these devices have been demonstrated to closely simulate moving wheel load deflections. This allows, in principle, the direct use of the deflection, bending strain, and modulus data without correlations.

The wave propagation methods both produce moduli of the pavement layers that correspond to a light load. Consequently, to use the wave propagation techniques it is necessary to develop the required correlation between layer moduli at different load levels. This is the only required correlation that can be used with wave propagation methods.

CORRELATIONS BETWEEN NDT DEVICES

Because correlation between NDT devices is the most common correlation used in overlay design procedures, additional discussion is presented.

In general, a different correlation should be developed for each major pavement type and for different pavement thicknesses within particular types of pavements because the correlation is not unique, as was noted quite clearly by Majidzadeh and Ilves (3). Correlations will also change with loading frequency, as illustrated by Kentucky's method (9), in which there is a correction to a standard loading frequency of 25 Hz.

Because several of the overlay design procedures currently available were developed based on AASHO Road Test data and other deflection data from the Benkelman beam, deflection measurements from other devices have often been converted to equivalent Benkelman beam deflections by several agencies. A few for the Dynaflect are summarized to illustrate the variability that can be expected. In Arizona the conversion is

$$BBD = 22.5\ (DMD) \qquad (1)$$

where BBD is the Benkelman beam deflection and DMD is the Dynaflect maximum deflection. No data based on correlation were given. Arizona also uses the California overlay design method with their correlation between Dynaflect and traveling deflectometer (20).

In Virginia the equivalents are as follows:

No. of Points Correlated	Tests	r	Se (0.001 in.)	Regression Equation
All points flexible	107	0.852	9.8	BB = 30.5 D - 12.3
Stabilized base	72	0.918	5.4	BB = 24.0 D - 8.0
Unstabilized base	35	0.877	9.6	BB = 32.8 D - 8.6

where BB is the Benkelman beam deflection (in. x 10^{-3}) and D is the Dynaflect deflection (in. x 10^{-3}).

Benkelman beam deflections are taken approximately as recommended in AASHTO T 256-77; however, the tip is placed only 2 ft (0.6 m) forward of the wheel at the start of the test versus 4 to 4.5 ft (1.2 to 1.4 m) as recommended in T 256-77. Also, the final position of the truck differs from that recommended by T 256-77. The tests were taken from seven flexible projects. Four of the projects had stabilized bases (21).

The Asphalt Institute uses the following equation for equivalent measurements:

$$BB = 22.30\ D - 2.73 \qquad (2)$$

where BB is the Benkelman beam rebound deflection (in. x 10^{-3}) and D is the Dynaflect center deflection (in. x 10^{-3}).

Benkelman beam deflections are rebound deflections based on the Canadian Good Roads Association (CGRA) procedure. No information on the number of test points, test locations, pavement types, and so forth is provided for the regression equation; however, it does reflect a composite analysis (5).

In Louisiana the following equation is used:

$$BB = 20.63\ D \qquad (3)$$

where BB is the Benkelman beam rebound deflection (in. x 10^{-3}) and D is the Dynaflect deflection (in. x 10^{-3}). This equation is based on 54 comparisons on 20 pavement sections of flexible pavement. The correlation coefficient was 0.85 (10,22, 23).

Correlations between most other devices and the Benkelman beam have been developed by various agencies. Correlations have been developed between different dynamic deflection devices and between dynamic deflection devices and impulse devices. An agency that is developing such a correlation should use those developed by another agency as a guide only. The actual correlation must be developed for the agency's own test procedures, pavement sections, soil types, and environmental conditions to be valid. Even then, all of the problems discussed by Majidzadeh and Ilves (3) may be encountered. As discussed previously, there is no unique multiplier that will accurately relate the deflection measured by one NDT device to the deflection measured by another. Changes in pavement layer thicknesses and moduli will affect any such multiplier (3,13).

Table 2 was prepared to show typical correlations between Benkelman beam readings and Dynaflect readings. The data in the table indicate that there is a large range of values for equivalent Benkelman beam deflections calculated from the same Dynaflect reading. This is included primarily as a caution to highway engineers that a correlation developed by one agency may not be directly transferable.

It should be noted that NDT equipment that can reproduce design loads and simulate moving wheel load deflections eliminates the need for many of the correlations. They also eliminate the error associated with correlations.

INTERCHANGEABILITY OF DATA

Many times agencies vary in their testing programs, which makes use of another agency's data difficult even when they use the same type of equipment. For instance, agencies that use the road rater may vary considerably in the load, frequency, loading plate configuration, and sensor location, any of which will have a significant impact on the deflection data. Some agencies that use the Benkelman beam use the WASHO method (24) whereas others use the rebound method (5), thereby making it difficult to compare the results. Even the weights used for Benkelman beam measurements vary. Early California measurements used a 7,500-lb (33-kN) wheel load and later a 9,000-lb (40-kN) wheel load (7,8). The British use a 7,000-lb (31-kN) wheel load (25), and Florida uses a 10,000-lb (44-kN) axle load (26).

These data indicate the problems that can occur in trying to use data developed by another agency. The source, testing procedure, and equipment configuration used in developing the data must be fully understood before data collected by another agency can be used. Failure to consider these can lead to significant error if data, or correlations based on that data, are used.

CONCLUSIONS

The following conclusions were made based on the data presented in the report:

1. Several overlay design procedures for flexible pavements that use deflections have been developed. The mechanistic-based procedures can be used more directly by agencies other than the developing agency. Some field verification is still necessary with mechanistic procedures.
2. In developing or selecting a deflection-based overlay design procedure, the following items should be considered: seasonal influences on the deflections, location of test points on the pavement surface, frequency of testing, need for cores and laboratory testing, type of NDT measurements (i.e., maximum deflection, basin characterization), additional field measurements that are required, corrections to NDT measurements for temperature, pavement properties calculated or inferred from the NDT mea-

TABLE 2 Benkelman Beam Readings Determined from Correlations with Dynaflect

Dynaflect Reading (0.001 in.)	Benkelman Beam Readings (10^{-3} in.)			
	Arizona	Asphalt Institute	Virginia (all flexible)	Louisiana
0.5	11.2	8.4	3.0	10.3
1.0	22.5	19.6	18.2	20.6
1.5	33.8	30.7	33.4	30.9
2.0	45.0	41.9	48.7	41.3
2.5	56.2	53.0	64.0	51.6
3.0	67.5	64.2	79.2	61.9

Note: 1 in. = 25.4 mm.

surements, method used to distinguish between different design sections, relationships that are used to convert NDT measurements to design parameters, relationships that relate the design parameters to the useful life of the pavement, the NDT devices that are available for use, and consideration of existing deterioration of the pavement.

3. If an NDT device produces a load less than the design load, one of three general methods must be used to convert the measured deflections into usable parameters: (a) correlate the NDT deflection measurements from the light load device with those produced by the design load, (b) correlate the material properties calculated from the NDT device with those same properties that would be developed for the design load, and (c) correlate the light load deflection measurements with some measure of performance directly. All of these methods may produce questionable results because of the stress sensitivity of the pavement and subgrade.

4. There are significant advantages in using an NDT load that equals that of a heavily loaded truck wheel load [e.g., 9,000 lb (40 kN)]. The response of the pavement to this heavy load can be accurately measured and directly used for structural evaluation and overlay design without questionable correlations or stress-sensitivity assumptions.

5. Available correlations are valid only for the typical pavement sections, materials, and environmental conditions that affect the pavement sections for which the correlations were developed.

RECOMMENDATIONS

1. Correlations of deflection measurements between devices should be used only with a complete understanding of the conditions for which they are applicable and with an understanding of the magnitude of error involved.

2. NDT response is load dependent. Analytical procedures to accurately characterize and model material properties that are stress dependent should be improved and refined. This becomes more critical as additional layers of overlays are added to pavements.

3. Any overlay design procedure developed or adopted by an agency must be carefully field calibrated for local conditions and materials. This will require the use of actual in-service pavement sections.

4. Computerized overlay design procedures should be made available to the field engineer who evaluates pavements and designs overlays. Computerized methods should be developed for use with microcomputers (256 K or less).

ACKNOWLEDGMENTS

The work discussed in this paper was sponsored by the Office of Research and Development, FHWA. The contracting officer's technical representative was Richard M. May. The assistance of the several states contacted and the equipment manufacturers is gratefully acknowledged.

REFERENCES

1. R.E. Smith and R.L. Lytton. Synthesis Study of Nondestructive Testing Devices for Use on Overlay Thickness Design of Flexible Pavements. Report FHWA/RD-83/097. FHWA, U.S. Department of Transportation, 1983.
2. Austin Research Engineers, Inc. Asphalt Concrete Overlays of Flexible Pavements--Volume 1: Development of New Design Criteria. Report FHWA-RD-75-75. FHWA, U.S. Department of Transportation, Aug. 1975.
3. K. Majidzadeh and G. Ilves; Resource International, Inc. Flexible Pavement Overlay Design Procedures--Volume 1: Evaluation and Modification of the Design Methods. Final Report FHWA/RD-81/032. FHWA, U.S. Department of Transportation, 1981.
4. K. Majidzadeh and G. Ilves; Resource International, Inc. Flexible Pavement Overlay Design Procedures--Volume 2: User Manual. Final Report FHWA/RD-81/033. FHWA, U.S. Department of Transportation, 1981.
5. Asphalt Overlays for Highway and Street Rehabilitation. Manual Series 17. The Asphalt Institute, College Park, Md., 1983.
6. A.I.M. Claessen and R. Ditmarsch. Pavement Evaluation and Overlay Design. Proc., 4th International Conference on Structural Design of Asphalt Pavements, Ann Arbor, Mich., 1977.
7. R.W. Bushey et al. Structural Overlays for Pavement Rehabilitation. Report CA-DOT-TL-3128-74-12. California Department of Transportation, Sacramento, 1974.
8. Asphalt Concrete Overlay Design Manual. California Department of Transportation, Sacramento, 1979.
9. H.F. Southgate, G.W. Sharpe, and R.C. Deen. A Rational Thickness Design System for Asphaltic Concrete Overlays. Research Report 507. Division of Research, Bureau of Highways, Kentucky Department of Transportation, Lexington, Oct. 1978.
10. R.W. Kinchen and W.H. Temple. Asphaltic Concrete Overlays of Rigid and Flexible Pavements. Report FHWA/LA-80/147. Louisiana Department of Transportation and Development, Baton Rouge, Oct. 1980.
11. A.C. Bhajandas, G. Cumberledge, and G.L. Hoffman. Flexible Pavement Evaluation and Rehabilitation. ASCE Symposium on Pavement Design, Atlanta, Ga., June 1975.
12. J.L. Brown and H.E. Orellana. An Asphaltic Concrete Overlay Design Subsystem. Research Project 1-8-66-101. Highway Design Division, Research Section, Texas Highway Department, Austin, 1970.
13. D.E. Peterson et al. Asphalt Overlays and Pavement Rehabilitation--Evaluating Structural Adequacy for Flexible Pavement Overlays. Report 8-996. Utah Department of Transportation, Salt Lake City, Jan. 1976.
14. N.K. Vaswani. Method for Separately Evaluating Structural Performance of Subgrades and Overlaying Flexible Pavement. In Highway Research Record 362, HRB, National Research Council, Washington, D.C., 1971, pp. 48-62.
15. M.S. Hoffman and M.R. Thompson. Mechanistic Interpretation of Nondestructive Pavement Testing Deflections. Department of Civil Engineering, University of Illinois, Urbana-Champaign, 1981.
16. M.R. Thompson. Concepts for Developing a Nondestructive-Based Asphalt Concrete Overlay Thickness Design Procedure. Illinois Department of Transportation and Department of Civil Engineering, University of Illinois, Urbana-Champaign, 1982.
17. R.L. Lytton. Comments on FAA Overlay Design Procedure. Consulting Report. U.S. Army Corps of Engineers Waterways Experiment Station, Vicksburg, Miss., Feb. 8, 1982.
18. P.E. Paris and F. Erdogan. A Critical Analysis

of Crack Propagation. Trans., ASME Journal of Basic Engineering, Series D-85, No. 3, 1963.
19. H.F. Southgate and R.C. Deen. Temperature Distribution in Asphaltic Concrete Pavements. In Transportation Research Record 549, TRB, National Research Council, Washington, D.C., 1975, pp. 39-46.
20. Deflection Overlay Design Procedure. Section 501.05. In Arizona DOT Materials Manual, Arizona Department of Transportation, Phoenix (undated).
21. C.S. Hughes. Correlation Between Benkelman Beam and Dynaflect. Virginia Research Council, Charlottesville, 1966.
22. AASHO Correlation Study. Research Report 63-4SC, Interim Progress Report 1. Louisiana Department of Highways, Baton Rouge, 1967.
23. J.W. Lyon, Jr. Louisiana Experimental Base Project, Interim Report 1. Report FHWA/LA-79/126. Louisiana Department of Transportation and Development, Baton Rouge, Nov. 1979.
24. Standard Recommended Practice for Pavement Deflection Measurements. AASHTO Designation T 256-77. In Standard Specifications for Transportation Materials and Methods of Sampling and Testing, Part II, AASHTO, Washington, D.C., 1982.
25. C.K. Kennedy, P. Fevre, and C.S. Clarke. Pavement Deflection: Equipment for Measurement in the United Kingdom. TRRL Report 834. Transport and Road Research Laboratory, Crowthorne, Berkshire, England, 1978.
26. R.L. McNamara and G.C. Page. Benkelman Beam Versus Dynaflect Deflection Correlation for Flexible Pavements in Florida. Research Report FL/DOT/OMR-81/237. Florida Department of Transportation, Gainsville, 1981.

Comparison of Falling Weight Deflectometer with Other Deflection Testing Devices

OLLE THOLEN, JAY SHARMA, and RONALD L. TERREL

ABSTRACT

Pavement modeling has always been a complex and difficult problem for the highway engineer. Currently, there are complex and precise computer programs that provide the engineer with a means of computing theoretical behavior. However, full-scale field testing has not kept pace, and new testing devices are just now becoming readily available. For many years the Benkelman beam was the standard, and later developments tended to be compared with this method for acceptance. However, it became apparent that better methods were required for adequate representation of pavement behavior under moving wheel loads. In this paper a summary of comparison tests conducted in Scandinavia is presented. The comparison included two designs of falling weight deflectometers (FWDs), Dynaflect, plate bearing, traveling deflectograph, vibrators, and Benkelman beam. These devices were used to test a variety of pavement structures. The results have revealed a wide range of deflections depending on the pavement section. These differences are caused by the magnitude and nature of applied load, time of loading, pavement thickness, and other factors. It appears that the FWD is well suited to a wide range of pavements and provides uniformly accurate results that are consistent with actual pavement loading and behavior.

Modeling of highway and airport pavements has been a difficult task since the beginning of road building. A pavement has many variables, such as thickness and type of materials, environment, traffic, and others. To account for many of these variables simultaneously, full-scale testing, such as deflection measurements, has proved to be beneficial.

The basic assumption in the behavior of pavements is that a pavement can withstand a number of repetitions of a given load before it fails. Failure can mean many forms of distress under some form of loading. If this loading is representative of traffic, then the strain or deformation could be related to performance by a failure model.

During the past several decades a large volume of data from Benkelman beam testing has been compiled and in various ways compared with pavement performance. This large bank of knowledge has become the principal reason for continued reliance on the Benkelman beam. Therefore the correlation between

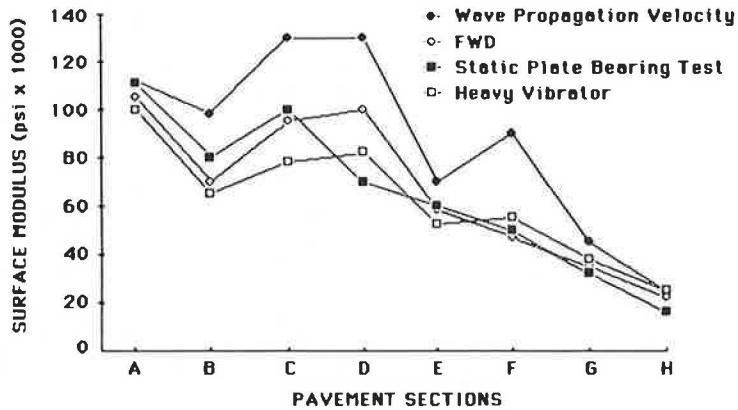

FIGURE 1 Comparison of different bearing capacity measurement methods on different road structures.

the Benkelman beam and other devices has become the apparent test of acceptability. Some engineers have reasoned that the understanding of pavements and their behavior is applicable only if the Benkelman beam or some similar device is used. That sort of reasoning may lead to the conclusion that a new testing device with increased capability (accuracy) may be desired, but that it should still give results closely correlated to the Benkelman beam. This prerequisite may be required by many engineers, in spite of the fact that the method does not relate to strain at traffic loading.

In this paper an attempt is made to demonstrate the factors involved and the range of results that might be expected from several of the pavement testing methods that are available to the engineer.

COMPARISON OF DIFFERENT METHODS

The comparison of various pavement devices has been an ongoing process, and many of these comparisons were made in Scandinavia, where much of the early work on falling weight deflectometers (FWDs) was done (1-11). The goal of most of these studies was to determine the behavior of pavements under different types of loading rather than to make a direct comparison of testing devices.

Two particular studies are of note and have been well documented. The first study (5) by the Swedish Road and Traffic Research Institute included eight different pavement structures that were tested on eight occasions over a time period of slightly more than a year. Also, four testing methods were used: static plate bearing tests, FWDs, heavy vibrators (15 Hz), and a wave propagation test. Figure 1 shows the surface moduli of the eight different pavement sections; these have been averaged with time for each pavement structure.

The second study (6) included the evaluation of 12 testing methods used in the Nordic countries on 12 different pavement sections. Figure 2 shows the surface deflection for five of the testing methods for a range of pavements. The values plotted in Figure 2 are normalized to 11,250 lb. The data in Table 1 give an explanation of the various pavement types included in this study, and Table 2 gives a list of the deflection testing devices used.

Examination of Figures 1 and 2 indicates that the use of the various testing methods results in the same general trends over the range of pavement structures. When both static and dynamic testing methods are used on the same pavement, the FWD seldom results in extreme values, as compared with some of the other methods.

Tables 3 (5) and 4 (6) are correlation matrices from the two research projects. It is apparent that most of the correlation coefficients are rather high. However, it must be kept in mind that the

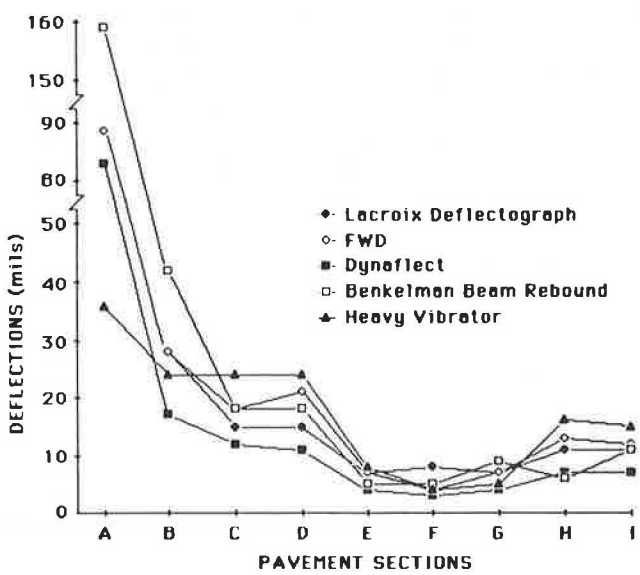

FIGURE 2 Comparison of different bearing capacity measurement methods on different road structures, with deflections normalized to 11,250-lb load.

TABLE 1 Description of Pavement Sections

Section	Wearing Course[a]	Base Course Type	Base Course Depth (in.)	Subbase Type	Subbase Depth (in.)	Subgrade
A	Gravel	Gravel		Sand		Peat on clay
B	Asphalt	Gravel	12	Bark	40	Peat and mud on clay
C	Asphalt	Cement slab	6	Gravel	12	Till and clay
D	Asphalt	Gravel	28	–		Till and clay
E	Asphalt	Crushed rock	51	–		Soil embankment
F	Asphalt	Asphalt	12	Sand	12	Clay
		Gravel	2			
G	Asphalt	Asphalt	8	Sand	16	Clay
		Gravel	2			
H	Asphalt	Gravel	10	Sand	16	Clay
I	Asphalt	Gravel	10	Sand	28	Clay

[a]All pavement sections with an asphalt wearing course are about 2 in. thick or less.

TABLE 2 Identification of Testing Devices

Symbol	Testing Device
I	Danish traveling deflectograph
II	La Croix deflectograph
III	Benkelman beam
IV	FWD (one-mass system)
V	FWD (two-mass system)
VI	Heavy vibrator (39 kN, 17 Hz)
VII	Dynaflect (5 kN, 8 Hz)
VIII	Static plate bearing test method 1
IX	Static plate bearing test method 2
X	Dynamic plate bearing test

TABLE 3 Correlation Coefficients (r) from Comparison of Surface Moduli Measured by Different Methods (*5*)

	Static Plate Bearing	Heavy Vibrator	Wave Propagation Velocity
FWD	0.84	0.90	0.86
Static plate bearing test		0.75	0.77
Heavy vibrator			0.78

coefficients are not universal values that represent the two methods being compared; they also depend on the choice of tested structures. In fact, it would be relatively easy to find populations with correlation coefficients near zero.

Further evaluation indicates that a high correlation coefficient does not prove that the two methods are accurately measuring the parameter desired. For example, in Table 4 the coefficient for the two static plate bearing tests (VIII and IX) is 0.98. When the regression line was examined, the two tests on one pavement indicated the same static surface modulus, whereas on the other structure there was a difference of a factor of two.

The correlation coefficients in these studies were consistently high, which indicates that the translation between different test methods may be reasonable, but only within a certain narrow range of pavement structures. Therefore, within these boundaries, a reasonable correlation could be developed.

It can be noted that the FWDs, particularly the two-mass FWDs, show high correlation coefficients when compared with the other most important families of testing devices--the vibrator and the Benkelman beam--along with their relatives. The correlation between the heavy vibrator and members of the Benkelman beam family is poor.

The fact that most test methods result in about the same measure of bearing capacity is not too surprising. It is not likely that a method would be used if it gave poor results. With some experience a pavement engineer can estimate the strength or bearing capacity without testing. However, when more accurate and useful information is required, accurate testing becomes more desirable. Therefore, an approximate agreement between methods may make the method useful for approximate surveys, but the choice of testing method for more precise evaluations is important.

When a more detailed comparison of testing methods is made, greater differences begin to appear. A complete analysis might be interesting, but would also be too lengthy. The following sections give examples of how the FWD compares with other methods.

FWD Versus Wheel Load

It is generally known that the deflection that occurs under a moving wheel load is dependent on vehicle speed. There may be a considerable difference between the deflection at normal traffic speed and at creep speed, which is used when testing with the Benkelman beam and the traveling deflectograph (2,12-15). Among other factors, the temperature of asphalt pavements plays a significant role, and uniform results are more easily attainable at normal traffic speed. The goal in developing the FWD was to obtain the same deflection as that measured under traffic loads at normal speed.

On one Danish test road with an asphalt pavement, deflections at traffic loads, FWD tests, and Benkelman beam tests were compared by means of accelerometers buried in the pavement (2). The results conclusively demonstrated that the FWD deflections were similar to those caused by traffic loads, whereas the Benkelman beam deflections were considerably larger.

It was further noted in the tests shown in Figure 2 that time of loading was a factor in pavements with thick asphalt layers and a peat subgrade. On pavements without these layers, the wheel load tests indicated smaller deflections than the FWD tests. This difference was most likely because the deflections of the wheel load tests were not measured in the loaded area and because the reference beam may have had its feet within the deflection bowl. Typical values of the deflection ratio between FWD and wheel loading at creep speed on these pavements ranged from 1.05 to 1.35. In another comparison, the difference between the two traveling deflectograph deflections was greater than the difference between deflections measured by FWD and traveling deflectographs.

TABLE 4 Correlation Coefficients (r) and Number of Test Points in Comparison Between Different Testing Devices (*6*)

Testing Device	Testing Device I	II	V	VII	IV	III	VIII	X	IX	VI
I		0.89	0.85	0.89	0.78	0.96				0.66
II	55		0.96	0.95	0.95	0.94				0.75
V	55	77		0.96	0.95	0.88		0.91	0.67	0.95
VII	55	76	128		0.93	0.91				0.84
IV	41	58	109	111		0.92		0.86	0.73	0.87
III	42	59	99	100	99				0.85	0.76
VIII								0.50	0.98	
X			32		32		32			0.98
IX			33		33	33	33			0.49
VI	42	58	64	65	64	65		31	32	

Note: Correlation coefficients are given in the upper half of the table and the number of test points is given in the lower half of the table. A description of the testing devices is given in Table 2.

Two-Mass Versus One-Mass FWD

Commercially available FWDs operate on similar principles, but have three important differences:

1. The force generating unit,
2. The method of distributing load on the pavement, and
3. The method of measuring deflection.

Force Generation

Typical force pulses from the one-mass system are shown in Figure 3 (16). The sharp rise of the force pulses does not accurately simulate moving wheel loads. Further, one-mass force pulses often exhibit high frequency distortions, as noted at the top of the second and third pulses in Figure 3. If this distortion occurs before the main peak, then the peak force measured is not compatible with deflections measured by sensors farther away from the load plate. This phenomena could then be a source of greater variation, which results in nonreproducible values of bearing capacity.

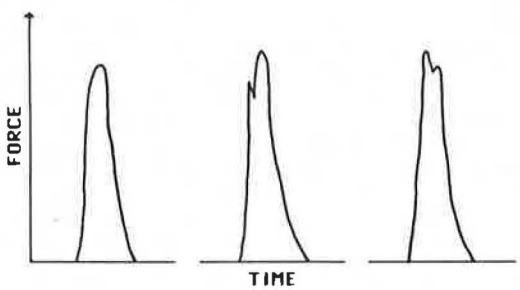

FIGURE 3 Examples of force pulses by measurement with one-mass FWD at different normal conditions (*16*).

To improve on this system the two-mass system was developed for the KUAB FWD. Typical examples of force pulses produced by this system are shown in Figure 4. The more gradual rise in the force pulses and the shape of the pulses are the same as those produced by moving wheel loads. The shape of the force pulses are always smooth for a wide range of pavement sections, and they are reproducible.

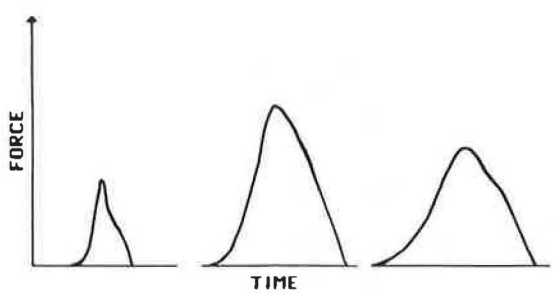

FIGURE 4 Representative examples of different force pulses from two-mass FWD system with rubber buffers.

Load Distribution

Deflection tests are generally conducted on pavements in need of rehabilitation; the surface is often uneven because of wheel ruts, cracks, and so forth. Several tests were conducted (1,16) on uneven roads, and it was found that deflection errors ranged from 10 to 20 percent. To improve accuracy, the KUAB FWD was designed with a segmented circular loading plate as shown in Figure 5. Each of the four segments can move independently; thus a uniform load is applied to each even though the vertical position may be different. This is achieved by loading each plate with a plunger that is connected to a common oil chamber. The spherical bearings are designed such that the center of rotation is low, thus permitting controlled lateral movement of the plates when they are tilted.

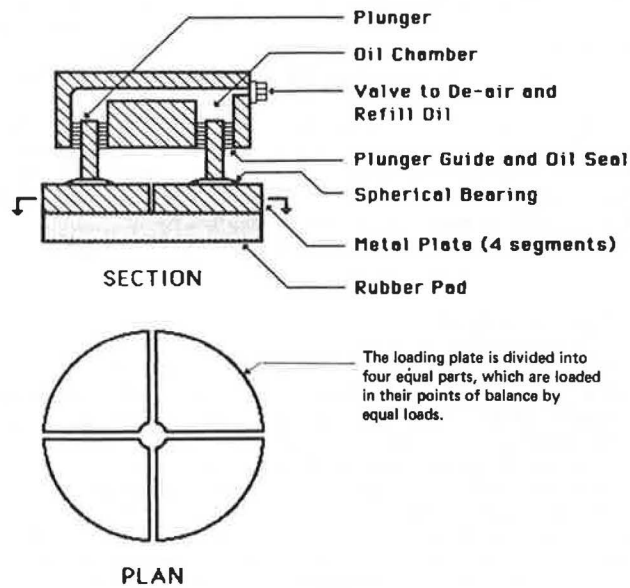

FIGURE 5 Principle of hydraulic load distribution plate.

Deflection Sensors

Deflection measurement has frequently been a difficult task in dynamic loading situations. Most FWDs use velocity transducers or geophones, and by integration of the measured velocity the deflection is obtained. However, a problem with this method is the difficulty with field calibration. Relative calibration is possible by placing all geophones next to or on top of each other and noting the similarity in deflection. This may be considered a reasonable method to check the device, but to give full proof of correct operation the comparison would have to be made on one pavement with a deflection rise time in the low range and on one pavement with a deflection rise time in the high range thus requiring an analogue recording of the deflection or some other means of measuring rise time and pulse shape. In addition, the comparison could be made on both small and large deflections, and finally some variables may be expected to influence all geophones in a similar manner.

The primary disadvantage of the relative calibration method is that when a calibration change is discovered, the test does not supply any data for correcting the change. In other words, the relative calibration does not indicate what has changed (i.e., frequency of the geophone, the damping ratio of the geophone, or some part of the electronics).

To improve field calibrations, special seismometers were designed for the KUAB FWD. The seismometers use a mass-spring system as a reference and the sensing element is a differential transformer (LVDT). This system permits direct measurement of deflections, and because the mass and LVDT core are

suspended with springs, there is no problem of reference. Calibration is accomplished with a micrometer provided with each seismometer. Thus each seismometer can be accurately calibrated in the field to measure deflections in the range of 0 to 5 mm (0 to 200 mils).

FWD Versus Static Plate Bearing Test

Many comparisons of FWD and static plate bearing test methods have been made (1,5,6,8,10,11), and the general conclusion is that there is no unique ratio between the deflections measured with each device. The static tests result in higher deflections on bituminous materials and on softer subgrades such as peat. Typical ratios of deflections for these situations range from about 1.5 to 3.

On stiffer materials, such as glacial till and gravels, the deflection ratios appear to approximate unity. On such materials there was no evidence that the scatter or difference between FWD and static plate bearing tests was any greater than the difference between various plate bearing test procedures.

FWD Versus Vibrators

Testing with the FWD and heavy vibrators often results in similar deflections. In one study (5) the overall ratio of the two deflections was unity. However, there was a range in values: the FWD indicated 10 to 20 percent higher modulus on thick asphalt pavements, but the reverse was true for unbound rock surfaces. During most of these tests only one frequency was used with the vibrator, thus interpretation of the results was difficult. It was noted that a 10- to 30-percent difference in modulus resulted by altering the frequency; most likely this was the result of the time dependence of the asphalt layer, but phenomena related to resonance also could have been involved.

Some testing agencies (17-19) believe that a single testing frequency with vibrators is insufficient to obtain reliable data. Also, resonance may be an important influence on results. FWDs appear to be somewhat less affected by this phenomena, however (17). Some data (6) have clearly revealed this independence, as noted in Figure 6. In this figure the ratio of deflections is shown for several pairs of testing devices. The testing devices and pavement structures shown in this figure are noted in Tables 1 and 2. There is a reasonably wide range of force and frequency represented by the vibrator and Dynaflect. There is also a difference in impact time between the two FWDs. Deflections shown in Figure 6 are mean values that have been normalized to 11,250 lb. Pavement structures A and B are on peat subgrade and have low resonant frequency.

Although there is a wide range of parameters among the various testing procedures, the difference between the vibrators is rather large. The validity of vibrators can certainly be questioned over a range of pavement types. Also noted in Figure 6 is the reasonable agreement between the two FWDs, in which the ratio of deflection values is approximately unity.

PRECISION OF TESTING DEVICES

Variation in most testing is to be expected when a pavement is tested at several locations on the surface. The variation (or coefficient of variation) is caused by true variation in the quantity measured as well as lack of precision in the test. A small coefficient of variation means either that the variation in bearing capacity (or deflection) is small, or that the test method is incapable of detecting the variation. If the bearing capacity variation within the pavement section is small, then the precision of the test method may be determined on the pavement.

From the data in the Nordic study (6), those sections in which the coefficient of variation was less than 10 percent for at least one of the test methods were selected for further analysis (see Table 5). These values are given under the "Measured" columns. In this table the coefficient of variation of the bearing capacity within one pavement section is less than the lowest of the coefficients by the different methods. It could be assumed that a portion of the variation of each pavement is caused by bearing capacity variation and the remainder is caused by lack of precision of the test methods. The difference in precision among methods can be estimated by assuming that the lowest coefficient of variation of each section is equal to the sum of the portions, as noted previously. The numbers under the "Adjusted

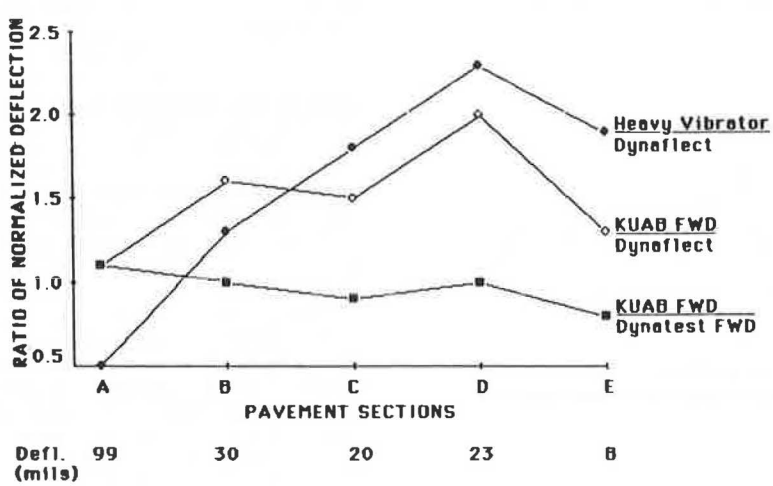

FIGURE 6 Ratio of normalized deflections measured by different testing devices. A ratio of unity means that they compare well, whereas deviations from unity indicate relatively less similarity. Note that the bottom line gives deflections at which comparisons are made for each pavement section.

TABLE 5 Coefficients of Variation of Different Bearing Capacity Tests on Homogeneous Road Sections (*16*)

	Coefficient of Variation (%) of Different Pavement Sections									
	C		C		D		D		E	
Test Device	Measured	Adjusted from Analysis	Measured	Adjusted from Analysis	Measured	Adjusted from Analysis	Measured	Adjusted from Analysis	Measured	Adjusted from Analysis
I	8	7	17	16	7	6	9	8	26	25
II	10	9	16	15	7	6	12	12	18	17
III	10	9	19	17	15	15	12	12	22	22
IV	13	12	19	17	6	5	12	12	16	15
V	6	4	10	8	4	3	5	4	6	4
VI	12	11	–	–	5	4	–	–	12	11
VII	10	9	9	6	4	3	12	12	16	15

Note: The numbers in the Adjusted from Analysis columns are estimates of the coefficient on a completely homogeneous section. The number of test points on each section and test method was 10.

from Analysis" columns in Table 5 are estimates of the coefficients for a completely homogeneous pavement section.

Another measure of quality of testing is to look at the width of 95 percent confidence intervals of the bearing capacity values at a test point. The data in Table 6 give these values for several of the test methods evaluated. The two-mass FWD revealed very good precision and very good repeatability--much better than the other devices evaluated.

TABLE 6 Relative Repeatability of Various Test Devices at a Given Test Point

Test Method	Width of 95 Percent Confidence Interval at Test Point (%)
FWD (two-mass system)	20
Dynaflect heavy vibrator and Danish traveling deflectograph	40
La Croix deflectograph and FWD (one-mass system)	50
Benkelman beam	60

CONCLUSIONS

The pavement studies conducted in the Nordic countries have provided an excellent opportunity for comparing a variety of testing devices. The devices have all been used by various agencies and have become a part of design and analysis procedures. Although most new methods have been traditionally compared with the Benkelman beam, there is no evidence that indicates that this method is any better than any other. Thus there is no particular reason to attempt correlations to gain acceptance of a method.

Pavement modeling that uses such approaches as elastic layer theory requires feedback from field tests that represent the actual behavior as closely as possible. Recent work in Europe and in the United States has demonstrated that load response using the FWD is very close to real-world conditions, and hence the FWD is being promoted as the best testing system.

The study reported herein has provided an opportunity to evaluate the relative merits of two FWD systems as well as compare them to other methods. Based on the study, the following conclusions appear warranted:

1. FWDs provide a force pulse shape that tends to simulate moving wheel loads better than the other devices compared in this study.
2. In a comparison of the two FWDs, the two-mass system appeared to have better precision and better repeatability qualities (Tables 5 and 6).
3. The Dynaflect compared well with other devices, both in precision and repeatability; however, it does a relatively poor job of simulating full-scale moving wheel loads.
4. Pavement vibrators compared favorably with other devices, except in pavements with soft subgrades, such as peat.

REFERENCES

1. B.O. Tholen. Barighetsmatning med fjadrad fallvikt vid VTI 1971-1973. VTI internrapport nr 173, Stockholm, Sweden, 1974 (Swedish).
2. P. Ullidtz. En studie af to dybdeasfaltbefaestelser. Technical University of Denmark, Copenhagen, 1973 (Danish).
3. H. Fritzsche. Neuzeitliche Tragfahigkeitsprufverfahren, forschungsbericht Versuchs - und Entwicklungsstelle des Strassenwesens. Abteilung, Berlin, undated (German).
4. A.O. Bohn et al. Danish Experiments with the French Falling Weight Deflectometer. Proc., 3rd International Conference on the Structural Design of Asphalt Pavements, Volume I, London, England, 1972 .
5. O. Andersson. Measurements of the Bearing Capacity of Roads--A Comparison Between Four Measuring Methods. Report 61A. National Swedish Road and Traffic Research Institute, Stockholm, Sweden, 1975.
6. Jamforande barighetsmatningar i Varmland 1976. Internordisk metodstudie. Statens Vagverk, Internrapport nr 17, Stockholm, Sweden, 1977.
7. N.N. Ivanof et al. New Methods for Fast Evaluation of the Bearing Capacity of Flexible Pavements. Avtomobilnyi Darogi, Vol. 24, No. 4, 1961 (Russian).
8. Schluns and Schlosser. Ein Beitrag zur Ermitlung dynamischer verformungskennwerte flexibler Strassen. Die Strasse, Juli 1976 (German).
9. I. Pliacek. Heat Conditions in Flexible Pavements and Their Influence on Pavement Strains. Proc., 14th World Congress, Permanent International Association of Road Congresses, Question II, Prague, Czechoslovakia, 1971.
10. H. Grunbaum. Dynamische tragfahigkeitsmessungen mit einem Fallgaret. Strasse und Verkehr, Vol. 56, No. 13, 1970 (German).
11. A.O. Bohn. Tragfahigkeitsmessungen mittels Fallgerats. Strasse und Autobahn, Vol. 1, 1968 (German).
12. Smirnow and Jordan. Besonderheiten der Formanderungen von Streassenkonstruktionen unter der Einwirkung von Bollenden Kraftfahrzeugbelastungen. Die Strasse, Mai 1973 (German).
13. Bleyenberg et al. Fully Monitored Motorway

Trials in the Netherlands Colloborate Linear Elastic Design Theory. Proc., 4th International Conference on the Structural Design of Asphalt Pavements, Volume I, Ann Arbor, Mich., 1977.
14. G. Baum. Ein Beitrag zur dynamischen beanspruchung der Tragschichtenunterlage in Beziehung zum Informations-inhalt des dynamischen Tragwertes E_{vd}. Strasse und Autobahn, Vol. 7, 1970 (German).
15. P. Leger and P. Autret. Utilisation des measures de deflexion pour le dimensionnement et al surveillance des chaussees. Bulletin de liason des Laboratoires des Ponts et Chaussees, No. 62, Nov.-Dec. 1972 (French).
16. B.O. Tholen. Provning av fallviktsdeflektometer pa en provvag med helbituminos overbyggnad pa moranlera och prov med olika stottider vid fallviktsbelastning. Vagbyggnad, KTH, Stockholm, Sweden, 1980 (Swedish, summary in English).
17. W. Heukelom. Analysis of Dynamic Deflections of Soils and Pavements. Geo-Technique, Vol. 11, 1961.
18. A.I.M. Claessen et al. Pavement Evaluation with the Falling Weight Deflectometer. Proc., Association of Asphalt Paving Technologists, Vol. 45, 1976.
19. G. Baum. Der dynamische Tragwert fur Strassenbefestigungen. Strasse und Autobahn, Vol. 3, 1969 (German).

Asphalt Concrete Overlay Design Procedure for Portland Cement Concrete Pavements

STEPHEN B. SEEDS, B. F. McCULLOUGH, and R. FRANK CARMICHAEL

ABSTRACT

The development and practical application of a reflection cracking analysis and overlay design procedure, which was developed for the Arkansas State Highway and Transportation Department, are described. The procedure is mechanistically based, but it is calibrated to the performance of experimental overlay sites in Arkansas and Texas. The procedure is incorporated into a computer program (ARKRC-2) for both existing pavement evaluation and overlay design. It considers asphalt concrete overlays and several techniques of reflection cracking control that may accompany overlay placement. These measures include bond breakers, stress-relieving interlayers, undersealing, and increased overlay thickness. The design procedure calls for a program of field measurements of vertical and horizontal slab movements to establish the potential for slab movement after overlay. Differential vertical slab movements are measured at joints (or cracks) by using a light-load deflection device (such as the Dynaflect). Measurements of horizontal slab movement are made over 2 or 3 daily temperature cycles at several existing joints (or cracks) by using a mechanical strain gauge. In the analysis procedure differential vertical slab movements are used to characterize load transfer and predict shear strains that will occur in the overlay under a simulated 18-kip axle load. Horizontal slab movements, on the other hand, are used to predict the maximum daily tensile strains that will be generated in the overlay during different seasons of the year. For both strain criteria, a fatigue-type approach is used to predict how long the overlay will last. A probabilistic distribution is then applied to the horizontal tensile (environmental) strain criteria, such that the overlay design can be based on a minimum tolerable level of reflection cracking over the design life. For joints (or cracked areas) that have problems with poor load transfer and would thus generate excessive overlay shear strains, it is recommended that some type of slab repair or undersealing operation be performed. (The findings of the original study for Arkansas indicated that other control measures such as increased overlay thickness and stress-relieving interlayers are not cost-effective compared with remedying the cause of the poor load transfer problem.) Besides providing a general description of the analytical models and the ARKRC-2 program (which can be adapted to almost any environment in the United States), examples of the overlay design nomographs developed for the specific construction materials and environmental regions found in Arkansas are also presented.

In this paper a design procedure for asphalt concrete overlays of existing rigid pavements is described. The procedure was developed for Arkansas (1) by extending and calibrating the original FHWA-Austin Research Engineers (ARE) procedure (2) based on field measurements and performance observations in Arkansas (by the University of Arkansas and the Arkansas State Highway and Transportation Department) and in Texas (by the Center for Transportation Research at the University of Texas). The primary emphasis of the design procedure is the control of overlay reflection cracking through the examination of the two principle failure mechanisms: temperature-related horizontal slab movements and wheel-load-related differential slab movements at joints.

The primary component of the procedure is a computer program (ARKRC-2) that uses a mechanistic analysis approach to predict the performance of asphalt concrete overlay alternatives that incorporate various crack deterrent measures, including bond breakers, cushion courses or other intermediate layers, undersealing, and increased overlay thickness. A secondary component of the procedure is one in which the computerized portion of the process is replaced by design charts and nomographs. These design charts were developed based on a statistical analysis of the ARKRC-2 program in which (a) a factorial experiment involving the major independent variables was designed, (b) the treatment combinations were generated by using the ARKRC-2 program, and (c) the regression analyses were performed to develop the coefficients for the design equations. These equations and nomographs are capable of accurately considering several of the factors and conditions associated with the design of asphalt concrete overlays in Arkansas. They are also compatible with the AASHTO Pavement Design Guide format, but do have their limitations and constraints (beyond those of the program) that limit their application in other environments.

This paper is organized such that the analysis and design for the two failure mechanisms are considered separately. Within each part a description is provided on field data collection, general input data, the method of analysis, and use of the design charts. Because of the detail that would be required, application of the actual ARKRC-2 program is not described.

OVERLAY DESIGN CONSIDERING TEMPERATURE EFFECTS

In this design procedure the adequacy of a given overlay strategy to withstand reflection cracking is established based on two types of failure criteria: overlay tensile strain and overlay shear strain. Shear strains are basically the result of the potential for differential vertical movements between adjacent slabs underlying the overlay. Tensile strains, on the other hand, are the result of thermal stresses and temperature-related horizontal movements of the underlying slab. Because these two types of distress mechanisms are both associated with the existing concrete pavement, it is possible to estimate the amount of influence they will have on the development of reflection cracking by making some field measurements of concrete movement before placement of the overlay. In this section the design for considering the effects of temperature-related horizontal slab movements on tensile strains and reflection cracking in the overlay is described.

Field Measurements of Slab Movement

In order to predict the effects of cyclic temperature changes, it is necessary to collect measurements of slab movement as a function of air temperature. The recommended procedure for doing this is to install metal reference points on both sides of several joints (or cracks) in the existing portland cement concrete (PCC) pavement and then measure the spacing between these points by using a Berry strain gauge over a range of air temperatures. To avoid some of the other external effects, it is recommended that these measurements be obtained at the rate of five different temperatures per day for a minimum of 2 consecutive days.

The recommended installation procedure to obtain these measurements is to first drill holes on both sides of a joint (crack) and securely glue bolts into these holes to act as reference points. The bolts should have small drilled holes on their heads that function as seats for the Berry strain gauge. Figure 1 shows the placement of these brass bolts. The bolts should be placed out of the wheelpaths (preferably 12 to 18 in. from the pavement edge) to minimize wheel load disturbance.

Although it is important to obtain a good sample of horizontal movement data from several joints (or cracks) in the existing PCC pavement, it is not an easy or safe process because of the need for traffic control. Consequently, it is up to the user or highway engineer to determine the number of joints (or cracks) that should be measured. It should be recognized, however, that the procedure calls for the joint (crack) movement to occur over a drop in air temperature, and the more locations that are measured, the more likely it is that joints (or cracks) with a high reflection cracking potential will be considered. For continuously reinforced concrete pavements (CRCPs), the measurements must be made in areas that exhibit the average crack spacing for the overlay design section.

Figure 2 shows a sample form for collecting the horizontal movement data from a single joint (crack). The grid at the bottom of the figure is provided to allow the user to plot the data after recording it. These plots will be used later as an aid in selecting design movement data.

General Input Data

In addition to the field data needed to characterize temperature-related horizontal slab movements, there are a number of other inputs that would be considered in a complete or comprehensive ARKRC-2 evaluation. These other inputs (which are too numerous to describe in detail) are summarized as follows:

1. Existing pavement characteristics, which include pavement type, joint or average crack spacing, slab thickness, concrete creep modulus (i.e., elastic modulus under creep loading conditions), thermal coefficient, and unit weight;
2. Reinforcement characteristics, which include longitudinal bar diameter and spacing, elastic modulus, thermal coefficient, and bonding stress;
3. Overlay characteristics, which include overlay thickness, creep modulus, thermal coefficient, unit weight, and bonding stress;
4. Characteristics of control methods considered, which include bond-breaker width, intermediate (cushion course) layer thickness, creep modulus, thermal coefficient, and unit weight; and
5. Environment, which refers to the frequency distribution of critical maximum daily temperature drops during the year.

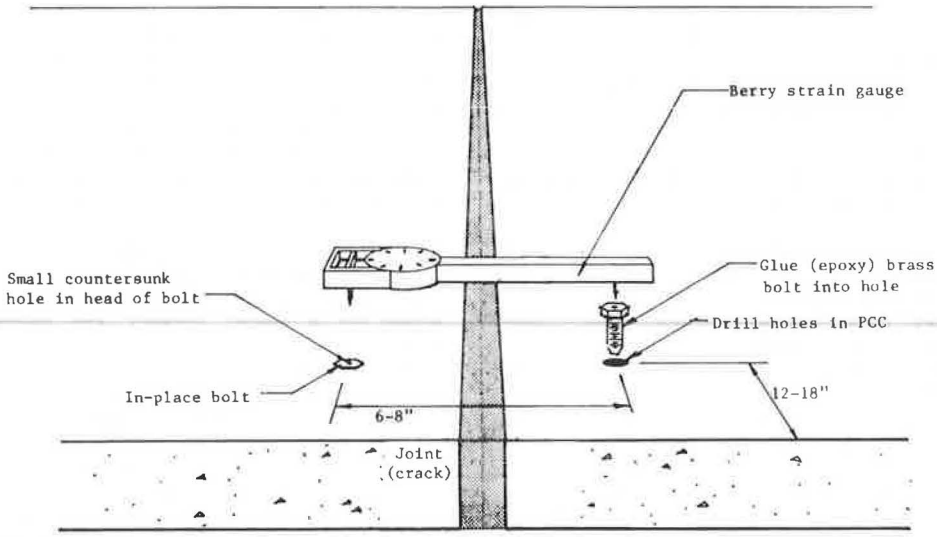

FIGURE 1 Placement of brass bolts for measurement of horizontal slab movement.

REFLECTION CRACKING ANALYSIS DATA
HORIZONTAL SLAB MOVEMENTS

Project: _____
Location: _____
Joint/crack No. _____ Recorder _____
Slab Lengths: Upstream side _____ Downstream side _____

Measurement Number	Date	Time of Day	Pavement Temperature °F	Joint/Crack Width (inches)
1				
2				
3				
4				
5				
6				
7				
8				
9				
10				
11				
12				
13				
14				
15				

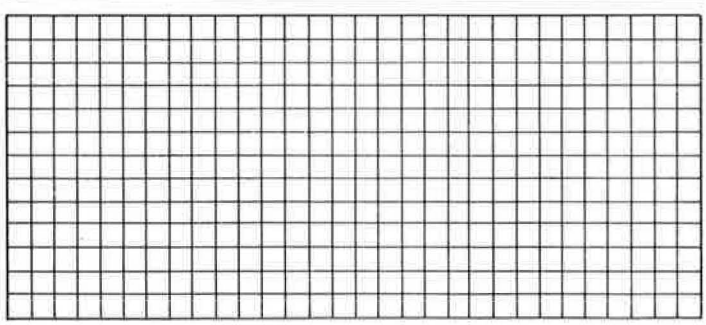

Pavement Temperature, °F

FIGURE 2 Sample form for collecting horizontal movement data.

METHOD OF ANALYSIS

The basic concept behind the method of analysis for temperature-related slab movements is to apply the mechanics of force equilibrium in a pavement structure so that critical tensile strains in the overlay (above a joint or crack) can be computed. These strains are determined for the different critical temperature conditions experienced by the pavement during a yearly cycle. A fatigue model is used to assess damage during each critical period. Miner's linear damage hypothesis is then used to accumulate

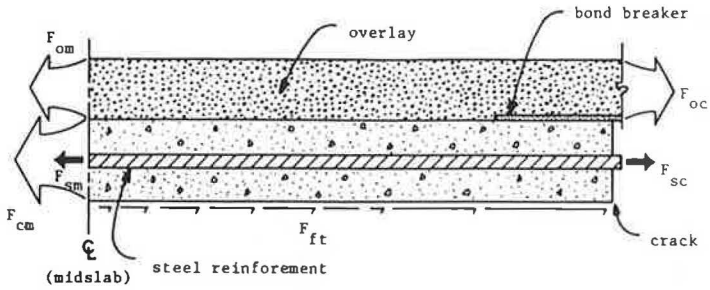

F_{om} = Force in overlay at midslab.

F_{sm} = Force in steel at midslab.

F_{cm} = Force in concrete at midslab.

F_{ft} = Slab-base friction.

F_{oc} = Force in overlay at crack (joint).

F_{sc} = Force in steel at crack.

FIGURE 3 Illustration of the force balancing method used to achieve equilibrium in the pavement structure after overlay for the design temperature drop.

the damage during these critical periods and predict the number of years to a certain level of reflective cracking.

More specifically, the field measurements of slab movement are first used to characterize the slab-based friction relationship. This relationship is then adjusted for conditions after overlay, and an iterative process is applied until equilibrium between all forces that act in the pavement structure (at a given design temperature) is achieved. A free body diagram of this is shown in Figure 3. The force in the overlay is ultimately translated into an overlay tensile strain by using its thickness and creep modulus. The bond breaker shown has the effect of increasing the length over which the overlay can absorb slab movements and thus reduces the maximum tensile strain. A cushion course, which is not shown in the figure, can also be considered and has the effect of absorbing a significant amount of strain (due to slab movement) before it reaches the overlay.

Because it is recognized that the tensile strains that induce reflection cracking come about as the result of both direct thermal stresses and the temperature-drop-related movements of the underlying slab, and because the temperature variations are cyclic in nature, the reflection cracking that develops in the overlay must be attributed to fatigue or the accumulation of damage brought about by cyclic loading. Therefore, it was considered essential that the fatigue damage concept be incorporated into the ARKRC-2 analysis and design procedure. The following is the fatigue equation that was developed on the basis of a calibration of observed overlay performance in Arkansas and Texas:

$$N_T = a_1(\varepsilon_T)^{a_2} \quad (1)$$

where

N_T = average number of fixed strain cycles needed to develop a reflection crack at a given location,

ε_T = asphalt concrete overlay tensile strain for a given critical temperature drop,

$a_2 = -3.70$,

$a_1 = 8.072 \times 10^{-4}\ (EOV)^{-1.118}$, and

EOV = asphalt concrete overlay creep modulus (psi).

The consideration of fatigue for a constant cyclic loading condition is basically simple. A small complication is introduced, however, when the effects of a variable cyclic load (such as that resulting from varying low temperature drops) are considered. This consideration of variable load effects requires the assumption that Miner's linear damage hypothesis is applicable to the analysis of fatigue in flexible overlays. This is not a bad assumption and has been used in several other problems that deal with the analysis and design of highway pavements.

Information on the distribution of daily temperature drops for Arkansas was obtained from the National Climatic Center (NCC). This information was collected from a 7-year period (1974 through 1980) for both the maximum daily temperature drop and the difference between 50° F and the minimum daily temperature. The latter data were obtained because a study conducted at the Texas Transportation Institute (3) indicated that the primary temperature-related damage suffered by asphalt concrete occurs when the temperature is less than 50° F. The results of the fatigue equation development verified this observation for conditions in Arkansas; therefore 50° F was selected as a reference temperature for calculating the overlay tensile strains. Inspection of the Arkansas temperature data from NCC indicates that the differences between 50° F and the daily temperature are divided into 10-degree frequency ranges (classes) that identify the average number of days during the year on which the temperature drops a certain magnitude less than 50° F. The total number of days from each range (class) for a given region is never equal to the total number of days in a year (365) because days on which the temperature stays higher than 50° F are not counted. The seven temperature drops and corresponding minimum temperature frequency ranges (classes) considered are given in Table 1.

The average temperature drops (less than 50° F) are used by the program to estimate the corresponding overlay tensile strains. After these tensile

TABLE 1 Temperature Drops and Corresponding Minimum Temperature Frequency Ranges

No.	Range of Temperature Drop (°F)	Range of Minimum Temperature (°F)	Avg Temperature Drop Below 50° F
1	1 to 10	49 to 40	5
2	11 to 20	39 to 30	15
3	21 to 30	29 to 20	25
4	31 to 40	19 to 10	35
5	41 to 50	9 to 0	45
6	51 to 60	−1 to −10	55
7	61 to 70	−11 to −20	65

strains $(\varepsilon_T)_i$ are determined for each average temperature drop, the fatigue equation is used to estimate the allowable number of cycles $[(N_T)_i]$ of a given strain the overlay can carry before it cracks. Next, the incremental damage (d_i) accrued each year by each given strain level is determined by using the following equation:

$$d_i = n_i/(N_T)_i \quad (2)$$

where n_i is the average number of days during the year on which the overlay is subjected to a given strain level $(\varepsilon_T)_i$. Because each strain level corresponds to a particular average temperature drop, n_i is determined from the temperature distribution data.

Next, the yearly damage due to each individual strain level is accumulated according to Miner's hypothesis:

$$D = \sum_{i=1}^{7} d_i = \sum_{i=1}^{7} n_i/(N_T)_i \quad (3)$$

where D represents the total damage experienced by the overlay during the course of 1 year.

Because by definition "failure" occurs when D is equal to 1.0, the number of years (Y_T) to failure of the overlay can finally be determined by using the following simple equation:

$$Y_T = 1.0/D \quad (4)$$

It is important to note that because the fatigue equation represents an average number of cycles to the development of a reflective crack at a given location, Y_T represents the number of years to a reflection cracking level of 50 percent. In the next section on use of the design charts, an explanation is given on how Y_T can be adjusted for a different reflection cracking level.

Use of Design Charts (Tensile Strain Criteria)

As mentioned previously, the asphalt concrete overlay design charts for the consideration of tensile strain criteria were developed by using a designed statistical experimental analysis of the ARKRC-2 computer program. Because it was necessary to limit the number of factors considered in the experiment, the resulting design charts do have certain constraints and limitations that pertain to material properties, construction methods, and climate (environment). Figure 4 shows the design chart recommended for overlays on existing jointed concrete pavements in one of Arkansas' five climatic regions. Similar nomographs were developed for other climatic regions and for existing CRCPs as well. (Figure 5 identifies Arkansas' five climatic regions). A discussion of the selection of inputs for the nomographs follows:

1. For each joint (or crack) measured and recorded in the form shown in Figure 2, the user should determine the slope ($\Delta/\Delta T$) of the best-fit straight line through the data. On the basis of the inspection of the slope values for each line, the user should select a data set or series of data sets for use in analyzing the potential for reflection cracking in the section characterized by the data set(s). This means that, for some overlay projects, it may be necessary to identify and design different overlay sections. In selecting these sections, the user should recognize that those that have the highest slope values will have the greatest potential for reflection cracking (at least from the standpoint of tensile strain). The user should note too that the slope value is the most important characteristic of the data and that it is not necessary to separate sections that have approximately the same slope but different intercepts. Also, because of the inverse relationship between joint (crack) width and temperature, $\Delta C/\Delta T$ should always have a negative value.
2. SPACE defines the spacing between the joints of a jointed pavement or the average spacing between the cracks of a continuous pavement. If the existing pavement is CRCP, then the average crack spacing can be determined by counting the number of cracks in a section of the highway of known length and dividing the section length by the number of cracks. It is important to note that this information is used in conjunction with the horizontal movement data that should have been recorded from areas that exhibited the average joint or crack spacing.
3. THOV defines the thickness (in inches) of the asphalt concrete overlay and represents one of the factors that can be varied in the selection of an adequate design for minimizing reflection cracking. THOV consists of the combined thickness of all binder and surface courses that are considered to increase the load-carrying capacity of the pavement structure. This variable should not include the thickness of any intermediate or strain-absorbing layers (such as an open-graded base course).
4. TH2 is the variable that defines the thickness (in inches) of the intermediate layer that will be placed before the overlay (TH2 equals zero if there is no intermediate layer). An intermediate layer represents a material of certain thickness placed before the overlay to help minimize reflection cracking brought about by underlying slab movements. The layer is different from a bond breaker layer in that it is designed to internally absorb some of the underlying slab movements before they reach the overlay layers. It is not effective in reducing reflection cracking brought about by poor load transfer across joints or cracks.

In this design procedure TH2 can have a large effect on the critical tensile strain developed in the asphalt concrete overlay, particularly if the creep modulus of the layer is low. The strain-absorbing open-graded course used in Arkansas is such a material, but it does have its thickness limits. It can not be less than 3 in. because some of the aggregate particles are as large as 2.5 in. Also, because of possible rutting and compaction problems, the open-graded course thickness should not be greater than 5 or 6 in. Consequently, if the user intends to use some other type of intermediate layer, care should be taken to ensure that its possible thickness limits are considered.

After all the necessary data have been obtained, the following simple design chart procedure may be used to arrive at a suitable asphalt concrete overlay design alternative that considers the temperature effects on critical tensile strains. (It will then be necessary to check this design alternatively

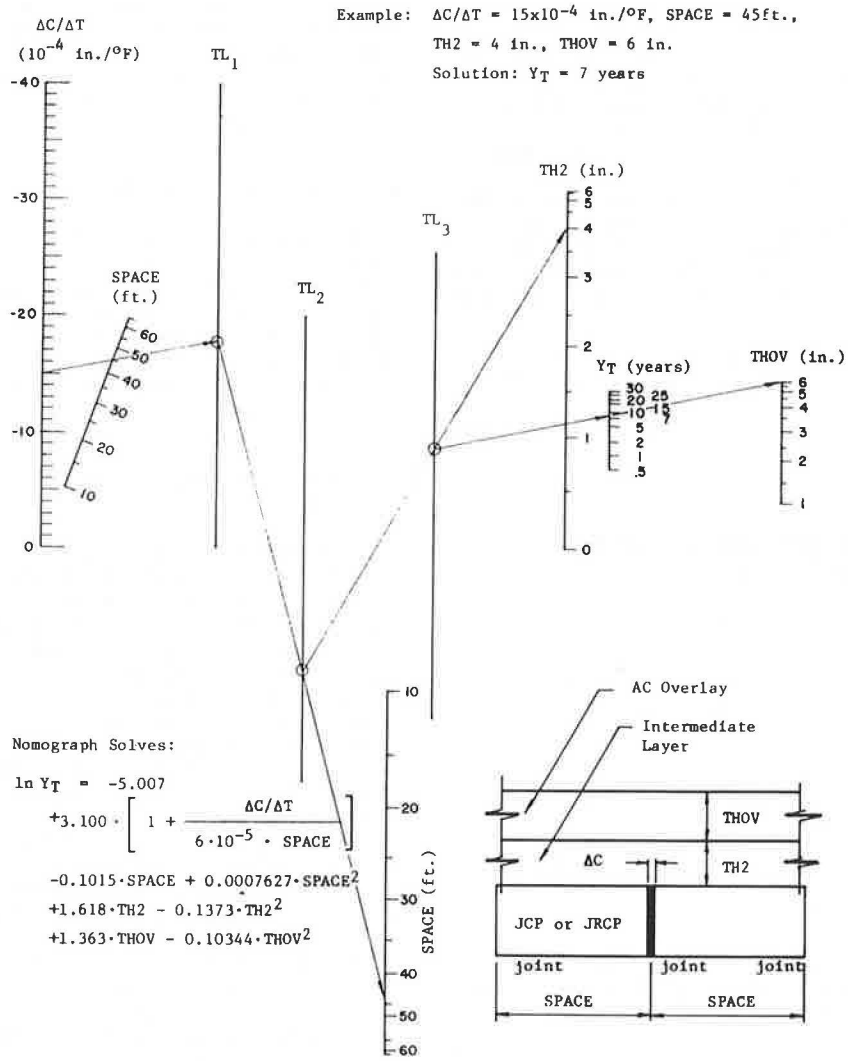

FIGURE 4 Asphalt concrete overlay design nomograph for jointed pavements in Arkansas Region B. (Caution: Be aware of restrictions on use of this nomograph.)

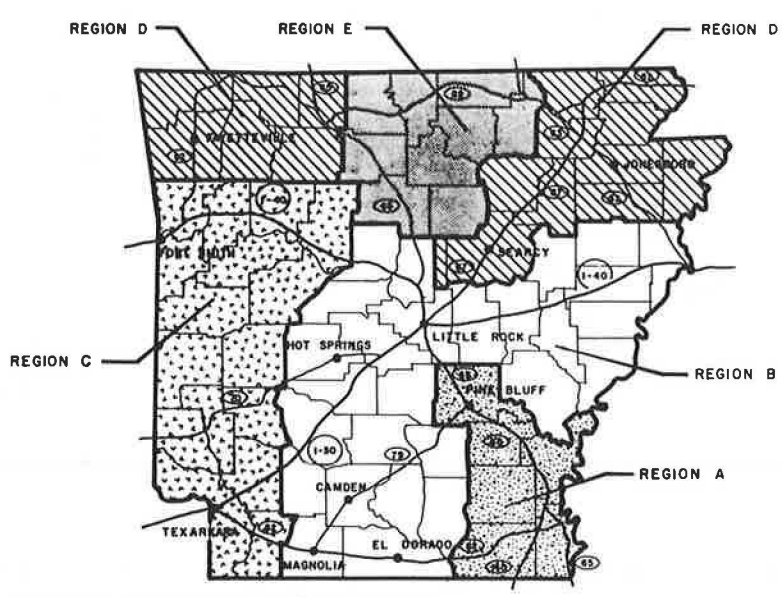

FIGURE 5 Five composite Arkansas regions.

by using the shear strain criteria discussed in the next section).

First, the appropriate nomograph is selected based on the pavement type and region considered. Second, different overlay and intermediate layer thickness combinations (THOV and TH2) are tried until an optimum design alternative for tensile strain criteria is reached.

Finally, if the user is interested in either using a different failure criteria (other than 50 percent reflection cracking) or estimating when different levels of reflection cracking will be reached (based on tensile strain criteria), the following procedure may be applied:

1. Select the level of reflection cracking considered as a limit. This will range anywhere from 1 to 99 percent.
2. Use the data in Table 2 to determine the z-value that corresponds to the selected reflection cracking level.

TABLE 2 z-Values Corresponding to Different Levels of Reflection Cracking

Reflection Cracking (%)	z-Value	Reflection Cracking	z-Value
1	-2.330	55	0.126
5	-1.645	60	0.253
10	-1.282	65	0.385
15	-1.037	70	0.524
20	-0.841	75	0.674
25	-0.674	80	0.841
30	-0.524	85	1.037
35	-0.385	90	1.282
40	-0.253	95	1.645
45	-0.126	99	2.330
50	0.000		

3. Solve for the number of years (Y) that corresponds to the desired level of reflection cracking by using the following formula:

$$Y = (1.585)^{z} \times Y_{50} \quad (5)$$

where Y_{50} is the number of years before 50 percent reflection cracking is reached (as determined from nomographs), and z is the standard normal variate (from Table 2). It should be noted that the accuracy of this prediction is decreased for very high or very low levels of reflection cracking.

OVERLAY DESIGN CONSIDERING WHEEL LOAD EFFECTS

This part of the asphalt concrete overlay design procedure is used to check the adequacy of the design (developed in the first part) for the effects of wheel load on overlay shear strain. As in the first part, the description of this model is provided in four segments: field data collection, general input data, method of analysis, and use of the design charts.

Field Measurements of Slab Deflection and Load Transfer

Because overlay shear stresses and strains develop primarily as a result of differential vertical movements at joints (or cracks) between adjacent slabs, it is important that some field measurements be made before the overlay is placed to characterize this distress mechanism. The best way to do this is as follows: for a number of joints (or cracks) within a given design section, load one side of the joint and measure the deflection on both the loaded and unloaded sides. A light load is desirable so that the differential deflections measured will approximate those after placing the overlay. The Dynaflect is well suited for this measurement and was recommended for use in Arkansas.

Figure 6 shows the recommended position of the Dynaflect and its geophones within the lane and with respect to the joint or crack. Note that the deflection measurements are taken in the outside wheelpath of the outside lane. Note also that the load wheels and geophone 1 are located on the upstream side of the joint, whereas geophone 2 must be detached from the mounting bar and placed on the downstream side

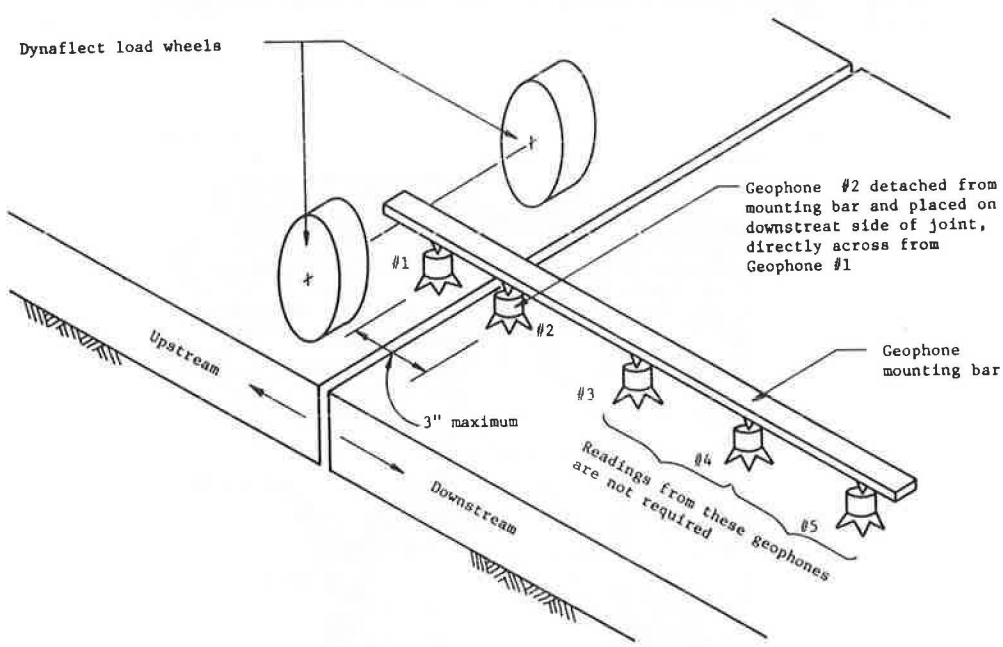

FIGURE 6 Required positioning of Dynaflect load wheels and geophones for load transfer deflection measurements.

of the joint, directly across from geophone 1. Readings from the other geophones may be recorded, but are not required. Henceforth, the deflections from geophones 1 and 2 (when in this configuration) will be designated as w_ℓ (loaded side) and w_u (unloaded side), respectively.

It is recommended that the deflections be obtained during a period representative of the base support conditions after overlay. In other words, measurements should not be made during spring thaw or after a significant rainfall because these saturated conditions are not representative of those after overlay. Late spring, summer, and autumn are probably the best times to obtain representative deflection measurements.

In order to achieve good reliability of the results, it is also important to obtain a good sample of deflection measurements. The number of measurements recommended is dependent on the spacing between the joints (or cracks) and the possibility of the use of some type of undersealant to improve poor load transfer areas.

For the case of jointed pavements [jointed concrete pavement (JCP) and jointed reinforced concrete pavement (JRCP)], it is desirable to obtain measurements at every construction joint. This is especially true if an undersealant is being considered, because certain criteria will be provided later for the selection of which joints to underseal. If an undersealant is not considered and the joint spacing is less than 25 ft, it is probably adequate to obtain measurements at every other joint, so long as there are not any apparent problems with joint pumping.

For the case of CRCP, it is recommended that deflection measurements be obtained for a series of three to five cracks at intervals of approximately 200 ft. Intervals of 100 ft are recommended if an undersealant is to be considered in areas where pumping is observed.

After the data have been recorded, processing should begin by computing the deflection factor (F_w) for each joint (or crack) by using the following equation:

$$F_w = (w_\ell - w_u)/(w_\ell + w_u) \tag{6}$$

where w_ℓ is the deflection on the loaded side of the joint, and w_u is the deflection on the unloaded side. This data reduction is probably best accomplished with the aid of a computer. After the data are reduced, it is then useful to prepare a longitudinal profile plot of F_w versus distance along the roadway for later analysis.

General Input Data

Besides the field measurements of slab deflection, there are some inputs required for the overlay shear strain analysis:

1. Overlay characteristics, which include dynamic modulus and the combined thickness of any binder and surface (wearing) courses;
2. Intermediate layer characteristics, which include the dynamic modulus and thickness of any type of cushion course or stress-relieving layer placed before the overlay; and
3. Traffic, which refers to the number of 18-kip equivalent single-axle loads that can be expected over the design period.

Method of Analysis

The design for shear strain in an asphalt concrete overlay is based on a theoretical analysis of the Dynaflect deflection measurements made on the slab before placement of the overlay (field measurement program). The difference in deflection across a joint or crack is indicative of the load transfer and therefore the shear forces that will be carried by the overlay. Figure 7 shows the Dynaflect load and geophone configuration used to give the loaded and unloaded deflection values (w_ℓ and w_u). Figure 8 shows how these deflection values make it possible to estimate the amount of shear force (V_O) that will be carried by the overlay layers. The deflections w_ℓ and w_u on either side of a joint due to a load P (Figure 8a) can be simulated by two forces (P_1 and P_2) acting separately (Figure 8b). From slab (or beam) theory, the magnitude of a slab's deflection is directly proportional to the applied load; therefore

$$P_1/P_2 = w_\ell/w_u \tag{7}$$

Because the total force that causes the deflection on both sides (P) is equal to $P_1 + P_2$, and be-

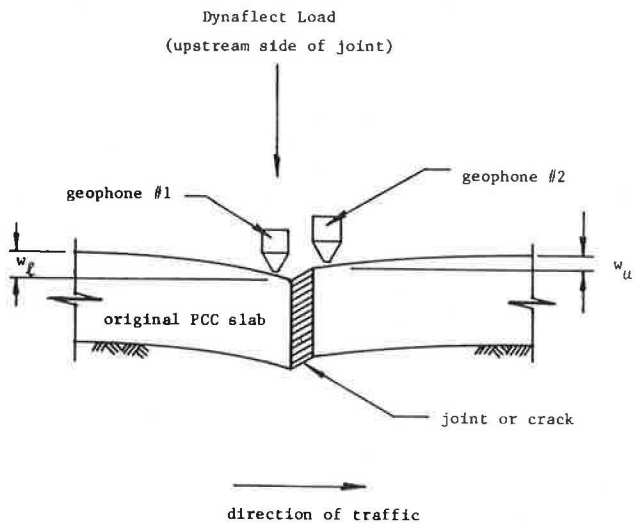

FIGURE 7 Illustration of Dynaflect deflection load and geophone configuration for determining required deflection values.

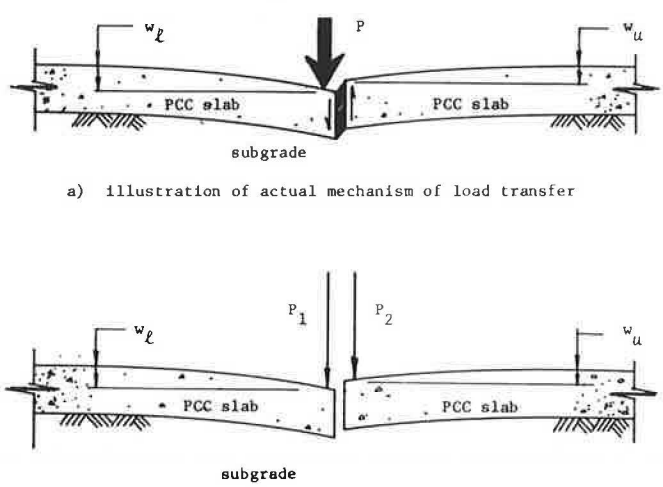

a) illustration of actual mechanism of load transfer

b) model showing effective forces P_1 and P_2, which result in identical deflections

FIGURE 8 Load transfer diagrams.

cause the shear force after overlay (V_o) is equal to $P_1 - P_2$, the equation can be rearranged to solve for V_o:

$$V_o = P \cdot (w_\ell - w_u)/(w_\ell + w_u) \quad (8)$$

The next step in the determination of the maximum shear strain is to estimate the shear moduli of the overlay layer(s). This is accomplished by using the following equation:

$$G = E/2(1 + \nu) \quad (9)$$

where

- G = shear modulus (psi), with G_{OV} for the overlay and G_2 for the intermediate layer;
- E = design dynamic modulus of the layer during critical temperature conditions (psi); and
- ν = Poisson's ratio for the layer (0.30 recommended for asphalt cement hot-mix overlay, 0.35 for open-graded course intermediate layer).

These shear moduli are then used to determine an effective overlay thickness, D_e (in inches):

$$D_e = THOV + (G_2/G_{OV})\ TH2 \quad (10)$$

where THOV and TH2 are the thicknesses (in.) of overlay and intermediate layers, respectively.

Next, the maximum shear stress in the overlay layers is determined. If a section (A-A) is taken out of the overlay in the region where the shear force acts, then the distribution of shear stress along that section will be as shown in Figure 9. The following general equation defines the shear stress at any location along the face:

$$\tau = VQ/Ib \quad (11)$$

where

- τ = shear stress (psi),
- V = shear force (lb),
- Q = first moment of the area above (or below, depending on the position of the neutral axis) the location where strain is desired (in.^{3}),
- I = moment of inertia (in.^{4}), and
- b = width of section (in.).

Note that for equilibrium of a small element taken at the top (or bottom) of the section, the shear stress must be zero.

A simplification of this equation can be used to estimate the maximum shear stress at the neutral axis of the cross section:

$$\tau_{max} = 3V/2bh \quad (12)$$

where

- V = V_o, i.e., overlay shear force (lb),
- b = width of the section (in.); for purposes of the overlay shear calculations, this value should be the width of the region of shear, which is approximately 25 in. for a dual-tired axle; and
- h = height of cross section (in.); for the effective overlay thickness (D_e) for overlay shear calculations.

Next, the maximum shear strain in the overlay (γ_{OV}) is determined by using the following equation:

$$\gamma_{OV} = \tau_{OV}/G_{OV} \quad (13)$$

where $\tau_{OV} = \tau_{max}$, the maximum shear stress in the overlay (psi), and G_{OV} is the overlay shear modulus (psi).

Finally, the overlay life for a given shear strain is determined by using a fatigue-type relationship based on asphalt shear strain. Unfortunately, the available literature did not provide a relationship that could be used effectively in the model. Therefore, it was necessary to adapt the overlay tensile strain equation (developed in this study) to consider the effects of shear strain. This was accomplished by using known relationships between tensile and shear stress in the indirect tensile test and between normal and shear moduli [note

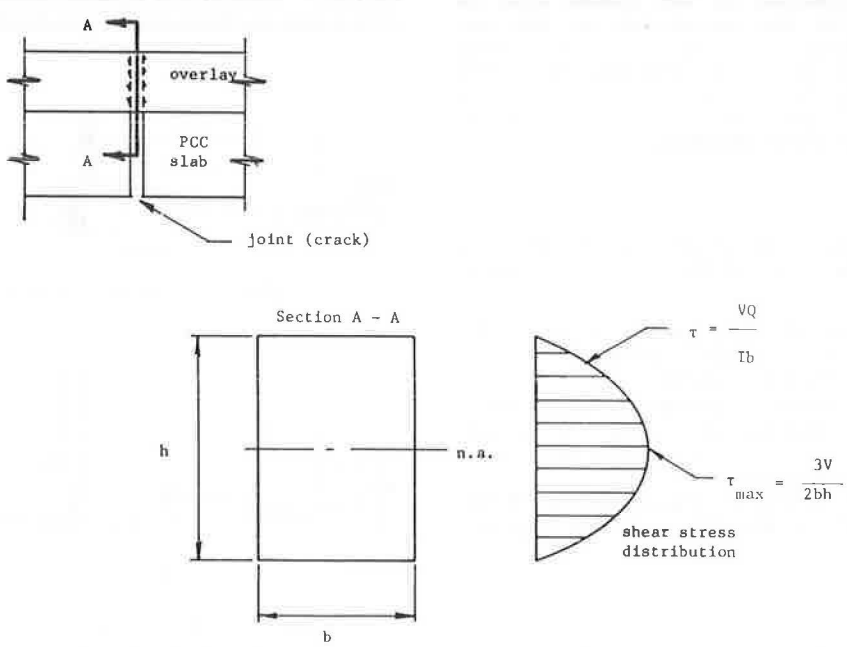

FIGURE 9 Distribution of shear stresses in the overlay.

that Equation 14 is from Anagnos and Kennedy (4) and Equation 15 is from Timoshenko and Gere (5)]:

$$\tau = 2 \cdot \sigma_T = 2 \cdot EDV \cdot \varepsilon_T \quad (14)$$

$$G_{OV} = EDV/[2 \cdot (1 + \nu_{OV})] \quad (15)$$

where ν_{OV} is Poisson's ratio for the overlay. Thus, overlay tensile strain can be converted to shear strain by using the following equation:

$$\varepsilon_T = \gamma_{OV}/[4(1 + \nu_{OV})] \quad (16)$$

Then, when this is substituted into the tensile strain fatigue equation and rearranged to solve for allowable overlay shear strain, the result is the following equation (which assumes a value of 0.30 for Poisson's ratio of the overlay material):

$$\gamma_{OV} = 0.7587 \cdot (EDV)^{-0.3002} \cdot (N_T)^{-0.2703} \quad (17)$$

where N_T = DTN18, the design 18-kip equivalent single-axle load (ESAL) applications that will be carried by the overlay before the development of reflection cracking; and EDV is the dynamic modulus of the overlay material (psi).

This section has thus far described the mechanics of the shear strain model in predicting the allowable 18-kip ESAL traffic. The design model incorporated into the ARKRC-2 program is based on the same concepts, but is formulated in reverse order. The user specifies a design 18-kip ESAL traffic and a possible overlay strategy and the program back-calculates a critical deflection factor (F_w). This factor is then used to single out the joints (or cracks) that are particularly damaging and may require structural maintenance to reduce the potential for generating reflection cracking after overlay.

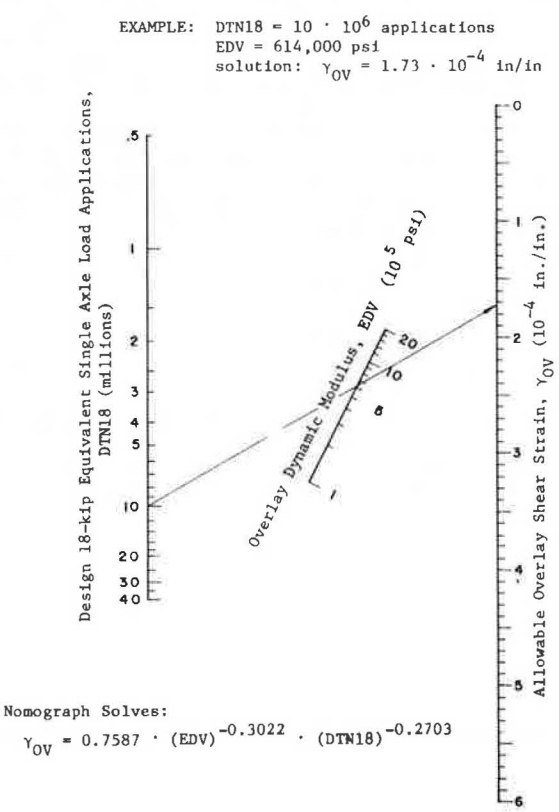

FIGURE 10 Nomograph for estimating allowable overlay shear strain.

Thus if the F_w value for a given joint (crack) calculated by using Equation 6 [$F_w = (w_\ell - w_\mu)/(w_\ell + w_\mu)$] is greater than the critical F_w, then it is recommended that that joint or crack be undersealed before placing the overlay.

Use of Design Charts (Shear Strain Criteria)

Because of the simple form of the overlay design equation for shear strain criteria, it was possible to develop a series of nomographs in which all of the independent variables (factors) are considered. In this final section of the second part of the design procedure a description of how the design charts should be applied is given.

First, with the overlay dynamic modulus (EDV) and the design traffic (DTN18), use Figure 10 to estimate the allowable overlay shear strain. Then with the trial design (from tensile strain criteria), use the allowable overlay shear strain to determine the allowable deflection factor from Figure 11. Finally, draw a horizontal line on the longitudinal plot of the deflection factor that indicates the level of the allowable deflection factor (as shown in Figure 12). If inspection indicates that a point or series of points exceeds the allowable deflection factor, then it will be necessary to either underseal those joints or use an increased overlay thickness. The design for the latter may be accomplished by reusing

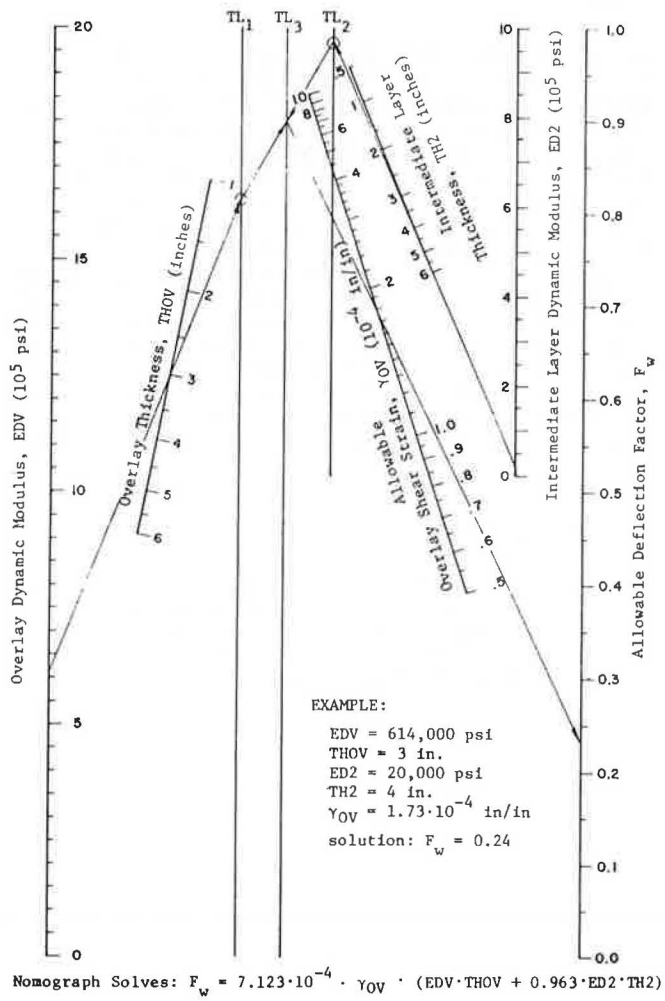

FIGURE 11 Nomograph for determining allowable deflection factor.

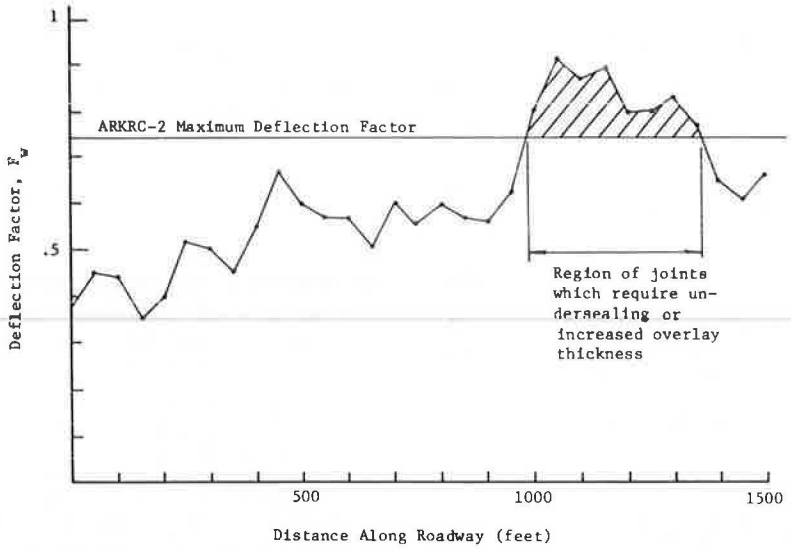

FIGURE 12 Graph of field deflection factors for 50-ft JCP illustrating application of ARKRC-2 maximum deflection factor in detecting joints that will cause premature reflection cracking in the overlay design considered.

Figure 11 with various increased levels of overlay thickness (THOV).

SUMMARY

A new procedure that has been developed for the design of asphalt concrete overlays on existing PCC pavements is described. The procedure uses a mechanistic analysis to evaluate field measurements of slab movement and predict overlay performance in terms of future reflection cracking. The method has been incorporated into both computerized and design chart (nomograph) procedures. The computer-based procedure considers several methods of controlling reflection cracking. Although the inherent fatigue equation is based on environmental conditions in Arkansas and Texas, the procedure is suitable for calibration and adaptation in almost any environment. The design chart procedure described is based solely on environmental conditions and construction practices common to Arkansas, but it is possible to develop similar nomographs for conditions in other states.

ACKNOWLEDGMENTS

The authors wish to recognize Robert Welch of the University of Arkansas, and Earl Kirkpatrick, Mike Limbird, and Brooks Nichols of the Arkansas State Highway and Transportation Department (AHTD) for their advice and technical support in collecting the field data, developing the models, and implementing the design procedure for application by AHTD. The authors also wish to acknowledge the work of Harold Von Quintus and Peter Jordahl, who were primarily responsible for developing the original reflection cracking analysis program for FHWA.

REFERENCES

1. S.B. Seeds, B.F. McCullough, and R.F. Carmichael; ARE, Inc. Arkansas Reflection Cracking Analysis and Overlay Design Procedure. Report UA-3/1. University of Arkansas and Arkansas State Highway and Transportation Department (Contract TRC-61), Little Rock, Feb. 1982.
2. Austin Research Engineers, Inc. Overlay Design and Reflection Cracking Analysis for Rigid Pavement--Volume 1: Development of New Design Criteria. Report FHWA-RD-77-66. FHWA, U.S. Department of Transportation, Aug. 1977.
3. H.-S. Chang, R.L. Lytton, and S.H. Carpenter. Prediction of Thermal Reflection Cracking in West Texas. Research Report 18-3. Texas Transportation Institute, Texas A&M University, College Station, March 1976.
4. J.N. Anagnos and T.W. Kennedy. Practical Method of Conducting the Indirect Tensile Test. Research Report 98-10. Center for Highway Research, University of Texas, Austin, Aug. 1972.
5. S.P. Timoshenko and J.M. Gere. Mechanics of Materials. Van Nostrand, New York, 1972.

Project-Level Structural Evaluation of Pavements Based on Dynamic Deflections

WAHEED UDDIN, A. H. MEYER, W. R. HUDSON, and K. H. STOKOE II

ABSTRACT

The framework of a structural evaluation system for pavements, which is based on the mechanistic evaluation of dynamic deflection data, is described. The computer program RPEDD1 has been developed for the evaluation of dynamic deflection basins measured on rigid pavements by nondestructive testing devices (a falling weight deflectometer and a Dynaflect). The analysis models presented in this paper include (a) a self-iterative procedure to determine in situ moduli of pavement layers, assuming a layered linearly elastic medium; (b) a self-iterative procedure for determining nonlinear strain-dependent moduli of granular layers and subgrade; and (c) a procedure for predicting fatigue life and existing structural capacity. A methodology has been developed to eliminate any need for assuming initial values of moduli. This has also improved efficiency of the self-iterative basin matching procedure and ensured unique values of the in situ moduli. Implementation of the proposed computerized evaluation procedures also provides a rational way to delineate sections for rehabilitation design.

Nondestructive testing (NDT) for structural evaluation of pavements is an important part of selecting rehabilitation and reconstruction strategies in the project-level pavement management process. The development of mechanistic overlay design procedures (1-3) has placed more emphasis on obtaining in situ material properties by analyzing deflection data. The realization that pavement response is affected by applied stress level, rate, and mode of loading and demand for faster and easier test methods have led to the development of several other types of NDT devices, such as the road rater and the falling weight deflectometer (FWD). The widespread use of applying a mechanistic approach to structural evaluation of pavement has resulted in (a) the measurement of deflection basins by recording dynamic deflections at more than one point during the test, and (b) the application of multilayered linear-elastic theory for analyzing the measured basin to derive in situ Young's moduli, assuming a pavement model as shown in Figure 1.

In this paper investigations performed for developing a computerized structural evaluation system based on dynamic deflection basins are described. A computer program [RPEDD1 (a rigid pavement structural evaluation system based on dynamic deflections--version 1.0)] has been developed and is described in this paper.

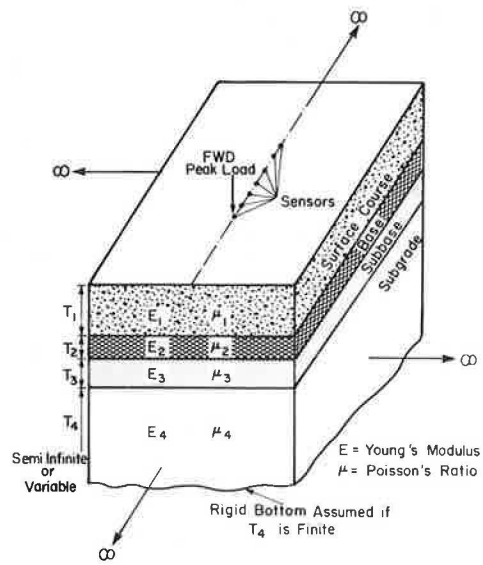

FIGURE 1 Multilayer linearly elastic model of pavement.

NDT DEVICES AND DYNAMIC DEFLECTION BASIN MEASUREMENT

Only the Dynaflect and the FWD are considered in this study. Standard configurations of load and deflection sensors (geophones) for the Dynaflect are assumed. Detailed descriptions of the Dynaflect and the test procedure are given elsewhere (4,5). The Dynaflect applies a sinusoidal vibrating load of a 1,000-lb peak-to-peak amplitude through two steel wheels that are 20 in. apart. Peak-to-peak surface deflections are measured by five geophones spaced 12 in. apart, with the first geophone located midway between the loading wheels. The radial distances of the geophones from each loading wheel are 10.00, 15.62, 26.00, 37.36, and 49.03 in. Basically, the FWD applies an impulse load by dropping a known mass from a predetermined height on a loading plate, which is assumed to be 11.8 in. in diameter in this study. An array of seven geophones is assumed in this research. The sensor at the center of the loading plate measures maximum deflection. Other geophones are assumed to be 12 in. apart, with radial distances at 0.0, 12.0, 24.0, 36.0, 48.0, 60.0, and 72.0 in.

FWD results are presented graphically as a deflection basin in this paper, plotted with radial distances as abscissas and normalized deflections as ordinates. FWD deflections are normalized with re-

spect to a 1,000-lb force to remove the influence of test load variations on deflections.

NDT EVALUATION OF IN SITU MODULI

An NDT device positioned far from the pavement edge and midway between two transverse joints or cracks can be used for the purpose of in situ material characterization and structural evaluation. Uddin et al. (6) have reported that Dynaflect deflection basins measured this way on continuously reinforced-concrete (CRC) pavements were practically free of temperature effects. A review of existing practices for the evaluation of deflection data and formulation of the self-iterative model developed in this study is presented in the following sections.

Review of NDT Evaluation Procedures

A detailed review of the published research on back-calculating moduli of two- or three-layer pavements using deflection basin parameters and layered theory is presented by Uddin et al. (7). A summary of deflection basin parameters is presented in Table 1. Finite element models have also been used by some researchers (8). These methods were generally developed by assuming fixed values of some parameters. Basin parameters do not use all the information that can be extracted from the use of the complete deflection basin. Another limitation is that each procedure has been developed for a specific NDT device and for some specific ranges of moduli. Generally, a bottom layer is assumed to be semi-infinite, which can result in considerable overestimation of error in the subgrade modulus if a rock layer exists within 20 ft (9). These considerations are often overlooked when a user applies these procedures in practice.

Inverse application of layered theory by fitting a measured deflection basin with a predicted deflection basin using an iterative procedure is the most promising method for calculating in situ moduli. In the past few years a number of self-iterative computer programs have been developed that use this approach, as summarized in Table 2. Some of the major features of these self-iterative procedures are as follows:

1. Generally these procedures are designed to handle only flexible pavements.
2. Semi-infinite subgrade is assumed in nearly all procedures. Effects of the existence of a rigid layer at a finite depth of subgrade on computed deflections and derived moduli are not addressed in the development of these methods.
3. Corrections to the derived moduli for nonlinear behavior of granular layers and subgrade are not considered in these procedures, with the exception of OAF and ISSEM4.
4. All these procedures are user dependent as far as the influence of initially assumed moduli on the convergence process and final moduli is concerned.
5. Dynamic aspects of the dynamic deflection data and effect of loading mode are ignored in all these procedures.

Research related to the self-iterative procedure developed in this study is presented in the following section.

Parameters Affecting Deflection Basin

To be precise, NDT data should be evaluated by using a dynamic analysis model. Dynamic loading on a pavement surface causes disturbances in the pavement subgrade system. If the pavement subgrade system is assumed to be linearly elastic, then a true dynamic analysis is possible by the application of the theory of stress wave propagation in layered elastic media. This theory is already being applied in the evaluation of dynamic moduli and layering in a pavement by the spectral analysis of surface waves (4). At the present state of knowledge, the layered linearly elastic theory can be used for mechanistic interpretation of dynamic deflection basins for all practical purposes. Therefore, the ELYSM5 computer program was selected for structural response analysis in this study.

Young's Moduli

A parametric study to investigate the sensitivity of theoretical deflection basins to the rate of change of moduli for a rigid pavement was performed in earlier research work (4). In that study one of the E values was varied by ±100 percent whereas the other E's were fixed at their original levels. Thicknesses and Poisson's ratios were fixed at constant values. An interesting conclusion was that a

TABLE 1 Summary of Deflection Basin Parameters (7)

Parameter	Definition[a]	NDT Device[b]
Dynaflect maximum deflection (DMD)	$DMD = d_1$	Dynaflect
Surface curvature index (SCI)	$SCI = d_1 - d_2$	Dynaflect, road rater model 400
Base curvature index (BCI)	$BCI = d_4 - d_5$	Dynaflect
Spreadability (SP)	$SP = \left(\sum_{i=1 \text{ to } 5} d_i / 5d_1\right) \times 100$	Dynaflect
	$SP = \left(\sum_{i=1 \text{ to } 4} d_i / 4d_1\right) \times 100$	Road rater model 2008
Basin slope (SLOP)	$SLOP = d_1 - d_5$	Dynaflect
Sensor 5 deflection (W_5)	$W_5 = d_5$	Dynaflect
Radius of curvature (R)	$R = r^2 / \{2 \cdot d_m [(d_m/d_r) - 1]\}$	Benkelman beam
Deflection ratio (Q_r)	$Q_r = r/d_o$	FWD, Benkelman beam
Area, in inches (A)	$A = 6[1 + 2(d_2/d_1) + 2(d_3/d_1) + (d_4/d_1)]$	Road rater model 2008
Shape factors (F_1, F_2)	$F_1 = (d_1 - d_3)/d_2$ $F_2 = (d_2 - d_4)/d_3$	Road rater model 2008
Tangent slope (TS)	$TS = (d_m - d_x)/x$	–

[a] d = deflection; subscripts 1, 2, 3, 4, 5 = sensor locations; o = center of load; r = radial distance; m = maximum deflection; x = distance of tangent point from the point of maximum deflection.

[b] The NDT device for which the deflection parameter was originally defined.

TABLE 2 Summary of Self-Iterative Procedures for Evaluation of Pavement Modulus from Deflection Basins (7)

Procedure Title	Source	Pavement Model (n = no. of layers)	Layered Theory Program for Analysis	NDT Method	Input	Output
*[a]	Anari and Wang, 1979; Pennsylvania State University	Four layers, flexible	BISAR	Road rater 400	d_i i = 1 to 4	E_1, E_2, E_3, E_4
ISSEM4	Sharma and Stubstad, 1980; Dynatest	Four layers, flexible	ELSYM5	FWD	d_i i = variable	E_1 to E_4 for four layer input
CHEVDEF[b]	Bush, 1980; U.S. Army Corps of Engineers Waterways Experiment Station	Four layers (not to exceed number of deflections)	CHEVRON	Road rater 2008	d_i i = 1 to maximum 4 (i = 1 + n)	E_j j = 1 to n
OAF[c]	FHWA, 1981; Resource International	Three or four layers, flexible	ELSYM5	Dynaflect, road rater, or FWD	d_i i = variable	E_j j = 1 to 3 or j = 1 to 4 (overlay thickness)
INVERSE	Hou, 1977; University of Utah	n = *	CHEV5L	*	d_i i = variable	E_j j = 1 to n
*	Tenison, 1983	Three layers, flexible	Chevron's N LAYER	Road rater 2000	d_i i = 1 to 4	E_j j = 1 to 3
RPEDD1[d]	Uddin et al., 1984; University of Texas	Three or four layers, rigid	ELSYM5	Dynaflect, FWD	d_i i = 1 to 5 or i = 1 to 7	E_j j = 1 to 3 or 4 (remaining life)
FPEDD1[d]	Uddin et al., 1984; University of Texas	Three or four layers, flexible	ELSYM5	Dynaflect, FWD	d_i i = 1 to 5 or i = 1 to 7	E_j j = 1 to 3 or 4 (remaining life)

Note: * = not known or available.

[a]Thickness, Poisson's ratio, initial seed modulus of each layer (except the thickness of bottom layer) are required input. Allowable ranges of moduli are also required. d_i = deflection reading measured at i^{th} sensor.
[b]Can be easily modified to handle other NDT devices.
[c]Another program, OAR, has also been developed recently by the same researchers (for rigid pavement overlay design).
[d]These procedures are developed in the present study (7).

deflection basin is least sensitive to a change in the moduli of intermediate layers and highly sensitive to even a small change in the subgrade modulus. It is inferred from this study that, to obtain a best fit, a change in the modulus of the ith layer (ΔE_j) can be predicted from the discrepancy (Δd_j) between an original deflection and its present value that corresponds to the jth sensor. For a four-layer rigid pavement, the following conceptual relationships are formed for later use in the convergence process designed for the self-iterative model:

$$\Delta E_4 \approx f(\Delta d_j) \quad (1)$$

where d_j is the deflection at the 5th sensor of the Dynaflect and the 6th or 7th sensor of FWD,

$$\Delta E_3 \approx f(\Delta d_k) \quad (2)$$

$$\Delta E_2 \approx f(\Delta d_1, \Delta d_k) \quad (3)$$

where d_k is the deflection at intermediate sensors located between the first and last sensors, and d_1 is the deflection at the first sensor (maximum deflection), and

$$\Delta E_1 = f(\Delta d_1) \quad (4)$$

A cycle of iterations starts by predicting the approximate change in the subgrade modulus and then proceeds to the corrections of the moduli of upper layers. This is the basis of an algorithm developed for the convergence process.

Thickness Information

The other important input parameter that influences theoretical deflection response is thickness. Deflection basins were calculated by varying the original thickness of a layer by factors of 2 and 0.5 while keeping all other input data fixed at original levels. This study indicates that, if design thicknesses are assumed for deflection basin analysis, slight variations in actual thicknesses of intermediate layers are not as critical as those of the surface concrete layer.

Development of a Self-Iterative Model

Assumptions

A set of simplified assumptions is necessary to validate the application of layered theory for determining in situ moduli from deflection basins. The assumptions can be separated into two groups:

1. Assumptions inherent in the use of layered linear-elastic theory to calculate pavement response. These are related to material properties, thickness information, boundary conditions, and so forth.
2. The second group of assumptions is required for NDT evaluation of a pavement in existing condition.

- The existing pavement is considered to be a layered elastic system (Figure 1). Therefore, the principle of superposition is valid for calculating response because of more than one load.
- The peak-to-peak dynamic force of the Dynaflect is modeled as two pseudo-static loads of 500 lb each uniformly distributed on circular areas (each 3 in.^{2}). The peak dynamic force of the FWD is assumed to be equal to a pseudo-static load uniformly distributed on a circular area represented by the FWD loading plate.
- Thickness of each layer is assumed to be known and exact.
- Subgrade is to be characterized by assigning an average value to its modulus of elasticity.

Methodology

A methodology has been formulated to determine in situ moduli based on a best fit of measured deflection basin within reasonable tolerances. The methodology relies on the iterative use of a procedure of successive correction until a best fit of the measured basin is obtained.

To start with, deflections are calculated from the initial input values of moduli (referred to as seed moduli in this study). The first cycle of iterations is equal to the number of layers in the pavement. In each cycle the first iteration is made to correct the subgrade modulus. ELYSM5 is then called to calculate theoretical deflections. Correction is then applied to the modulus of the next upper layer and ELYSM5 is again called to calculate theoretical deflections. The procedure of successive correction is continued until moduli of all layers have been checked for correction. Then another cycle of iterations starts again from the subgrade layer. The relationship used in the procedure of successive correction is given in the generalized form

$$ENEW_i = E_i(1.0 - CORR_i \cdot ERRP_k \cdot 0.5) \quad (5)$$

where

$ENEW_i$ = corrected value of Young's modulus of ith layer,
E_i = value of Young's modulus of ith layer in the previous iteration (for the first iteration it is seed modulus),
$CORR_i$ = correction factor for ith layer, and
$ERRP_k$ = discrepancy between measured deflection and predicted deflection (using E_i value) of kth sensor(s) as percentage error.

Only one-half of the discrepancy is meant to be removed in each iteration. Correction factors ($CORR_i$) are based on the parametric study described earlier. Iterations are stopped when one of the following criteria is reached: (a) the maximum absolute discrepancy between calculated and measured deflections is equal to or less than the permissible tolerance, (b) any correction in a modulus value causes the discrepancies between calculated and measured deflections to increase, or (c) the allowable number of iterations is maximum.

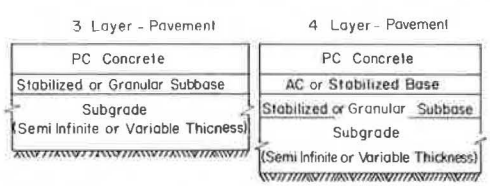

FIGURE 2 Typical rigid pavements analyzed by RPEDD1.

Description of BASINR

Subroutine BASINR is the self-iterative procedure to determine in situ moduli. The procedure can be used to analyze three- and four-layered pavements (as illustrated in Figure 2). The provision for a default procedure to obtain seed moduli from input data is an important part of BASINR and a significant improvement over other self-iterative procedures. Three types of tolerances allow ELYSM5 calculations to be skipped if the change in a modulus value is insignificant. The program is also designed to handle a rigid layer at some finite depth of subgrade.

Uniqueness of NDT-Based In Situ Moduli

A severe limitation in any deflection basin fitting method is the nonuniqueness of derived moduli. In addition, a basin matching procedure is generally sensitive to initially assumed seed moduli, especially if these values are drastically different from actual moduli. The approach used in this study to obtain a unique set of in situ moduli is to use the default procedure for seed moduli. Predictive equations have been developed for the Dynaflect and the FWD. Numerous theoretical deflection basins were generated for combinations of pavements based on a fractional factorial design (Table 3). The theoretical basins were later used to develop nonlinear predictive equations for Young's modulus (E_i) of each layer, with R^2 values ranging from 0.7 to 0.99. The provision for default seed moduli eliminates guesswork in selecting seed moduli and ensures a unique result.

Applications

The use of default seed moduli also results in fewer iterations for convergence. Generally, two to eight iterations are sufficient to reach a unique set of moduli. For validation of BASINR, theoretical deflection basins generated by ELYSM5 with preselected moduli were used to predict moduli. An example for the Dynaflect is shown in Figure 3 (7). Moduli calculated from a theoretical FWD deflection basin are shown in Figure 4 (7). In both examples zero values for seed moduli were entered in the inputs.

NONLINEAR MODELING OF GRANULAR MATERIALS AND SUBGRADE

Stress-Dependent Moduli

Characterization of the nonlinear behavior of granular materials and subgrades is normally based on

TABLE 3 Fractional Factorial Design to Generate Deflection Basin Data for Development of Moduli-Predictive Equations

	Factors						
	T_1 (in.)	T_2 (in.)	T_3 (in.)	E_4 (psi)	E_3 (psi)	E_2 (psi)	E_1 (psi)
Levels							
Low	8	0	6	5,000	30,000	100,000	2,000,000
Medium	10	4	9	15,000	150,000	500,000	4,000,000
High	13	8	12	45,000	450,000	1,000,000	6,000,000
Semi-infinite subgrade in all cases	PCC thickness	Base thickness	Subbase thickness	$E_{Subgrade}$	$E_{Subbase}$	E_{Base}	E_{PCC}

Note: Full factorial = 3^7; 1/9th fractional factorial = 3^5 = 243 combinations; PCC = portland cement concrete.

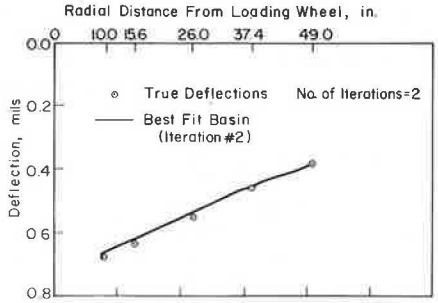

Assumed Pavement	True	Young's Moduli (psi) Input Seed	Default Seed	Predicted
8-in. P.C. Concrete	2,500,000	0	2,880,953	2,880,953
6-in Cement-Treated Base	200,000	0	263,467	263,467
6-in Granular Subbase	40,000	0	41,942	37,510
Semi-Infinite Subgrade	15,000	0	13,981	14,594

FIGURE 3 Young's moduli evaluated from a theoretical Dynaflect deflection basin *(7)*.

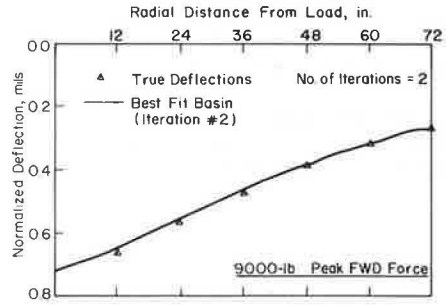

Assumed Pavement	True	Young's Moduli (psi) Input Seed	Default Seed	Predicted
8-in. P.C. Concrete	2,500,000	0	3,419,995	2,902,965
6-in. Cement-Treated Base	200,000	0	245,034	214,592
6-in. Granular Subbase	40,000	0	412,83	41,283
Semi-Infinite Subgrade	15,000	0	14,027	14,807

FIGURE 4 Young's moduli evaluated from a theoretical FWD deflection basin *(7)*.

laboratory tests from which the relationship between resilient modulus (M_R) and some stress parameter is determined. Review of research in this area can be found elsewhere (2,8,10-15). A stress-stiffening model is generally needed to characterize granular materials where M_R is a nonlinear function of bulk stress (sum of principal stresses). On the other hand, subgrade is characterized by a stress-softening model in which M_R is a nonlinear function of deviator stress. Uddin et al. (7) have discussed several limitations in using these procedures:

1. For certain combinations of pavement moduli, layered elastic theory predicts tensile stresses in granular layers even if gravity stresses are also considered (14). Researchers (14,16) have used a failure criterion or arbitrary procedures to overcome this problem of tensile stress.
2. There is a large scatter in M_R relationships obtained in the laboratory because of the influence of degree of saturation, water content and density, and so forth. Discrepancies may also arise from using total stress instead of effective stresses.
3. The discrepancies in current characterization procedures have been recognized (15) and attributed to laboratory M_R characterization of granular materials.

Uddin et al. (7) have discussed the possibility of using concepts developed in soil dynamics and geotechnical earthquake engineering to evaluate nonlinear moduli without using laboratory M_R relationships, as presented in the following section.

Equivalent Linear Analysis

Major findings from research related to the evaluation of the dynamic shear modulus (G) for use in soil dynamics and geotechnical earthquake engineering (16-19) are summarized in the following list:

1. Shear modulus (G) is a function of shear strain amplitude.
2. The primary parameters that affect G are shear strains (γ), mean effective principal stress ($\bar{\sigma}m$), void ratio (e), number of cycles of loading (N), and degree of saturation of cohesive soils.
3. There is a threshold strain amplitude (Figure 5) below which dynamic shear modulus is strain independent; it is typically referred to as G_{max}. Moduli associated with higher strain amplitude are strain sensitive.

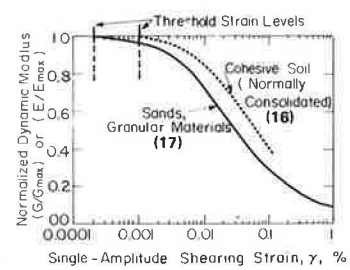

FIGURE 5 Typical relationships of normalized modulus versus shear strain for granular and cohesive soils.

TABLE 4 Maximum Shear Strain Response Under Different Loading Conditions

Loading Condition	Maximum Shear Strain[a] (%) from ELSYM5 Output: At Mid-Depth of Subbase Layer	At Top of Subgrade
Single-axle 18-kip design load[b]	5.227×10^{-3}	5.419×10^{-3}
FWD (9,000-lb peak force, radius of loading plate = 5.9 in.)	5.592×10^{-3}	5.683×10^{-3}
Dynaflect[c]	5.381×10^{-4}	5.729×10^{-4}

Note: The rigid pavement used in the analysis is divided as follows: top layer—portland cement concrete, 10 in. thick, 4,000,000 psi Young's modulus; 2nd layer—asphalt concrete base, 4.0 in. thick, 200,000 psi Young's modulus; 3rd layer—granular subbase, 6.0 in. thick, 75,000 psi Young's modulus; and 4th layer—subgrade, semi-infinite thickness, 30,000 psi Young's modulus.

[a] Largest of all values under the loading configuration.
[b] Dual wheels, 13.1 in. center to center; 75 psi tire pressure; 4,500 lb per wheel.
[c] For Dynaflect, equivalent single amplitude shear strain is half of the value given in each column.

4. Dynamic shear moduli data for gravelly soil are similar to that for sand, and an approximately unique curve can be obtained on a nondimensional plot of G/G_{max} versus shear strain (17), as illustrated in Figure 5. Stokoe and Lodde (16) present similar curves for cohesive soils using the resonant column test.
5. If G_{max} is known, then G associated with any higher shear strain amplitudes can be determined

from Figure 5. G_{max} can be obtained in the field with seismic tests (like the crosshole or downhole tests) or by the surface wave technique.

These concepts can also be extended to pavement analysis because G and E are related by the following relationship for a homogeneous and isotropic material:

$$E = 2G(1 + \mu) \quad (6)$$

where μ is Poisson's ratio.

Therefore G/G_{max} data can be translated to E/E_{max} data (20). The strain-softening behavior is exhibited by granular materials as well as by cohesive soils. In terms of NDT evaluations, varying strain amplitudes are associated with Dynaflect, FWD, and design loads (Table 4). It is observed that, at higher peak force levels, the peak shear strain amplitude generated by the FWD are approximately the same as those under the design load. In other words, in situ moduli derived from an FWD basin (at 9000-lb peak force) are the effective nonlinear moduli and need no further correction.

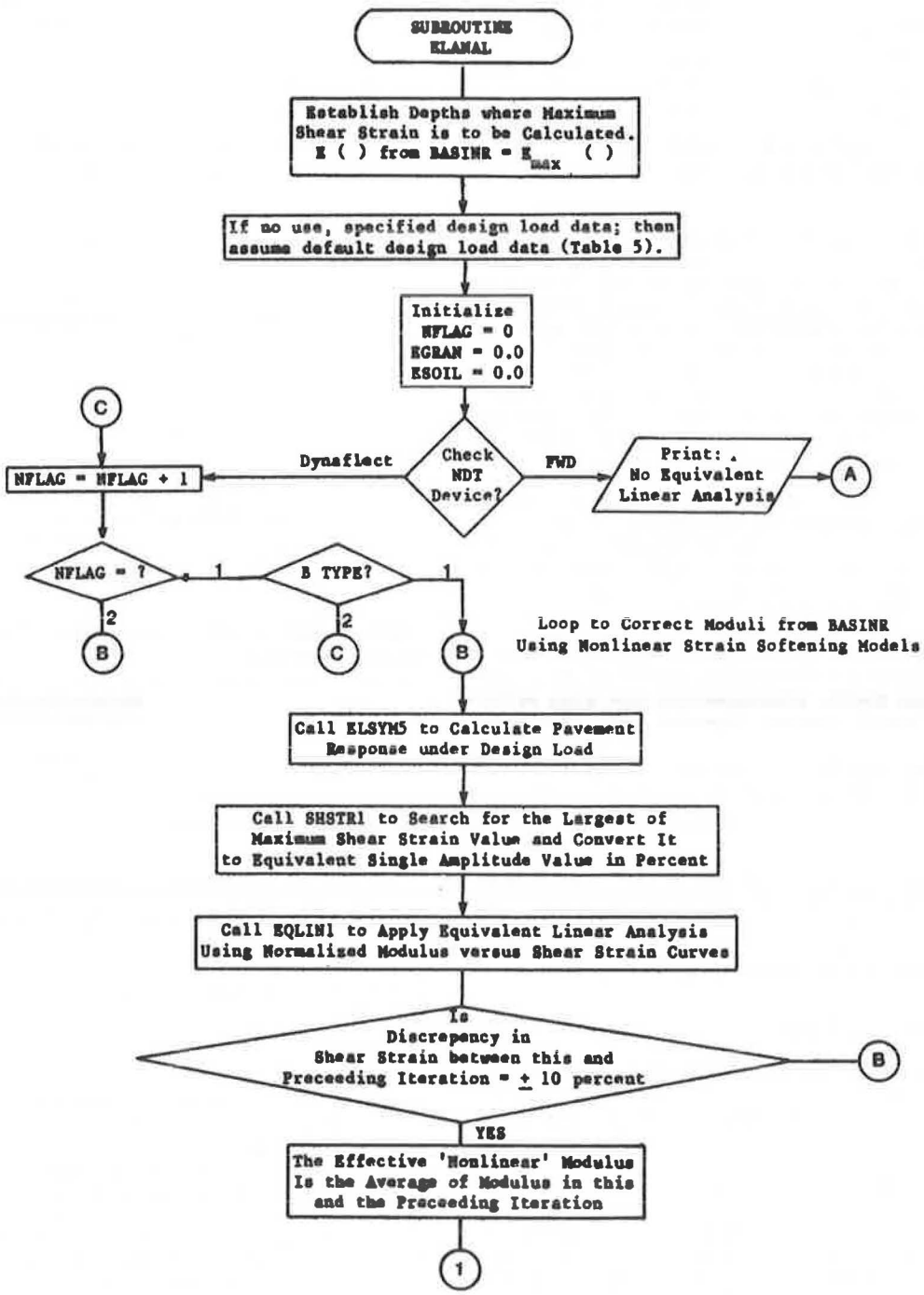

FIGURE 6 Simplified flow diagram for equivalent linear analysis to determine nonlinear strain-sensitive moduli of granular subbase and subgrade.

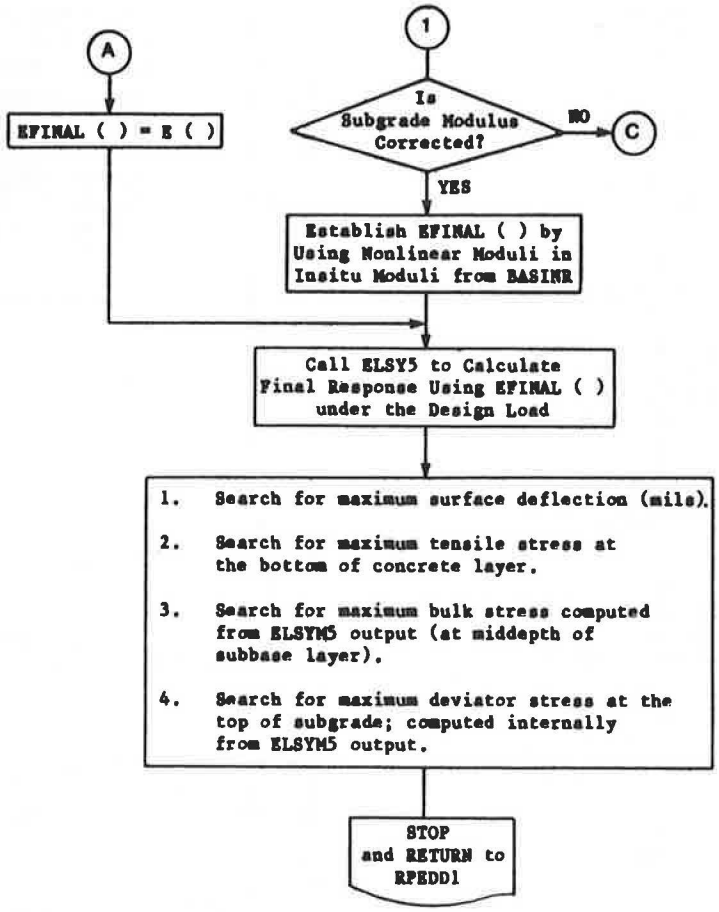

FIGURE 6 continued.

However, in situ Young's moduli calculated for nonlinear granular materials and subgrade from a Dynaflect deflection basin are associated with low amplitude shear strain and can be considered as E_{max}. A self-iterative procedure based on an equivalent linear analysis (subroutine ELANAL) has been developed for the evaluation of nonlinear moduli by using the E/E_{max} versus shear strain relationships of Figure 5. A simplified flow diagram of ELANAL is shown in Figure 6.

EVALUATION OF STRUCTURAL CAPACITY

Remaining life analysis is performed for the evaluation of structural capacity. ELYSM5 is called to calculate maximum horizontal tensile stress (σ_c) at the bottom of the concrete layer under the design load that is then corrected for pavement discontinuities by using the critical stress parameter (c_p) recommended by Seeds et al. (21). Past 18-kip equivalent single-axle load (ESAL) data (n_{18}) and flexural strength data (5) are required as additional input. Remaining life analysis is based on the approach used by several researchers (1,21):

$$R_L = [1.0 - (n_{18}/N_{18})] \times 100 \qquad (7)$$

where R_L is the remaining life (percent) and N_{18} is the maximum number of 18-kip ESAL applications. N_{18} is calculated by using the following equation developed for the fatigue of concrete pavement (9):

$$N_{18} = 46{,}000[S/(c_p \cdot \sigma_c)]^{3.0} \qquad (8)$$

where S and σ_c are in psi.

APPLICATION AND IMPLEMENTATION OF PROPOSED STRUCTURAL EVALUATION SYSTEM

A simplified flow diagram of RPEDD1 is shown in Figure 7. The final output of RPEDD1 is a table, which may be detailed (with the results of the remaining life analysis) or in summary form (without traffic and remaining life data). RPEDD1 is capable of analyzing 50 deflections in one run.

The general practice of an NDT evaluation--to analyze an average deflection basin obtained from all the basins measured in a design section--is not recommended for the application and implementation of RPEDD1. Figure 8 shows an example of analyzing deflection basins measured on a CRC pavement. The evaluation of individual deflection basins provides the user with a global look at the tested pavements. The tabulated results, printed in output, can be plotted as shown in Figure 9. A remaining life profile (Figure 9, top) can be used to identify sections that should be considered for an overlay analysis if the remaining life is below a threshold limit (e.g., 40 percent). Plots of subgrade modulus (Figure 9, bottom) can be used to delineate design sections. Finally, design moduli based on mean and standard deviations in each design section can be

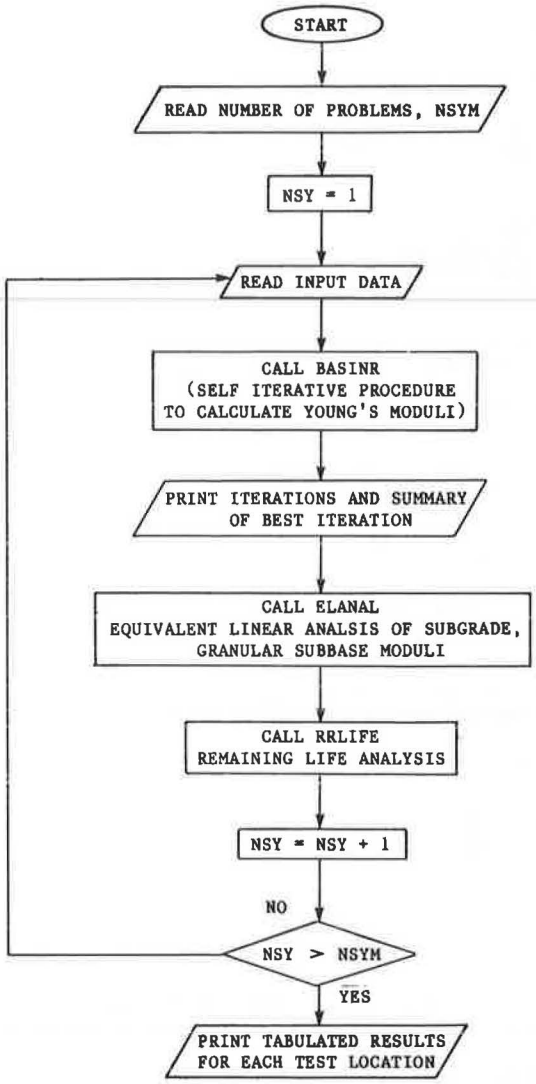

FIGURE 7 Simplified flowchart of RPEDD1.

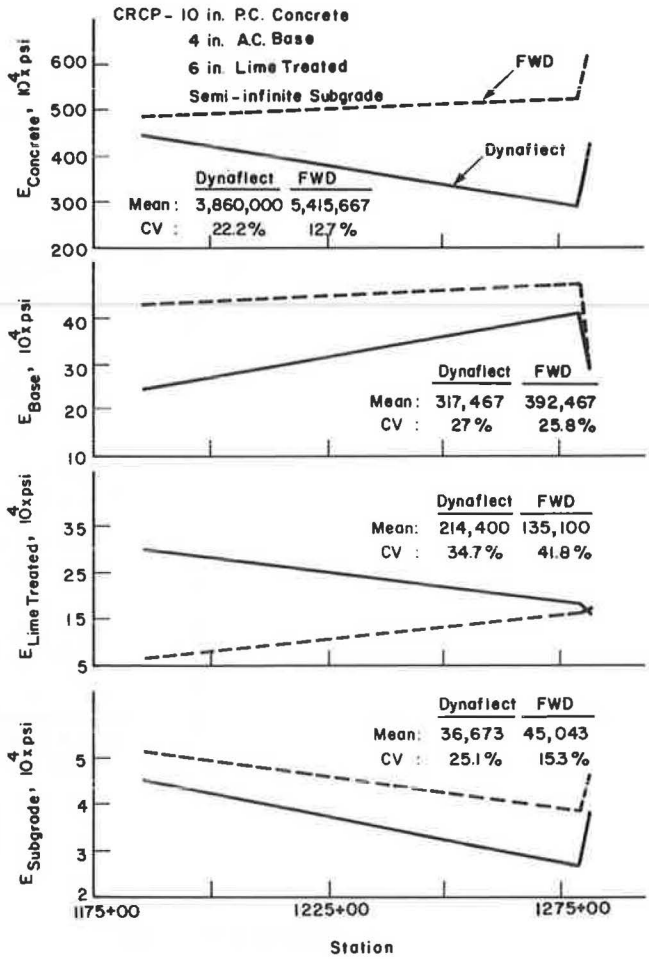

FIGURE 8 Evaluation of in situ moduli from deflection basins measured on a CRC pavement (SH-71) at Columbus, Texas.

determined for later use in a mechanistic overlay and rehabilitation design program such as RPRDS (21).

CONCLUSIONS

A complete framework for NDT evaluation of rigid pavements has been presented in this paper. The computer program RPEDD1 has been developed in this study for evaluation of dynamic deflection basins measured by the Dynaflect or the FWD. The principal conclusions based on the research presented in this paper are as follows:

1. The self-iterative model yields unique moduli, is not user dependent, and eliminates guesswork in assuming seed moduli.
2. NDT evaluation of nonlinear moduli of granular and cohesive materials using the concept of strain sensitivity is a rational approach. It also eliminates the derivation of laboratory M_R relationships.
3. Guidelines for the application and implementation of RPEDD1 provide the user with a global look at the structural condition of pavement, variability of in situ moduli along the pavement, overlay analysis, selection of design sections, and design moduli for later use in comprehensive overlay design.

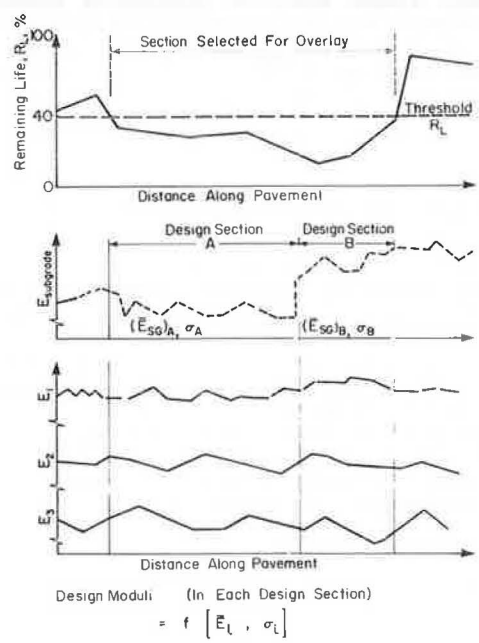

FIGURE 9 Application and implementation of RPEDD1.

Using a similar approach, another computer program, FPEDD1--a flexible pavement structural evaluation system based on dynamic deflections--has been developed; it is described elsewhere (7).

ACKNOWLEDGMENTS

The research presented in this paper was conducted as part of the Cooperative Highway Research Program sponsored by the Texas State Department of Highways and Public Transportation and FHWA. Appreciation is extended to B.F. McCullough and J.M. Roesset, Professors of Civil Engineering at the University of Texas at Austin, for their interest during the course of this research.

REFERENCES

1. H.J. Treybig, B.F. McCullough, P. Smith, and H. van Quintus. Overlay Design and Reflection Cracking Analysis for Rigid Pavements--Volume 1: Development of New Design Criteria. Report FHWA-RD-77-66. FHWA, U.S. Department of Transportation, Aug. 1977.
2. Austin Research Engineers, Inc. Asphalt Concrete Overlays of Flexible Pavement--Volume 2: Design Procedures. Report FHWA-RD-75-76. FHWA, U.S. Department of Transportation, Aug. 1975.
3. K. Majidzadeh and G.J. Ilves; Resource International, Inc. Flexible Pavement Overlay Design Procedures--Volume 1: Evaluation and Modification of the Design Methods. Report FHWA-RD-81-032. FHWA, U.S. Department of Transportation, Aug. 1981.
4. W. Uddin, S. Nazarian, W.R. Hudson, A.H. Meyer, and K.H. Stoke II. Investigations into Dynaflect Deflections in Relation to Location/Temperature Parameters and In Situ Material Characterization of Rigid Pavements. Research Report 256-5. Center for Transportation Research, University of Texas, Austin, Dec. 1983.
5. W. Uddin, V.T. Verdin, W.R. Hudson, A.H. Meyer, B.F. McCullough, and R.B. Rogers. Dynaflect Testing for Rigid Pavement Evaluation--Volume 1: Background. CTR Report 256-6F. Center for Transportation Research, University of Texas, Austin, Oct. 1983.
6. W. Uddin, A.H. Meyer, and W.R. Hudson. Study of Factors Influencing Deflections of Continuously Reinforced-Concrete Pavements. In Transportation Research Record 993, TRB, National Research Council, Washington, D.C., 1984, pp. 47-54.
7. W. Uddin, A.H. Meyer, W.R. Hudson, and K.H. Stokoe II. A Structural Evaluation System for Pavements Based on Dynamic Deflections. Research Report 387-1. Center for Transportation Research, University of Texas, Austin, Sept. 1984.
8. M.S. Hoffman and M.R. Thompson. Mechanistic Interpretation of Nondestructive Pavement Testing Deflections. Report FHWA-IL-UI-190. University of Illinois, Urbana, June 1981.
9. A. Taute, B.F. McCullough, and W.R. Hudson. Improvements to the Material Characterization and Fatigue Life Prediction Methods of the Texas Rigid Pavement Overlay Design Procedure. Research Report 249-1. Center for Transportation Research, University of Texas, Austin, March 1981.
10. H.B. Seed, F.G. Mitry, C.L. Monismith, and C.K. Chan. Prediction of Flexible Pavement Deflections from Laboratory Repeated-Load Tests. NCHRP Report 35. HRB, National Research Council, Washington, D.C., 1967, 117 pp.
11. R.G. Hicks. Factors Influencing the Resilient Properties of Granular Materials. Ph.D. dissertation. Institute of Transportation and Traffic Engineering, University of California, Berkeley, May 1970.
12. W.S. Smith and K. Nair; Materials Research and Development. Development of Procedures for Characterization of Untreated Granular Base Course and Asphalt Treated Base Course Materials. Report FHWA-RD-74-61. FHWA, U.S. Department of Transportation, Oct. 1973.
13. G. Rada and M.W. Sitczak. Comprehensive Evaluation of Laboratory Resilient Moduli Results for Granular Material. In Transportation Research Record 810, TRB, National Research Council, Washington, D.C., 1981, pp. 23-33.
14. A.F. Stock and S.F. Brown. Nonlinear Characterization of Granular Materials for Asphalt Pavement Design. In Transportation Research Record 755, TRB, National Research Council, Washington, D.C., 1980, pp. 14-20.
15. P.A. D'Amato and M.W. Witczak. Analysis of In Situ Granular-Layer Modulus from Dynamic Road-Rater Deflections. In Transportation Research Record 755, TRB, National Research Council, Washington, D.C., 1980, pp. 20-30.
16. K.H. Stokoe II and P.F. Lodde. Dynamic Response of San Francisco Bay Mud. Proc., ASCE Earthquake Engineering and Soil Dynamics Conference, Volume II, 1978, pp. 940-959.
17. H.B. Seed and I.M. Idriss. Soil Moduli and Damping Factors for Dynamic Response Analysis. Report EERC-70-10. Earthquake Engineering Research Center, University of California, Berkeley, Dec. 1970.
18. B.O. Hardin and V.P. Drnevich. Shear Modulus and Damping in Soils: Measurement and Parameter Effects. ASCE, Journal of Soil Mechanics and Foundations Division, Vol. 98, No. SM6, June 1972, pp. 603-624.
19. B.O. Hardin and V.P. Drnevich. Shear Modulus and Damping in Soils: Design Equations and Curves. ASCE, Journal of Soil Mechanics and Foundations Division, Vol. 98, No. SM7, July 1972, pp. 667-692.
20. S. Nazarian and K.H. Stokoe II. Nondestructive Testing of Pavements Using Surface Waves. In Transportation Research Record 993, TRB, National Research Council, Washington, D.C., 1984, pp. 67-79.
21. S.B. Seeds, B.F. McCullough, and W.R. Hudson. A Design System for Rigid Pavement Rehabilitation. CTR Report 249-2. Center for Transportation Research, University of Texas, Austin, Jan. 1982.

Pavement Elastic Characteristics Measured by Means of Tests Conducted with the Falling Weight Deflectometer

AURELIO MARCHIONNA, MAURIZIO CESARINI, MASSIMO G. FORNACI, and MAURO MALGARINI

ABSTRACT

In this paper a procedure is described that obtains the elastic moduli of both flexible and semi-rigid pavements from tests carried out with a falling weight deflectometer (FWD). The pavements are schematized as an elastic four-layer body. For bituminous and hydraulic-bound layers, a linear elastic law was adopted, whereas a nonlinear elastic law was used for unbound layers (subbase and subgrade). The behavior of a large number of pavements subjected to the FWD load was analyzed by using a finite-element model. A wide range of layer thicknesses and moduli were included in the pavement sections tested. From this analysis and by using the multiple regression technique, it was possible to determine analytical functions between deflections and moduli. The procedure allows an evaluation of the moduli of the different pavement layers by using these functions and the deflections measured under the FWD load. An example of a practical application of this procedure to the elastic characteristics of semi-rigid pavements of some Italian motorways is presented in the paper.

To optimize the use of available resources, agencies in charge of the management of roads are increasingly concerned with the need to develop a program of pavement maintenance operations that provides the most cost-effective strategy. Therefore it is essential to define carefully the structural condition (bearing capacity) of the pavements.

For the purpose of evaluating the structural condition of pavements, it is possible to use different types of load tests. Currently the use of dynamic tests, carried out by means of stationary load (vibrators) or impulse load (falling weight) instruments, has become common. In comparison to the dynamic load applied to the pavement, the latter are light in weight and are convenient to use (1).

A way of estimating the bearing capacity is to use the deflection values, obtained by tests carried out with the falling weight deflectometer (FWD), to determine the real elastic characteristics of pavement materials. On the basis of these deflection values it is possible to evaluate the pavement remaining life in terms of fatigue distress (2-5).

The objective of this study is to define a method that determines the elastic characteristics of pavements. Specifically, a method suitable for the flexible and semi-rigid pavements that exist on the Italian motorways network was the goal (6,7).

DETERMINATION OF ELASTIC CHARACTERISTICS

The basic data are represented by the deflections of the pavement produced by the Dynatest 8000 FWD (Figure 1). The deflections are measured by means of seven geophones (Figure 2), one of which is placed at the center of the plate; the others are installed on a bar placed radially from the center of the load. The following distances were chosen:

Transducer	1	d_1	=	0	mm
Transducer	2	d_2	=	300	mm
Transducer	3	d_3	=	450	mm
Transducer	4	d_4	=	600	mm
Transducer	5	d_5	=	900	mm
Transducer	6	d_6	=	1200	mm
Transducer	7	d_7	=	1500	mm

Because of the degree of accuracy with which the machine measures the deflection values (±2 μm) and the high stiffness of the pavements to be examined,

FIGURE 1 View of the FWD.

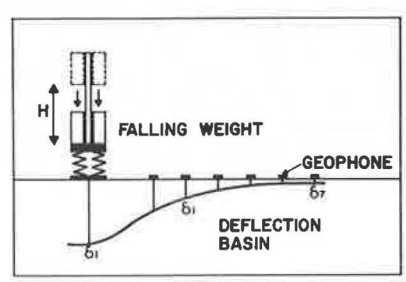

FIGURE 2 Deflection basin of the FWD.

it was decided to carry out measurements with the maximum possible load (falling height H = 400 mm).

The deflection (δ_{di}) measured at a point of the pavement located at a di distance from the center of the plate is a function of the elastic characteristics of the materials that make up the layers, of the layer thickness, of the load applied, and of the di distance.

As a general rule, it is assumed that

$$\delta_{di} = \delta_{di}(CM_{1,1}\ldots, CM_{K,J}\ldots, S_1\ldots, S_K, F) \quad (1)$$

where

δ_{di} = deflection at the point located at di distance,
$CM_{K,J}$ = Jth elastic characteristic of the Kth layer material,
S_K = thickness of the Kth layer, and
F = load applied.

Once the analytical forms of such relations have been found, they can be used to obtain the elastic or geometric characteristics of pavements on the basis of the measured deflection values. In the case of the FWD, there are seven deflection measurement positions; therefore it is possible to determine up to seven unknown characteristics.

CALCULATION MODEL

The determination of the δ_{di} functions was accomplished by using the deflections obtained by simulating with a computer the behavior, under the FWD load, of a large number of pavements varying in mechanical characteristics and thickness.

The first problem was the selection of the calculation model to be adopted. Measurements carried out with the FWD at three different falling heights and three different load values indicated that the pavements had a nonlinear response. This means that there is nonproportionality between the load applied and the strain measured (see Figure 3). Therefore it was necessary to use a nonlinear elastic model to analyze pavement behavior.

It was assumed that the granular materials that form the subbase and the subgrade had a nonlinear behavior and that their stiffness changed from point to point according to the state of stress (8-11). The model used was the nonlinear elastic multilayer structure; the analysis was carried out using the finite-element method (12-16) and the Nonlinear Structural Analysis Program (NONSAP) (17,18). New subroutines were added to this program to schematize the behavior of nonbound road materials.

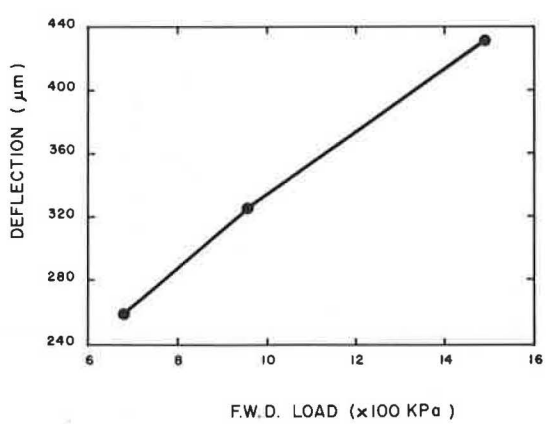

FIGURE 3 Deflection of the pavement surface as a function of the load applied by the FWD.

The basis of the finite-element technique (19, 20) is the replacement of a continuous elastic structure with a number of finite dimension elements. For elements with nonlinear behavior, it is necessary to increase the external load time in increments, recalculating each time the stiffness as a function of the state of stress of the previous step (step by step). In the analysis it is implicitly assumed that within a load step the constitutive law of the material can be considered linear; therefore the smaller the increase, the more this is true.

ELASTIC CHARACTERISTICS OF MATERIALS

All of the pavement types examined have been referred to the behavior of an elastic four-layer body. In the case of flexible pavements, the thickness of the first layer includes the wearing course and the binder, and the second layer represents the bitumen-bound base course. In the case of semi-rigid pavements, the first layer represents all the bitumen-bound layers and the second layer represents the cement-treated-base layer. The third and the fourth layers correspond to the subbase and the subgrade, respectively. Therefore the following laws were adopted:

1. A linear elastic law (E = const, ν = const) for the materials that form the bound layers (asphalt concretes and cement-treated materials); and
2. A nonlinear elastic schematization [E = E(σ), ν = const] for unbound materials (granular mixes in subbase and subgrade layers).

The analytical forms of the relations between elastic modulus and the material state of stress were chosen on the basis of the experimental relations determined by different researchers on the subject of materials subjected to states of dynamic triaxial stress (7-10). The following law was adopted for the elastic modulus (E_3) of the materials that form the subbase layer:

$$E_3 = K_{1,subbase} \cdot I_1^{K_{2,subbase}} \quad (2)$$

where

I_1 = first invariate of the tensor of stresses (3 times the average stress) (these values are expressed in terms of total stresses, and compressive stresses are assumed to be positive),
$K_{2,subbase}$ = exponent larger than zero, and
$K_{1,subbase}$ = modulus that corresponds to the state of stress characterized by $I_1 = 1$.

For the modulus of the subgrade (E_4), the following law was adopted:

$$E_4 = K_{1,subgrade} \cdot (\sigma_1 - \sigma_3)^{K_{2,subgrade}} \quad (3)$$

where

σ_1 = maximum principal stress,
σ_3 = minimum principal stress,
$K_{2,subgrade}$ = exponent smaller than zero; and
$K_{1,subgrade}$ = modulus that corresponds to the state of stress characterized by $(\sigma_1 - \sigma_3) = 1$.

Thus a linear behavior takes place in both laws when the exponent is equal to zero. For $I_1 \to 0$, $E_3 \to 0$ and

for $(\sigma_1 - \sigma_3) \rightarrow 0$, $E_4 \rightarrow \infty$, this is unacceptable from the physics point of view. The validity of these laws, therefore, was limited to following fields: $I_1 \geq 0.01$ MPa and $(\sigma_1 - \sigma_3) \geq 0.01$ MPa. A factor in the selection of these limits is that experimental tests in stress fields lower than these limits have apparently not been carried out. The values of the moduli determined at such limits are assumed to be valid for all the lower field (Figure 4). It is finally to be noted that the values of the stresses introduced in the calculation take into account the actual weight of layers.

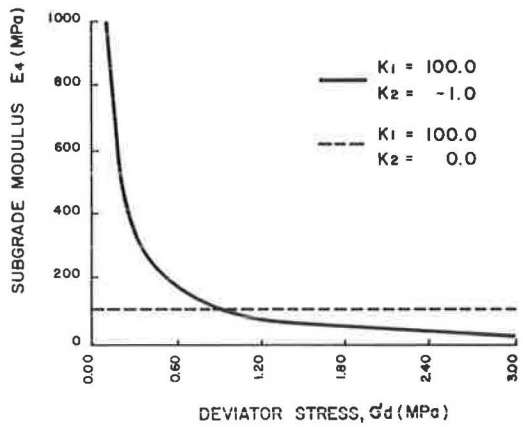

FIGURE 4 Modulus of subgrade versus deviator stress.

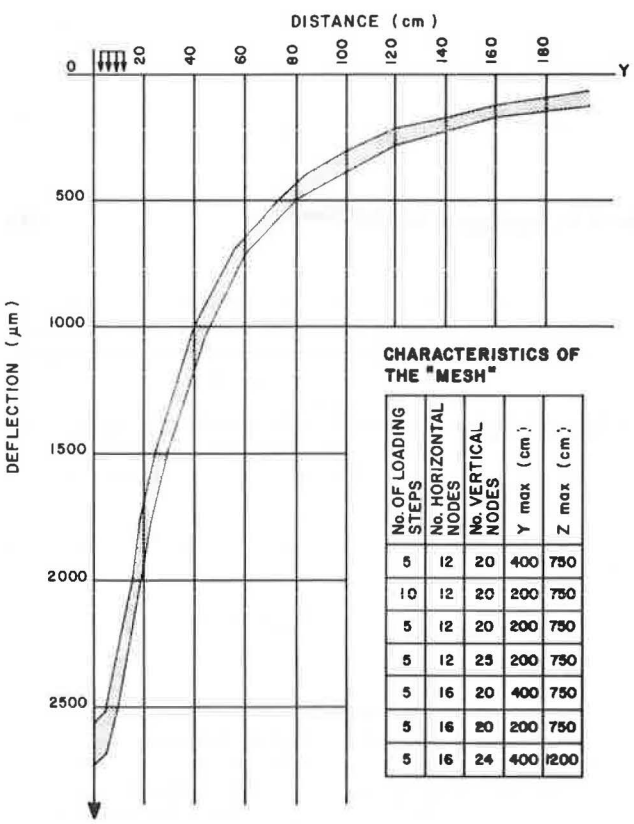

No. OF LOADING STEPS	No. HORIZONTAL NODES	No. VERTICAL NODES	Y max (cm)	Z max (cm)
5	12	20	400	750
10	12	20	200	750
5	12	20	200	750
5	12	25	200	750
5	16	20	400	750
5	16	20	200	750
5	16	24	400	1200

FIGURE 5 Influence of mesh geometric characteristics on the deflection basin. The shaded area shows the basins that correspond to the mesh data in the figure.

GEOMETRIC CHARACTERISTIC OF THE MESH

After the characterization of materials, the geometric definition of the problem was considered. A load test on a plate must be simulated. Toroidal elements with rectangular radial cross sections were used to form a model that has axial symmetry (21). In order to determine the optimal configuration of the "mesh" (i.e., its size, the size of the elements, and the position and type of constraints at the boundary), the deflections for different geometric configurations were calculated (see Figure 5). This analysis has produced the following general indications:

1. It is advisable to use elements whose side lengths (L) meet the conditions $5L_{min} \geq L_{max}$, and
2. It is opportune to use a mesh that fulfills the condition (Figure 6) $4Y_{max} \geq Z_{max}$.

On the basis of these results a configuration that permits a stable solution without exceedingly long calculation times was chosen (the time increases as the mesh is subdivided into smaller elements). A stable solution is one that produces deflections as close as possible to those that would be produced by a more subdivided "mesh." The characteristics of the configuration adopted (Figure 6) are the following:

1. Size of the mesh: Y_{max} = 400 cm, Z_{max} = 750 cm;
2. Size of the elements: side length ratio ($L_{min}/L_{max} \geq 1/5$) in the areas with high stress gradient;

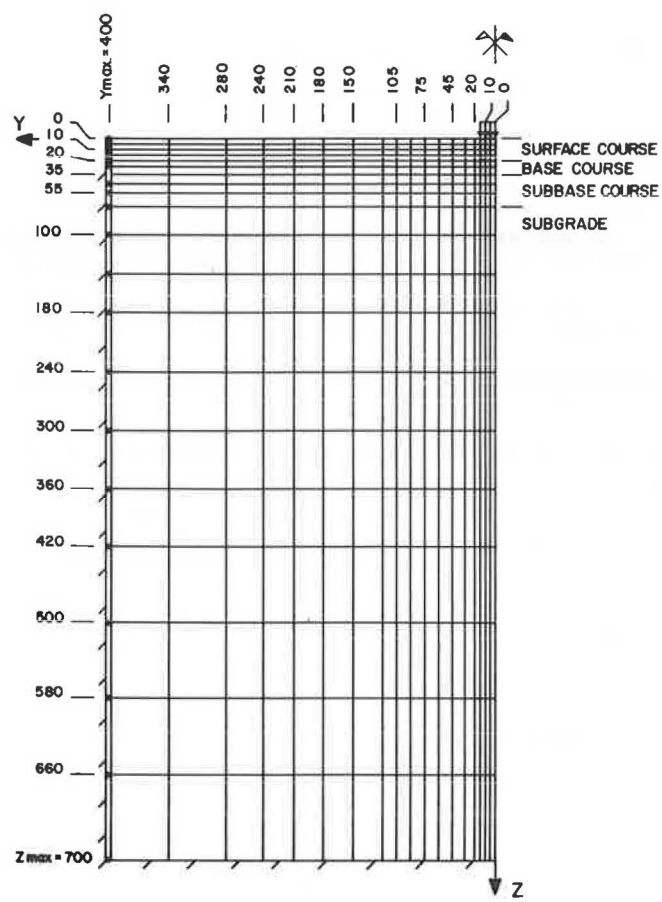

FIGURE 6 Pavement finite element mesh.

3. Number of horizontal nodes (19); and
4. Number of vertical nodes (21).

APPLIED LOAD

The FWD applies a load to the pavement that rises in a short time from 0 to the maximum value with a virtually sinusoidal trend. In the computer simulation the same load increase law was adopted. The minimum number of steps into which the load must be subdivided in order to obtain a stable solution was found to be seven. As a maximum load, the value that corresponds to a pressure of 1450 kN/m² on a 30-cm-diameter plate was assumed. This is the average value obtained with the FWD at a falling height of 400 mm.

RANGE OF ELASTIC AND GEOMETRIC CHARACTERISTICS

By using the model briefly described, it was possible to determine the deflection values for pavements whose elastic and geometric characteristics vary within fixed limits. The upper and the lower limits of each variable were chosen according to the pavement types, the materials, and the environmental conditions of the motorway network (see Table 1).

TABLE 1 Elastic Characteristics of Variables, Scanned Ranges

Layer	Elastic Characteristic	Maximum	Minimum
Surface course	E_1 (MPa)	10,000	1,000
	ν_1	0.30	0.45
Base course	E_2 (MPa)	8,000	1,500
	ν_2	0.35	0.45
Subbase course	K_1(MPa)$^{1-K2}$	500	10
	ν_3	0.35	0.50
Subbase course	K_2 (adim.)	1.00	0.10
Subgrade	K_1 (MPa)$^{1-K2}$	400	10
	ν_4	0.40	0.50
Subgrade	K_2 (adim.)	−0.10	−1.00

Each of these ranges was then scanned. The analysis included nine variables: six refer to the layer elastic characteristics:

E_1 = modulus of the 1st bound layer,
E_2 = modulus of the 2nd bound layer,
$K_{1,subb}$ = 1st nonlinear constant of the subbase,
$K_{2,subb}$ = 2nd nonlinear constant of the subbase,
$K_{1,subg}$ = 1st nonlinear constant of the subgrade, and
$K_{2,subg}$ = 2nd nonlinear constant of the subgrade;

and three refer to the layer thicknesses:

H_1 = thickness of the 1st layer,
H_2 = thickness of the 2nd layer, and
H_3 = thickness of the 3rd layer.

The values of the Poisson ratios were connected, according to a proportionality relation, to the values of the moduli or of the K_1 coefficients.

If all the pavement schemes resulting from the combination of all the variables involved had been examined, the deflection values from a few million cases would have been calculated. Because the examination of such a large number of cases would have required a long time, their number was limited to about 3,500. These combinations were chosen so as to examine the whole range of each variable and exclude those that are unlikely from the physics point of view.

DETERMINATION OF δ_{di} FUNCTIONS

The next step of this study was to find, on the basis of the computer simulation results, the analytical form of the relations between the deflection values and the geometric and elastic characteristics of pavements. It was possible to write the seven deflection functions in the following form:

$$\delta_{di} = \delta_{di}(E_1, \nu_1, E_2, \nu_2, K_{1,subb}, K_{2,subb}, \nu_3, K_{1,subg}, K_{2,subg}, \nu_4, H_1, H_2, H_3) \quad (4)$$

where the symbols have the meanings previously described. If the following assumptions are taken into account: $\nu_i = f(E_i)$ or $\nu_i = f(K_1)$, then the previous expressions can be represented as follows:

$$\delta_{di} = \delta_{di}(E_1, E_2, K_{1,subb}, K_{2,subb}, K_{1,subg}, K_{2,subg}, H_1, H_2, H_3) \quad (5)$$

By using the multiple regression technique (22), it was possible to find the expression of the δ_{di} functions that best fit the available data and met the condition that in all seven functions (measured deflections at the seven geophones) the independent variables have the same form. The imposition of this constraint simplifies the algorithm for the determination of the elastic characteristics. To obtain the functions that produce as little residual as possible, the input data were subdivided into groups. This subdivision was done on the basis of the δ_{d1} deflection value at the center of the loading plate. The groups have a 200 μm width and cover the range 0 to 2000 μm.

The optimal form of the functions obtained in the range $0 < \delta_{di} \leq 200$ is given here as an example:

$$\begin{aligned}\log_{10}\delta_{di} = {} & \alpha_{i0} + \alpha_{i1}E_1^{-0.4} + \alpha_{i2}E_2^{-0.4} \\ & + \alpha_{i3}\log_{10}K_{1,subb} + \alpha_{i4}K_{2,subb}^{1.5} \\ & + \alpha_{i5}K_{1,subg}^{0.5} + \alpha_{i6}K_{2,subg}^{0.8} \\ & + \alpha_{i7}\log_{10}H_1 + \alpha_{i8}\log_{10}H_2 \\ & + \alpha_{i9}H_3^{-1}\end{aligned} \quad (6)$$

The α_{ij} coefficients, with j varying from 0 to 9, are given in Table 2, together with the multiple correlation coefficients.

PROCEDURE FOR THE DETERMINATION OF THE ELASTIC CHARACTERISTICS

The seven relations thus obtained can be easily made linear by means of opportune variable substitutions. This produces the following type of relation:

$$\Delta_i = \alpha_{i0} + \alpha_{i1}X_1 + \alpha_{i2}X_2 + \alpha_{i3}X_3 + \alpha_{i4}X_4 + \alpha_{i5}X_5 + \alpha_{i6}X_6 + \alpha_{i7}X_7 + \alpha_{i8}X_8 + \alpha_{i9}X_9 \quad (7)$$

$(i = 1, 2 \ldots 7)$

where

$X_1 = f(E_1)$,
$X_2 = f(E_2)$,
$X_3 = f(K_{1,subb})$,
$X_4 = f(K_{2,subb})$,
$X_5 = f(K_{1,subg})$,

TABLE 2 Regression Coefficients

Position	Coefficient (α_{ij})										Coefficient of Multiple Correlation
	α_{i0}	α_{i1}	α_{i2}	α_{i3}	α_{i4}	α_{i5}	α_{i6}	α_{i7}	α_{i8}	α_{i9}	
1	3.79549	20.54139	20.28920	−0.29050	−0.08299	−0.00297	−0.09884	−0.32069	−0.31931	−0.22259	0.96421
2	4.15608	5.4167	9.29284	−0.35625	−0.10659	−0.00509	−0.16611	−0.24143	−0.25143	−0.19759	0.96777
3	3.88933	3.29009	3.53888	−0.32385	−0.10179	−0.00636	−0.21087	−0.13816	−0.14479	−0.19006	0.97915
4	3.49727	1.93323	0.83324	−0.25615	−0.08685	−0.00754	−0.25449	−0.05093	−0.05055	−0.20079	0.98929
5	2.66276	0.53259	−2.44696	−0.09323	−0.04428	−0.00887	−0.30286	0.04110	0.04726	−0.22521	0.99555
6	2.09894	0.25548	−1.94043	0.00647	−0.02203	−0.00855	−0.28312	0.04726	0.05051	−0.12022	0.99719
7	1.76472	0.22652	−1.05182	0.04400	0.00565	−0.00735	−0.22472	0.02989	0.03034	−0.46531	0.99717

$X_6 = f(K_{2,subg})$,
$X_7 = f(H_1)$,
$X_8 = f(H_2)$,
$X_9 = f(H_3)$, and
$\Delta_i = f(\delta_{di})$.

The deflections obtained by means of the FWD are included in the seven previous relations together with the thicknesses H_1, H_2, H_3, which can usually be obtained from the design data. Another seven equations of this kind are thus obtained:

$$\alpha_{i1}X_1 + \alpha_{i2}X_2 + \alpha_{i3}X_3 + \alpha_{i4}X_4 + \alpha_{i5}X_5 + \alpha_{i6}X_6 = C_i \quad (8)$$

$$(i = 1, 2 \ldots 7)$$

where

$$C_i = \Delta_i - \alpha_{i0} - \alpha_{i7}X_7 - \alpha_{i8}X_8 - \alpha_{i9}X_9.$$

The complete series of these seven equations forms a system where the six unknown quantities are representative of the elastic characteristics of the pavement being considered.

Because the number of equations is larger than that of the unknown quantities, this system does not allow a solution. A different approach was then devised so as to obtain the elastic characteristics of the pavement. For this purpose it was necessary to set the condition that the sum of the square of the differences between the first and the second number of each of the seven equations (Equation 8) is kept minimal. Such sum, called S, is necessary to minimize the following quantity:

$$S(X_1, \ldots, X_6) = \sum_{i=1}^{7}\left(C_i - \sum_{j=1}^{6}\alpha_{ij}X_j\right)^2 \quad (9)$$

The previous condition is transformed into required conditions through the partial derivatives of $S(X_1, \ldots, X_6)$, which can be expressed by means of the following formula:

$$\partial S/\partial X_K = \sum_{i=1}^{7}\left(\sum_{j=1}^{6}\alpha_{iK} \cdot \alpha_{ij} \cdot X_j\right) - \sum_{i=1}^{7}\alpha_{iK}C_i \quad (10)$$

$$(K = 1, \ldots 6)$$

By imposing the condition of a minimum value for $S(X_1, \ldots X_6)$, it is possible to determine the elastic characteristics of the road pavements with the help of a simple desk computer (PA.STR.EV. Program). For this purpose it is possible to use the computer installed on the deflection measuring equipment.

COMPUTERIZED PROCEDURE

Figure 7 shows the flowchart that describes the automatic procedure used. The input for NONSAP was automated by means of two programs (COMBINE and GENERA). The result of the NONSAP processing--the printouts (stored on file 1)--are scanned by the READER program, which extracts the data necessary to perform the regressions and checks them with the initial data (file 2). The SELECT program organizes these data by dividing them into groups on the basis of the value of the δ_{d1} deflection. A regression analysis (REGRESSION program) was then performed, with the results obtained (stored in file 3) being used by the PA.STR.EV. program. The outputs of this program are the values of the elastic characteristics of the materials.

RELIABILITY OF THE PROCEDURE

A series of tests was carried out to verify the reliability of the procedure. The tests consisted of comparing the initial elastic characteristics (used by NONSAP) with those resulting from PA.STR.EV., starting from the deflections calculated by NONSAP. These tests indicated that with the level of accuracy currently achieved by the regression functions, the differences between initial and calculated values amount to about 15 percent. This result can be accepted if it is considered that some verifications done with the NONSAP program revealed that differences of this size lead to smaller stress variations (7 percent less).

FREQUENCY AND TEMPERATURE OF ASPHALT CONCRETE

For a complete characterization of asphalt concretes, which are materials with visco-elastic behavior, it is necessary to know the frequency and the temperature associated with the moduli obtained by means of the FWD. To determine the frequency of application of the FWD, load measurements were made on a test section on the Nardò by-pass (23). By using the strain-gauges installed at the bottom of bituminous layers, it has been possible to follow the trend of the strains produced by the FWD impulsive load over time. Figure 8 shows an example strain-versus-time diagram obtained from the tests carried out; the measurement point in this case was on the perpendicular line that crosses the center of the loading plate. On the basis of these measurements, it was possible to evaluate the frequency of application of the FWD load; a value of 8 Hz was found. The temperatures considered applicable from the E_1 and E_2 moduli are the average temperatures of the two layers that are assumed to constitute all of the bituminous pavement layers. It is possible to determine such average temperatures when the gradient of the temperature related to depth inside the pavement

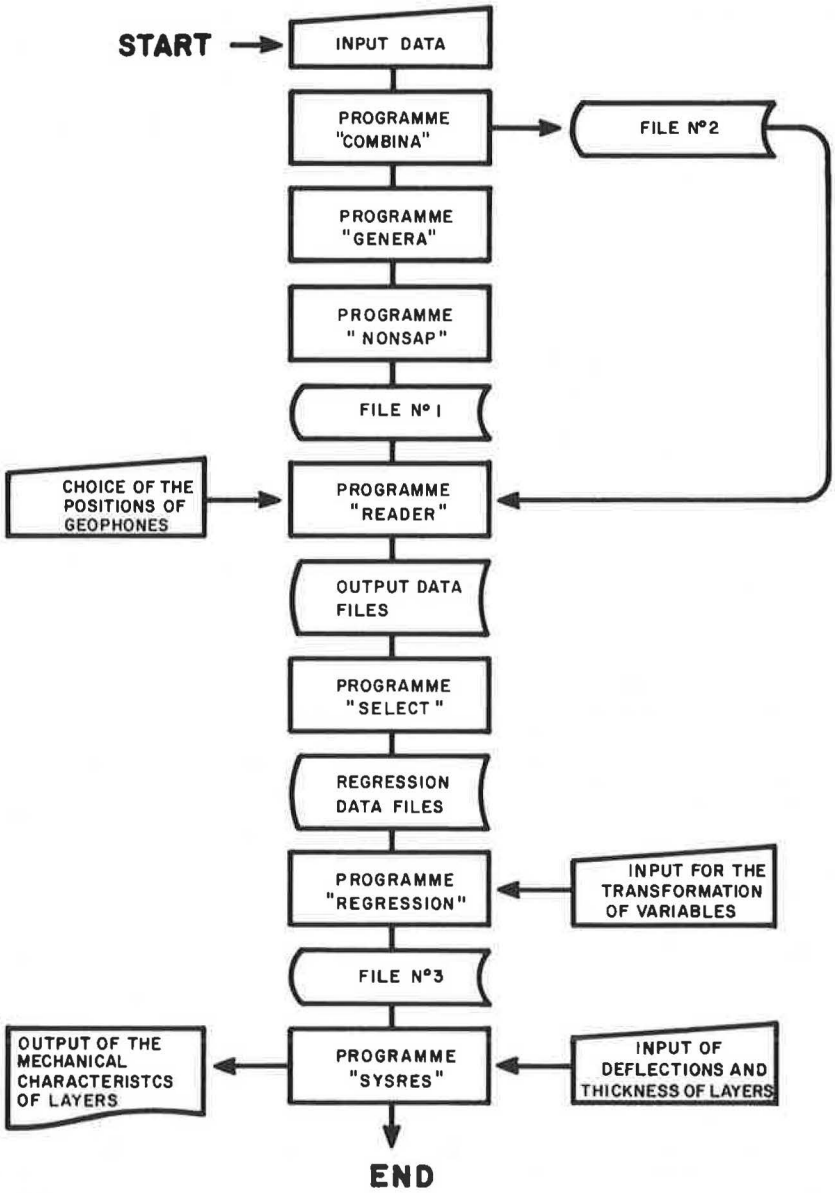

FIGURE 7 Flowchart of the procedure adopted.

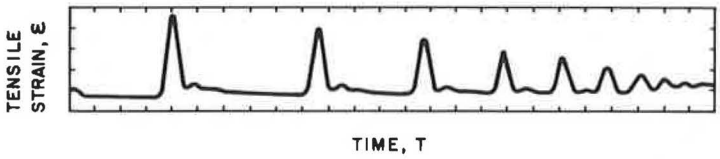

FIGURE 8 Tensile strain at the bottom of the bituminous layers due to the load applied by the FWD (the peaks following the first are caused by the bounces of the falling weight).

is known. For this purpose, the temperatures at the pavement surface and at a point located at a depth of about 5 cm were measured at the time of the test.

EVALUATION OF CEMENT-TREATED-BASE MODULI BY FWD

An interesting practical application of this method was the evaluation of the moduli of cement-treated bases in semi-rigid pavements.

The moduli of pavements with cement-treated bases are given in Tables 3 and 4, which relate to new and restored pavements, respectively. The data in Table 3 indicate that the cement-treated-base moduli of new pavements, for which the material was mixed in a plant with a cement content of about 2.5 percent), was in the range of 5000 to 6000 MPa.

This table also gives the elastic modulus of a layer obtained with a high-furnace-slag and lime mix. The elastic modulus of the layer was found to be quite high, ranking around 10 000 MPa.

In Table 4 data on two cement-treated bases (the

TABLE 3 Moduli Evaluated with PA.STR.EV. Program—New Pavements

Motorway	Years After Construction	Temperature of Asphalt Concrete (°C)	Percentage of Cement in Cement Mix Layer	Modulus of Bituminous Layers (MPa)	Modulus of Cement-Treated Base (MPa)
A14[a]	11	3	2.5	11,560	5,138
A30	6	25	2.5	5,912	5,312
Nardò test track	4	35	2.5	2,493	5,965
A14	8	24	–[a]	2,640[b]	9,561

[a]20 percent slag plus 1 percent hydrated lime.
[b]Cracked layers.

TABLE 4 Moduli Evaluated with PA.STR.EV. Program- Restored Pavements

Motorway	Time After Restoration	Temperature of Asphalt Concrete (°C)	Percentage of Cement in Cement Mix Layer	Modulus of Bituminous Layers (MPa)	Modulus of Cement-Treated Base (MPa)
A1	6 days	43	4.6	2,124	2,127
A1	8 days	34	4.6	5,089	2,731
A1	3 months	20	4.6	7,690	6,925
A1	2 months	22	4.6	6,473	4,824
A4	2 years	17	2.6	3,955	1,329

material was mixed in situ during a deep restoration work) with a high cement percentage are given. The modulus develops during the phase of mix hardening from a value of about 2500 MPa (about 1 week after its construction) to a value ranging between 4500 and 7000 MPa (approximately 3 months after its construction).

The final example refers to a restored pavement with an in-plant mixed cement-treated base. In this case transverse cracks were found every 50 cm. Thus the elastic modulus is rather low in comparison with the previous values (about 2000 MPa).

CONCLUSIONS

The most immediate use of the FWD appears to be related to the field of maintenance operations on distressed pavements, for which an optimum rehabilitation strategy must be selected. Once the real structural condition of the pavement is determined by means of the described procedure, it is possible to calculate the remaining pavement life on the basis of the stress distribution induced by traffic loads and by considering the pavement as a homogeneous section.

It is also possible to evaluate the remaining life that corresponds to different maintenance operations and to evaluate which is more likely to be successful. Planning of the preferable maintenance operations may follow. Another use of the FWD procedure is in recording the evolution of the elastic characteristics as a function of the traffic of the materials volume. Finally, this method can be used as a check on just constructed or restored pavements to determine compliance with new specifications regarding materials moduli.

REFERENCES

1. N.W. Lister and C.K. Kennedy. A System for the Prediction of Pavement Life and Design of Pavement Strengthening. Proc., 4th International Conference on Structural Design of Asphalt Pavements, Ann Arbor, Mich., 1977.
2. R.C. Koole. Overlay Design Based on Falling Weight Deflectometer Measurements. In Transportation Research Record 700, TRB, National Research Council, Washington, D.C., 1979, pp. 59-72.
3. J. Sharma and R.N. Stubstad. Evaluation of Pavement in Florida by Using the Falling Weight Deflectometer. In Transportation Research Record 755, TRB, National Research Council, Washington, D.C., 1980, pp. 42-48.
4. P. Ullidtz. Predicting Pavement Response and Performance for Full-Scale Testing. Presented at International Colloquium on Full-Scale Pavement Tests, E.T.H., Zurich, Switzerland, May 1982.
5. P. Ullidtz. Overlay and Stage-by-Stage Design. Proc., 4th International Conference on Structural Design of Asphalt Pavements, Ann Arbor, Mich., 1977.
6. A. Bohn, P. Ullidtz, R. Substad, and A. Sorensen. Danish Experiments with French Falling Weight Deflectometer. Proc., 3rd International Conference on Structural Design of Asphalt Pavements, London, England, 1972.
7. G. Camomilla and M. Malgarini. Nuovi metodi per la misura della capacità portante delle pavimentazioni. Autostrade, n. 5, May 1983.
8. R.W. May and M.W. Witczak. Effective Granular Modulus to Model Pavement Response. In Transportation Research Record 810, TRB, National Research Council, Washington, D.C., 1981, pp. 1-9.
9. J. Moossazadeh and M.W. Witczak. Prediction of Subgrade Moduli for Soil that Exhibits Nonlinear Behavior. In Transportation Research Record 810, TRB, National Research Council, Washington, D.C., 1981, pp. 9-17.
10. S.F. Brown and J.W. Pappin. Analysis of Pavement with Granular Bases. In Transportation Research Record 810, TRB, National Research Council, Washington, D.C., 1981, pp. 17-23.
11. G. Rada and M.W. Witczak. Comprehensive Evaluation of Laboratory Resilient Moduli Results for Granular Material. In Transportation Research Record 810, TRB, National Research Council, Washington, D.C., 1981, pp. 23-33.
12. J.M. Dancan, C.L. Monismith, and E.L. Wilson. Finite Element Analyses of Pavement. In Highway Research Record 228, HRB, National Research Council, Washington, D.C., 1968, pp. 18-33.

13. N.C. Yang. Design of Functional Pavements. McGraw-Hill, New York, 1977.
14. S.K. Wang, M. Sargious, and Y.K. Cheung. Advanced Analysis of Rigid Pavements. ASCE, Transportation Engineering Journal, Feb. 1972.
15. R. Pichumani, J.E. Crowford, and G.E. Triandafilidis. Finite Element Analysis of Pile-Supported Pavement Structures. ASCE, Transportation Engineering Journal, May 1974.
16. M. Agostinacchio. L'impiego del metodo degli elementi finiti per il calcolo delle pavimentazioni stradali. Presented at XIX Convegno Nazionale Stradale, Rimini, Italy, 1982.
17. K.J. Bathe, E.L. Wilson, and R.H. Iding. NONSAP: A Structural Analysis Program for a Static and Dynamic Response of Nonlinear System. Report UCSESM 74-3. University of California, Berkeley, Feb. 1974.
18. K.J. Bathe, H. Ozdemir, and E.L. Wilson. Static and Dynamic Geometric and Material Nonlinear Analysis. Report UCSESM 74-4. University of California, Berkeley, Feb. 1974.
19. C.A. Brebbia and J.J. Connor. Fondamenti degli elementi finiti. CLUP Edizioni (undated).
20. O.C. Zienkiewcz and K. Cheung. The Finite Element Method in Structural and Continuum Mechanics. McGraw-Hill, London, England, 1967.
21. E.L. Wilson. Structural Analysis of Axisymmetric Solids. A.I.A.A. Journal, Vol. 3, No. 12, 1967.
22. N.R. Draper and H. Smith. Applied Regression Analysis. Wiley, New York, 1967.
23. G. Battiato, G. Camomilla, M. Malgarini, and C. Scapaticci. Misure dell'aggressività del traffico merci sulle pavimentazioni. Autostrade, n. 1, Jan. 1983.

Influence of Relative Rigidity on the Problem of Reflection Cracking

A. O. ABD EL HALIM

ABSTRACT

Reflection cracking of bituminous overlays on rigid pavements has been known for a long time, and many studies have been conducted based on theoretical and experimental investigations. As a result a number of solutions were tried, but in most cases performance was reported as poor to fair. A recent investigation oriented toward the use of a plastic mesh to reinforce asphalt pavements resulted in the development of a new analytical approach that helps explain the actual causes of reflection cracking in bituminous overlays. The new approach adopts the principle of "relative rigidity" to analyze the pavement structure at the time of construction. Results of the analysis have indicated that the critical interface is the one at the top surface of the softer hot asphalt layer. In addition, the analysis points out the importance of selecting different types of compactors to keep the integrity of the underlying rigid layer. Finally, the analysis emphasized that experimental investigations must consider the critical conditions that occur at the time of construction.

As a result of an experimental program to investigate the effectiveness of plastic geogrid reinforced pavement (1-3), a number of on-road and off-road paved trials were planned and carried out, including two test locations in southern Ontario. (Note that data on the test locations are from two unpublished reports: R.C. Haas, "Notes on the Problems of Installing Tensar Geogrid in Asphalt Pavement Construction," March 29, 1983; and A.O. Abd El Halim, "Report on Tensor Mesh Paving Trial," December 8, 1981.) Some of the problems encountered were buckling of the mesh, cracks after the completion of compaction, and separation between the mesh and the asphalt. Preliminary analyses were conducted to find out what happened and how these problems could be overcome. If brief, the analysis indicated that two types of actions were the main contributors to the observed problems. The first type of action was caused by certain properties of the reinforcing layer, such as temperature effects, inadequate tension, and imperfection of the geometry of the mesh (still in initial stages at the time of the test trials). The other type of action was caused by the interactions among the compactor, the reinforcement layer, the asphalt layer, and the subgrade. It should be added here that several grid types were used in the second trial (off-road), including differing heat setting treatments, and different ten-

sion methods and fastening techniques. Observations of the problems in the latter trial suggested that the main cause of the problems was the interaction between the aforementioned components rather than the undesirable properties of the reinforcement.

Based on these observations, a third trial was carried out. (Note that data are from an unpublished report by A.O. Abd El Halim, J. Gough, and R.C. Haas, "Off-Road Paving Trials with Tensar Geogrid at Genstar Quarry, Burlington, Ontario, April 27-28, 1983," May 5, 1983.) The third trial differed from the previous two trials in the type of the subgrade under the reinforced layer. Although the underlying layer in both previous trials was relatively rigid (cold asphalt layer in the first and concrete layer in the second), the subgrade in which the third trial was carried out was soft clay. Observations of the third field trial suggested that most of the problems encountered on the other two sections were overcome. It is too early to claim that all the problems have been solved; nevertheless, the results were encouraging.

The most important conclusion drawn from these field trials was that a more in-depth analysis has to be conducted on to the exact structure at the time of construction (e.g., type of compactor, order of rigidities of the layers, and subgrade conditions).

It is postulated in this paper that investigating the pavement structure at the time of construction could provide important answers to one of the most troublesome problems facing the pavement engineers today, namely, reflection cracking. The role of relative rigidity or stiffness mismatch in the components of the structure are postulated as a primary contributor to these problems.

RELATIVE RIGIDITY OF PAVEMENT STRUCTURE

The transfer of stresses among the various components of a multiphase elastic material or a multicomponent elastic structure is influenced by the relative stiffness characteristics of the separate components. The influence of relative rigidity on the load transfer characteristics can be illustrated by a flexible plate resting on an elastic soil mass subjected to a uniform load distribution at the surface (Figure 1). The relative rigidity between the plate and the elastic soil mass is governed by two basic parameters: the modular ratio Ep/Es, where Ep is the modulus of elasticity of the plate and Es is the elastic modulus of the soil; and the ratio t/a, where t is the thickness of the plate and a is its radius. When the primary mode of load transfer between the plate and the soil mass is flexural interaction between the plate and the soil mass, the dominant relative rigidity parameter R takes the form (4):

$$F = (Ep/Es)\ (t/a)^3 \qquad (1)$$

When R became large (i.e., R >>1) the plate behaves as a rigid plate, and as R becomes small (i.e., R <<1) the plate exhibits flexible characteristics. The relative rigidity between the plate and the elastic soil medium affects the mode of load transfer between the two systems and results in displacement and stress distributions in the plate and the soil region. Figure 1 shows the typical contact stresses that will be observed at the plate-soil mass interfaces as the relative rigidity of the system varies from the flexible to the rigid case.

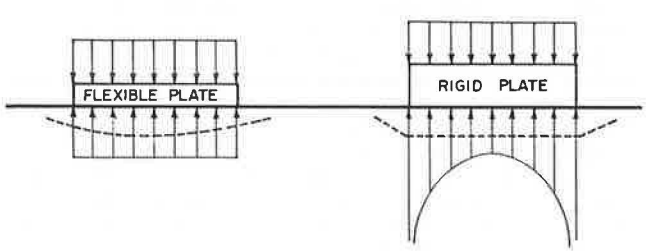

FIGURE 1 Stress and deflection distribution.

The pavement structure is also a system in which several components interact, and this interactive response is influenced by the relative rigidity characteristics of the various components. In the case of a new asphalt layer on top of a rigid concrete layer, the components include the subgrade, the rigid layer, the compacted and uncompacted hot asphalt, and the compaction device. At different stages of the construction of the pavement structure, the relative rigidity between the various components changes.

THEORETICAL MODELING

Figure 2 shows the four time stages that the existing pavement structure experiences. Case I represents the conditions just before overlay construction has started (time T_0). It can be seen that for this case the top layer is more rigid than the underlying layer, as indicated by the rigidity coefficients R_1 and R_2, respectively ($R_1 > R_2$).

This structure would be capable of transferring the applied stress due to the traffic load from the upper rigid layer to the underlying more flexible layer. Thus the first assumption is

> 1. In order to transfer stresses and strains between successive layers, the rigidity of the upper layer must be larger than the second upper layer, i.e., $R_i > R_{i+1}$ for all layers in the structure.

At the time of overlay construction [time T_1 (Case II)], a different structure is developed. First, one more layer with lower rigidity is added to the existing structure; the hot asphalt layer clearly has a low value of rigidity when compared with the rigidity of the concrete layer. It is therefore postulated here that the structure in Case II represents a distorted system as far as the first assumption is concerned. As a result of this distortion in the order of stiffness in relation to the load's direction, the second assumption is as follows:

> 2. For any layered system, the addition of one or more layers on top of a given supporting structure would not result in any significant increase of the total rigidity of the system if any of the additional layers has a lower rigidity than the rigidity of any of the existing layers.

As shown in Figure 2 (Case II), R_2 of the hot asphalt layer is expected to be much smaller than R_1 of the concrete. As a result of this second assumption, the total rigidity of the system in Case II would be less than the total rigidity of the system in Case I, although more thickness was added. However, at this stage in the construction, the structure in Case II is in stable condition because loads have not been applied onto it. As the compaction of the asphalt starts, a complex situation results. The use of a steel compactor would result in a more distorted structure because of the immediate existence of a high rigid body on top of a structure of lower rigidity. Because of assumption 2, the

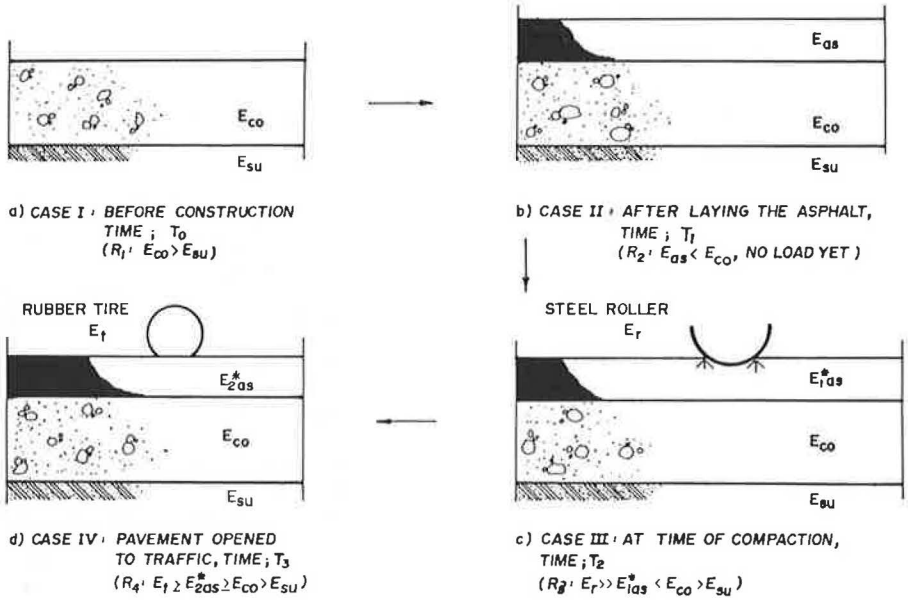

FIGURE 2 Four time stages of a new asphalt overlay.

distortion of the order of rigidities ($R_{load} > R_{asp} < R_{conct} > R_{sub}$) of the system in Case II, the third assumption could be stated:

> 3. For a distorted system, if a load is applied whose rigidity is extremely higher than the immediate underlying layer, deformation or "failure" should be expected to occur in this layer.

In other words, for the structure shown in Case II at time T_2, the top layer (hot asphalt) with the smaller value of R will deform under the effect of the steel compactor. This deformation is in addition to the compacting effect produced by the imposed stresses. Furthermore, it is postulated that this deformation is independent of the stress value and only occurs because of the extremely high relative rigidity of the steel compactor in addition to the disorder observed in the rigidities of the pavement. Clearly, this hypothesized deformation could take different modes or shapes, such as cracks, separation, or waving.

In the following section these assumptions are thoroughly investigated and verified by using a multilayer elastic computer program called BISAR (5).

APPROACH OF VERIFICATION

The approach for treatment of the pavement structure in the light of the theoretical discussion is based on the principle of distortion or failure caused by the disorder of the system rigidities. Therefore, the following steps were carried out to verify the presented theory:

1. Establish a criterion that relates distortion to relative rigidity,
2. Use the results of step 1 to prove the concept of disorder rigidities versus matched rigidities,
3. Demonstrate that this concept is independent of the value of the applied load on the pavement structure, and
4. Indicate how to apply this theory once it is approved to the problem of reflection cracking.

Distortion Criterion

In mechanics it is well-known that the radius of curvature of a deflected beam is a function of both the stiffness of the beam and the computed moment. For simplicity of the analysis, a coefficient termed α, which indicates the distortion criterion, is defined as "the slope of deflection of the deflected interface tan θ used instead of the radius of curvature; then for one layer a coefficient α would represent the ratio between tan θ_1 and tan θ_2 for the two interfaces of the layer in question, as shown in Figure 3."

From the definition,

$$\alpha = \tan \theta_2 / \tan \theta_1 = r_1 / r_2 \qquad (2)$$

Clearly, when $\alpha = 1$, the structure could be evaluated as sound (e.g., case of a simple beam), and when $\alpha \neq 1$, the structure is distorted.

For the values of $\alpha < 1$, the failure is at the location of tan θ_1 (i.e., upper interface) and when $\alpha > 1$, the failure is expected to be in the bottom interface. It is worth noting here that simple beams that fail in tension would have $r_1 > r_2$ at the time of failure (i.e., $\alpha > 1$).

Distorted Versus Stable Structures

The coefficient established in the previous step was used in the analysis of more than 60 different pavement structures (1). Figure 4 represents the geometry and variables considered in this step. The results of this analysis are shown in Figure 5. It is clear from the figure that two different systems exist. The first is group A, which represents the stable structures with relative rigidities in order (i.e., $E_i > E_{i+1}$), whereas the structures in group B represent distorted systems and therefore need to be corrected. The value of α for structures in group B is less than 1, which indicates failure at the top interface (i.e., surface of the structure).

Influence of Stress

The third step of the analysis was carried out to investigate the effect of increasing the load value

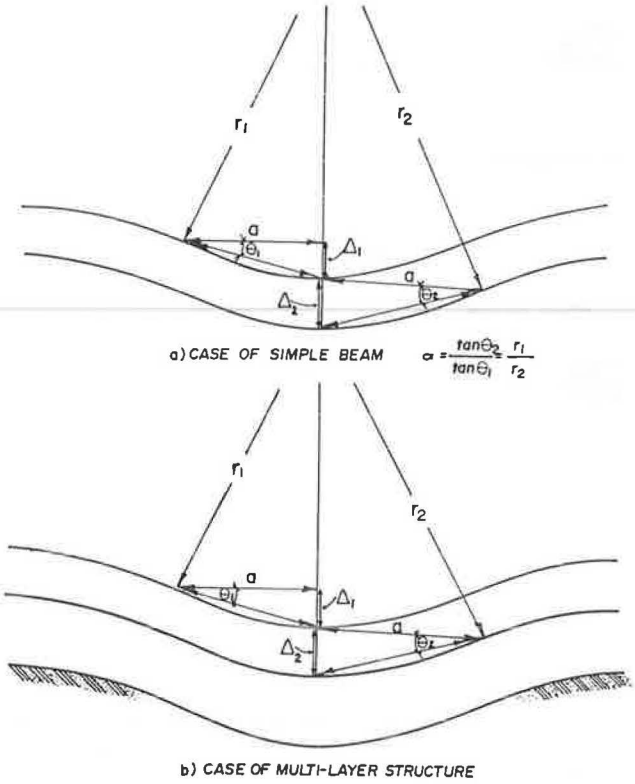

FIGURE 3 Details of the coefficient of distortion.

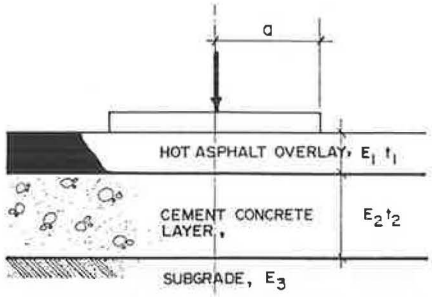

FIGURE 4 Outline of analyzed pavement structures.

and in turn the applied stresses on the computed value of α. As expected, the coefficient α proved to be independent of the value of the stress, as shown in Figure 6. This verifies the third assumption.

The results of these three steps could be summarized as follows:

1. The discussed theoretical modeling is sound;
2. The existence of a distortion in the pavement structures because of the disorder of the layer rigidities is proved;
3. The problem is not stress associated; therefore, reducing or increasing the loads has no effect on the output; and
4. The value of α in all the analyzed structures was less than unity, which indicates that the upper interface is a distorted one.

The presence of a soft layer with lower rigidity can be represented by the practice of overlaying cement concrete pavement at the time of construction. Therefore, the results of these analyses have led to the application of the same approach to investigate the problem of reflection cracking.

Influence of Relative Rigidity on Reflection Cracking

The problem of reflection cracking has been investigated and analyzed by many researchers (5-7). The recommended number of solutions for the problem to date has exceeded 10. These solutions range from using reinforced steel mesh in the asphalt overlay to the breaking of the existing rigid layer into smaller sizes (8-10). However, almost none of these investigations has looked into the problem at the time of construction. In the analysis carried out in this paper, two important results are related to reflection cracking. First, there is the existence of a distorted rigidity system in the pavement structure and the presence of a steel compactor on top of it. Second, the critical interface is shown to be the top one and not the one at the bottom. Most of these solutions treat the structure when it is opened to traffic and therefore analyze the structures in group A in Figure 5, which would suggest a stress-associated problem that must deal with the lower interface. Also, as is shown in the analysis, the

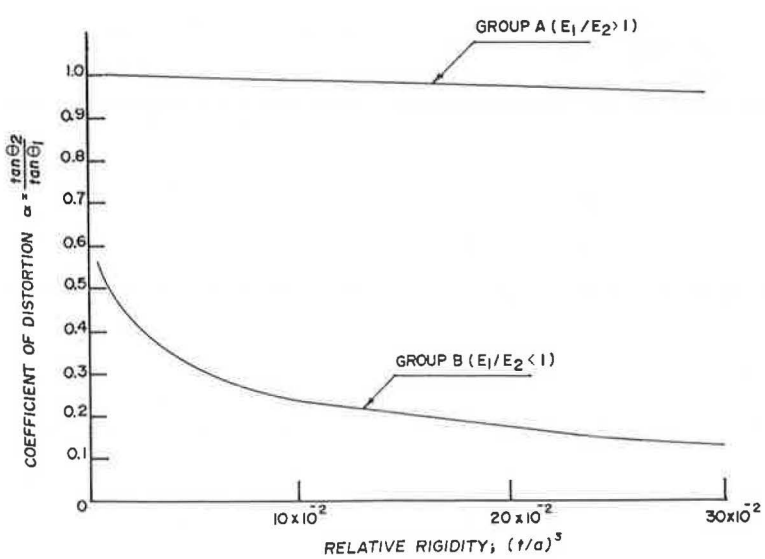

FIGURE 5 Influence of relative rigidity on pavement distortion.

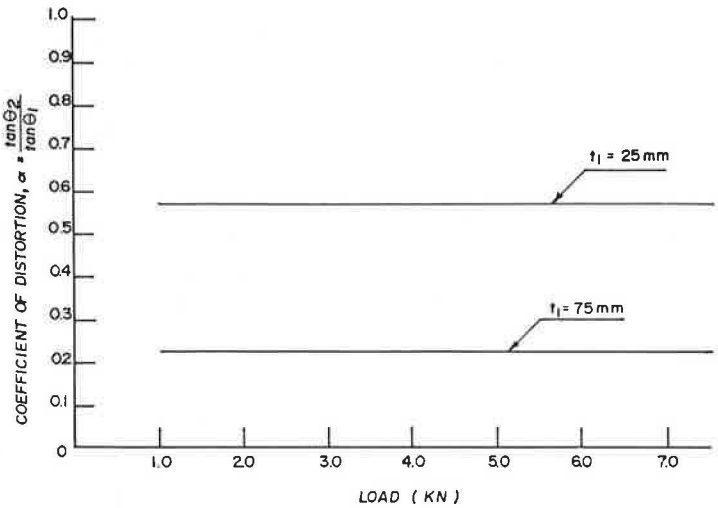

FIGURE 6 Relationship between applied load and coefficient of distortion.

presence of the crack in the existing rigid layer was not considered, yet the results indicate that cracks or deformation would exist in the top surface. Furthermore, the curve in Figure 5 would suggest that existance of cracks in the rigid layer (which could result in reducing its stiffness and therefore its rigidity) helps minimize the problem at the top. This is supported by field evidence that recommends the breaking of the rigid layer into small blocks, that is, increasing the number of cracks at the bottom (10,11). The analysis given in this section would suggest the following:

1. Reflection cracking is a construction problem that can develop at the very time the compactor rolls on the asphalt.
2. Very thin hair cracks could develop at the surface with the possibility of arresting them at the location of underlying crack.
3. These downward cracks would result in a loss in the total thickness of the overlayer and with traffic loading the remaining thickness would crack in fatigue over a short period of time.
4. The effect of cold cycles is not the main cause of reflection cracking; instead it represents a catalyst (the author heard of the same problem on a recent trip to Egypt, where the weather is hot).

CONCLUSIONS AND RECOMMENDATIONS

The analysis carried out in this paper has indicated that two different pavement structures exist, depending on the order of their relative rigidities. The first type is the structure that is designed on stress-strength criterion, whereas the other follows a geometric criterion. Of interest is the relationship between these latter structures and the problem of reflection cracking. Identifying the problem in the light of this new concept is a positive step in the right direction to solve the so-called reflective cracking problem.

Furthermore, the analysis indicated that the critical interface is the top one; therefore a more in-depth analysis has to be given to the interaction between the steel compactor and the new asphalt layer when it is laid on top of a rigid cement concrete layer. Also, although increasing the thickness of the asphalt layer represents a proven solution, it should be noted that the main purpose of this layer is the smooth surface rather than structural strength. Clearly, the analysis here would reveal that increasing the thickness results in increasing fatigue life, but it would not affect the development of hairline cracks on the top of the layer. From these analyses it would appear that the most promising solution is to reduce the rigidity of the existing concrete layer and hence move the structure from group B to group A of Figure 5.

Finally, the following points could represent a guideline for the solution of the problem of reflection cracking:

1. If the concrete layer is to be kept intact, another compactor such as one with pneumatic tires should be used.
2. If a reinforcement layer is to be used, it must first be considered based on its function in reducing fatigue cracking rather than solving the reflection cracking problem. Furthermore, the presence of a steel reinforcement directly on top of the rigid layer would complicate the problem of reflection cracking, because it would increase the rigidity of the concrete layer at the time of compaction.
3. Investigating the problem in the laboratory should be considered at the time of construction as well as at the time of service.

ACKNOWLEDGMENTS

The author would like to express his gratitude to A.P.S. Selvadurai, Chairman of the Department of Civil Engineering at Carleton University; R.C. Haas, Chairman of the Department of Civil Engineering at the University of Waterloo; the Transportation Group at Alexandria University; and A. Gad El Karim, Chairman of the Department of Civil Engineering at M.T.C. in Cairo, Egypt, for their valuable contributions. This research was supported by the National Science and Engineering Research Council.

REFERENCES

1. A.O. Abd El Halim. Geogrid Reinforcement of Asphalt Pavements. Ph.D. thesis. University of Waterloo, Waterloo, Ontario, Canada, Sept. 1983.
2. A.O. Abd El Halim, R.C. Haas, and W.A. Phang. Geogrid Reinforcement of Asphalt Pavements and Verification of Elastic Theory. In Transportation Research Record 949, TRB, National Re-

search Council, Washington, D.C., 1983, pp. 55-65.
3. A.O. Abd El Halim et al. A New Method for Effective Reinforcement of Asphalt Pavements. Presented at Road and Transportation Association of Canada, Halifax, Nova Scotia, Canada, Sept. 1983.
4. A.P.S. Selvadurai. Elastic Analysis of Soil-Foundation Interaction. In Development in Geotechnical Engineering, Volume 17, Elsevier Scientific Publishing Co., New York, 1976.
5. D.L. DeJong, M.G.F. Puetz, and A.R. Korswagen. Computer Program BISAR--Layered System Under Normal and Tangential Surface Loads. External Report. Koninklyke/Shell-Laboratorium, Amsterdam, Netherlands, 1973.
6. J.B. MacMaster and W.E. Blum. Preventing Reflection Cracking. Presented at Miniworkshop, Canada/Japan Science and Technology Consultations, Vancouver, British Columbia, Canada, Oct. 18-22, 1982.
7. J.E. Noonan and F.R. McCullagh. Reduction of Reflection Cracking in Bituminous Overlays on Rigid Pavements. Research Report 80. Engineering Research and Development Bureau, New York State Department of Transportation, Albany (undated).
8. P.G. Velz. Effect of Pavement Breaker Rolling on Crack Reflectance in Bituminous Overlays. In Highway Research Record 11, HRB, National Research Council, Washington, D.C., 1963, pp. 85-88.
9. S.M. Kanarowski. Study of Reflection Cracking in Asphaltic Concrete Overlay Pavements. U.S. Army Corps of Engineers, Vicksburg, Miss., March 1972.
10. G.R. Korfhage. The Effect of Pavement Breaker-Rolling on the Crack Reflectance of Bituminous Overlays. In Highway Research Record 327, HRB, National Research Council, Washington, D.C., 1970, pp. 50-63.
11. C. Crawford. Cracking and Seating of PCC Pavements Prior to Overlaying with Hot Mix Asphalt, State of the Art. Information Series 91-5. National Asphalt Pavement Association, Riverdale, Md., 1984.

Suitability of Using the Falling Weight Deflectometer in Determining Deteriorated Areas in Jointed Rigid Pavements

MANG TIA, JOHN M. LYBAS, and BYRON E. RUTH

ABSTRACT

In this study the suitability of using the falling weight deflectometer (FWD) to determine deteriorated areas in rigid pavements was investigated. The FWD deflection basins of a few hypothetical concrete pavements of three types of deficiency conditions were calculated by using the finite-element analysis computer program WESLIQUID. These computed deflection basins were then compared with the deflection basin of a reference pavement that was in good condition. The three types of deficiency conditions studied were pavements with (a) weak subgrades, (b) voids in the subgrade beneath the concrete slab, and (c) deteriorated concrete slabs. Two FWD loading positions were considered: loading at the center of a pavement slab, and loading near the joint of the slabs. The results of the study indicate that the three different types of concrete pavement distress give three distinctly different FWD deflection basin shapes. The distinction among these three types of FWD deflection basins can be more easily understood by considering the differences between the FWD deflection of the pavement considered and that of a standard pavement of the same dimension that is loaded at the same position ($D-D_S$). The type and extent of the pavement distress could be determined from the shape and the magnitude of the $D-D_S$ plot. The results of the study also indicate that the effects of the joint are insignificant when the applied FWD load is far away from the joint.

In recent years the falling weight deflectometer (FWD) has been used by many state highway agencies in the evaluation of the performance of rigid and flexible pavements. The FWD test system consists of a loading system, a series of six or seven deflection sensors, and an automatic data recording system. The test system measures the deflection basin caused by a dynamic load on the pavement structure. The test load is applied by a weight dropped from a specified height to a circular loading plate. The falling weight load simulates to some degree the dynamic vehicular load on the pavement structure. The FWD test configuration is variable in terms of the radius of the loading plate, the magnitude of the applied load (by changing the drop height), and the positions of the deflection sensors. Currently, there are still no commonly accepted standard test configurations. Further study is needed to determine the most appropriate test configurations as well as the most effective use of the FWD in pavement evaluation.

One of the main functions of a pavement structure is to protect the subgrade from excessive deformation under the expected vehicular loads. As a pavement deteriorates with use, the deflection of the pavement under the same load increases. Although the magnitude of the maximum pavement deflection caused by an FWD load can indicate the degree of pavement deterioration, it is believed that the deflection basin can give indications of the type of structural deficiency encountered. Deterioration in a concrete pavement may be caused by (a) problems in the concrete material, such as delamination and cracking, caused by the use of poor quality materials or improper design and construction; (b) a weak subgrade, caused by a high water level or freezing and thawing; or (c) voids in the subgrade beneath the concrete slab, caused by the pumping action of water. It is envisioned that the deflection basins of the concrete pavement obtained from the FWD tests can be used to identify these three types of deficiency and to determine the extent of the deteriorated areas. An accurate determination of the type and extent of deterioration in concrete pavements will facilitate the proper selection of maintenance or rehabilitation methods on these pavements.

In this study the FWD deflection basins of a few hypothetical concrete pavements of various conditions were computed by using a finite-element analysis computer program. The theoretically computed FWD deflection basins were then evaluated to determine if they could be used to identify the type and extent of distress in concrete pavements. The three major types of pavement deterioration considered in this study were (a) poor concrete pavement materials, (b) weak subgrades, and (c) voids in the subgrade beneath the pavement slabs. Two FWD loading positions were considered in this study: loading at the center of a pavement slab, and loading near the joint of the slabs. The results from this theoretical study will provide an assessment of the usefulness of the FWD and a theoretical basis for further field testing and verification.

DESCRIPTION OF STUDY

Modeling of Concrete Pavements

The finite-element analysis computer program WESLIQUID, developed by the U.S. Army Corps of Engineers Waterways Experiment Station (1), was used to perform the computations. The WESLIQUID program models a concrete pavement slab as an assemblage of rectangular plate bending elements, and models the subgrade as a dense liquid by means of a series of linear elastic springs. It has the capability to model subgrade voids, slab boundaries, and joint conditions. Subgrade voids are modeled as gaps between the concrete slabs and the springs. Load transfers across a joint are modeled by means of shear and moment efficiencies. The efficiency of shear transfer is the ratio of vertical deflection along the joint between the unloaded (or less loaded) slab and the more heavily loaded slab. It is an effective way of modeling load transfer through dowel bars or aggregate interlocks at the joints. The efficiency of moment transfer is defined as the ratio between the actual moment and the full moment, which is determined by assuming that the rotations on both sides of the joints are the same. When a joint has a load transfer device such as a dowel or tiebar, which can resist a degree of bending moment, some moment transfer across a joint will be possible. However, in this study a moment transfer efficiency of zero was assumed in all analyses.

Modeling of FWD Loads

One of the higher FWD drops used by the Florida Department of Transportation (DOT) was used as the FWD load in the analyses in this study. This specific FWD drop produced a pressure of 217 psi (1500 kPa) on an 11.8 in. (300 mm) diameter load plate (2), with a total equivalent static load of 23.8 kips (106 kN). The FWD load was modeled as a static load of 23.8 kips applied uniformly over a 10.5 x 10.5-in. (266 x 266-mm) square area that resulted in a uniform pressure of 217 psi. The circular load plate was approximated by a square of the same area as required by the finite-element program.

Modeling of Distress Conditions

The three types of structural deficiency in concrete pavement as described earlier were considered in the analyses. Pavements with deterioration in the concrete slab were modeled as having a reduced stiffness (elastic modulus) in the concrete material. Pavements with a weak subgrade were modeled as having a reduced subgrade stiffness. Pavements with pumping problems and voids in the subgrade beneath the concrete slabs were modeled as having gaps of certain heights between the concrete slab and the spring support at the locations of the voids. These conditions are shown in Figure 1.

Research Approach

The deflection basins of a reference concrete pavement under an FWD load of 23.8 kips (106 kN) were computed for center load and joint load conditions. The reference concrete pavement used in the analyses represented a typical plain jointed concrete pavement of good condition. The concrete material was assumed to have an elastic modulus (E) of 4×10^6 psi (27.6 GPa), and a Poisson's ratio (μ) of 0.2. The subgrade stiffness was assumed to be 400 lb/in.^{3} (pci) (1.09×10^8 N/m^3), and there were no voids in the subgrade. The concrete slabs had a uniform thickness of 9 in. (229 mm), a length of 20 ft (6.1 m), and a width of 12 ft (3.7 m). When the center load was considered, a three-slab system was used in the analysis. When the joint load was considered, a two-slab system was used. These two cases are illustrated in Figures 2 and 3, respectively. Slabs farther away from the load do not have significant effects on the response of the pavement, and thus do not have to be considered in the analysis.

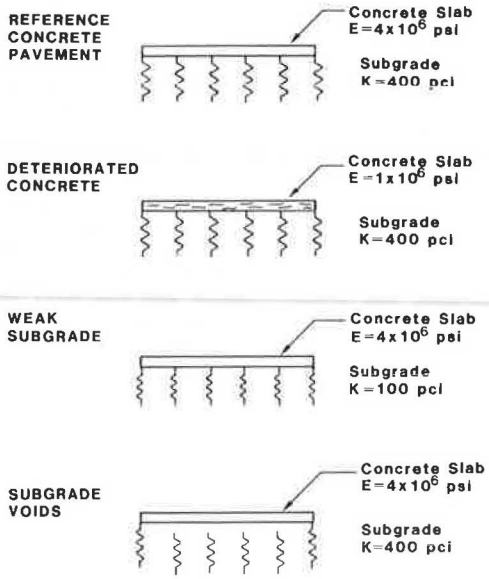

FIGURE 1 Modeling of distress conditions in concrete pavement.

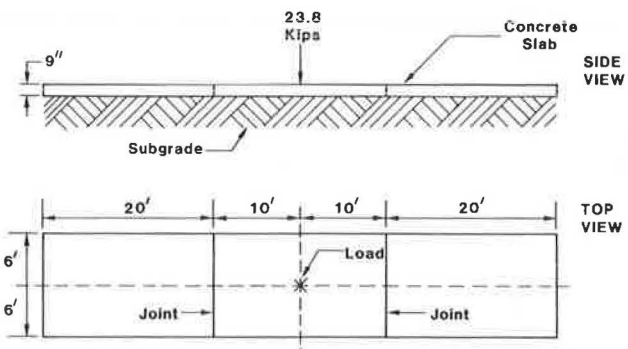

FIGURE 2 Three-slab system for analysis of center load.

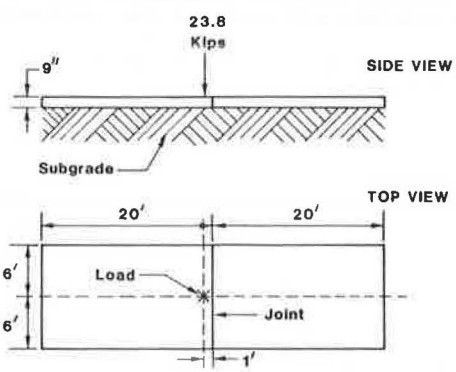

FIGURE 3 Two-slab system for analysis of joint load.

Computations were then made for the deflection basins of a few hypothetical deteriorated concrete pavements under the same FWD load (23.8 kips) at the same two positions (center and joint loads). The same dimensions (9 in. x 12 ft x 20 ft) of slabs were used. The computed deflection basins of these pavements were then compared with the deflection basins of the reference pavement.

RESULTS OF THE STUDY

Effects of Subgrade Stiffness and Joint Shear Transfer

The results of the analyses indicated that the FWD deflection basin would generally shift downward, while remaining in roughly the same shape, as the subgrade stiffness was reduced. The effects of subgrade stiffness on the computed FWD deflection basins of a concrete pavement loaded at the center of the slab are shown in Figures 4 and 5. Figure 4 shows the deflection plots along the longitudinal (or horizontal) line through the point of load, and

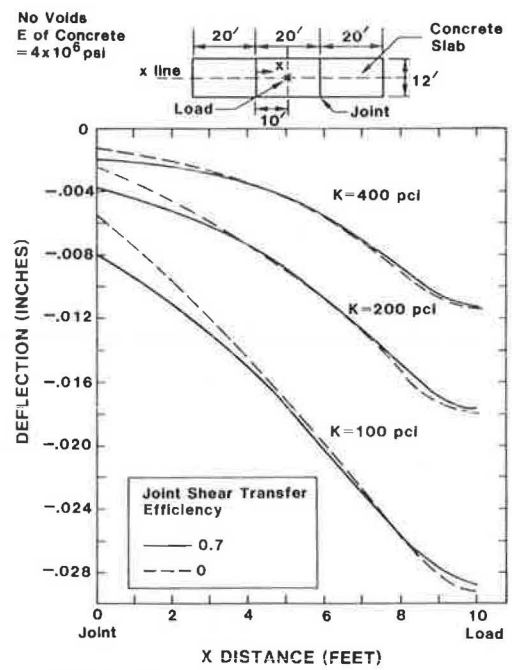

FIGURE 4 Effect of subgrade stiffness on computed longitudinal FWD deflection basins of a concrete pavement loaded at the center.

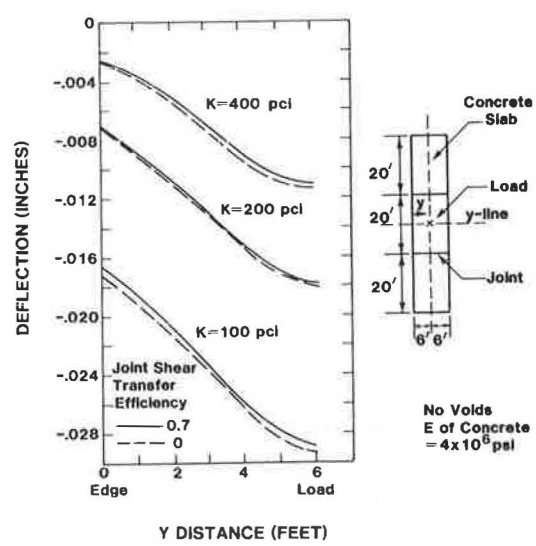

FIGURE 5 Effect of subgrade stiffness on computed transverse FWD deflection basins of a concrete pavement loaded at the center.

Figure 5 shows the deflection plots along the transverse (or vertical) line through the point of load.

Figures 6 and 7 show the effects of subgrade stiffness on the computed longitudinal and transverse FWD deflection basins of a concrete pavement loaded at a position 1 ft (305 mm) from the middle of the joint. The same trend can be observed here. As the subgrade stiffness was reduced from 400 to 100 pci (1.09×10^8 to 2.73×10^7 N/m^3), the FWD deflection basin shifted downward, while remaining in roughly the same shape.

Two joint shear transfer efficiencies were used in the analyses: 0.7 and 0. A joint shear transfer efficiency of 0.7 models the behavior of a good joint, across which a large portion of shear forces can be transferred. A joint shear transfer efficiency of 0 models a joint across which no shear forces can be transferred. The results of the analyses indicate that when the applied load is far away from the joint, the effects of joint shear transfer become insignificant. As seen in Figures 4 and 5, in the case of loading at the center of the slab, the FWD deflection basins computed from the use of a shear efficiency of 0.7 are not much different from ones that use a shear efficiency of 0. When the applied load is near the joint, the effects of the joint become significant. As shown in Figures 6 and 7, in the case of loading near the joint, the FWD deflection basins computed from the use of a shear efficiency of 0.7 are significantly different from ones that use a shear efficiency of 0.

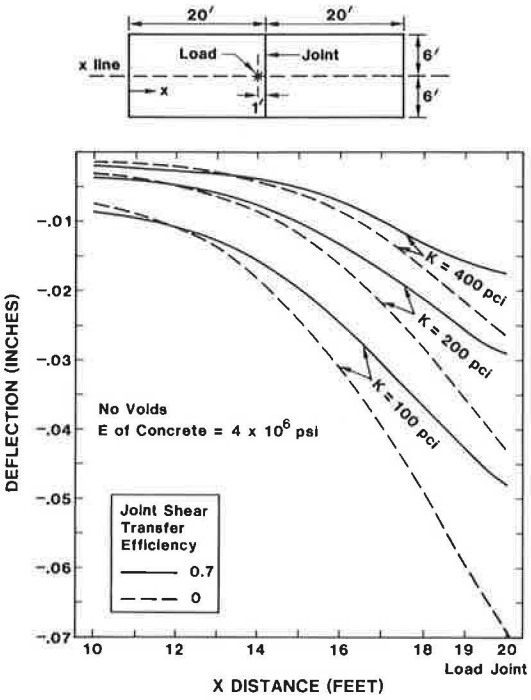

FIGURE 6 Effect of subgrade modulus on computed longitudinal FWD deflection basins of a concrete pavement loaded at the joint.

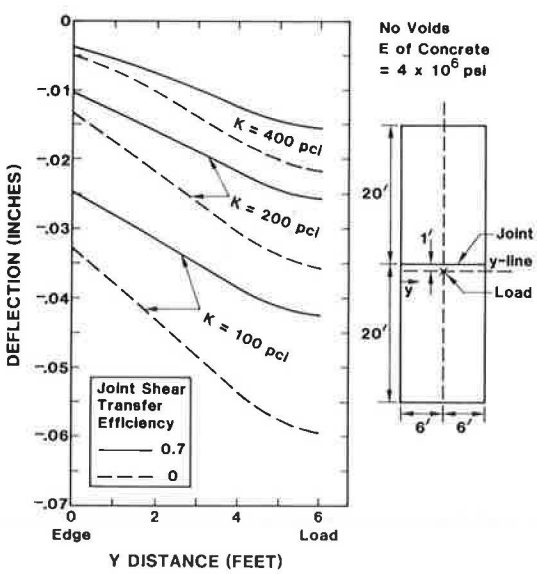

FIGURE 7 Effect of subgrade modulus on computed transverse FWD deflection basins of a concrete pavement loaded at the joint.

Effects of Subgrade Void Size

The effects of subgrade void size on the computed FWD deflection basins are presented in this section. Subgrade voids of a uniform depth of 0.75 in. (19 mm) and of various square areas were placed at the positions of the applied FWD load; deflection basins were computed by using a joint shear transfer efficiency of 0.7. The elastic modulus of the concrete was 4×10^6 psi (27.6 GPa) and the subgrade stiffness was 400 pci (1.09×10^8 N/m^3).

Figures 8 and 9 show the effects of subgrade void size on the computed longitudinal and transverse FWD deflection basins of a concrete pavement loaded at the center of the slab. It can be noted that the magnitude of the maximum deflection increases as the size of subgrade void increases. When compared with the deflection basin of the reference pavement that has no subgrade voids, it is noted that the more significant increase in deflection occurs at and near the locations of the voids.

Figures 10 and 11 show the effects of subgrade void size on the computed longitudinal and transverse FWD deflection basins of a concrete pavement loaded at a position 1 ft (305 mm) from the middle

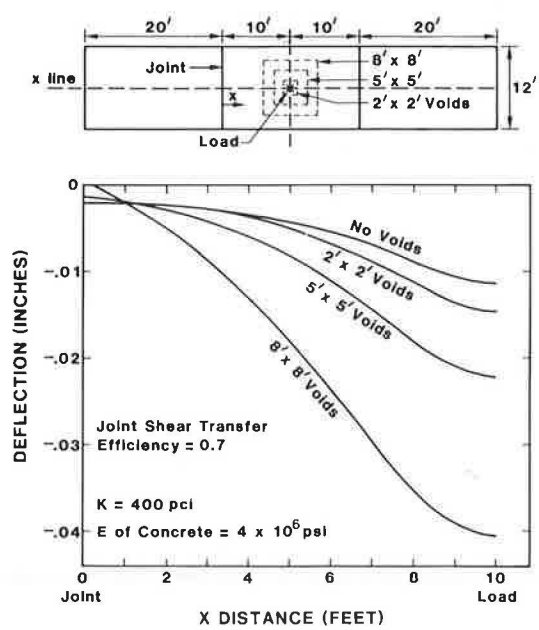

FIGURE 8 Effect of subgrade void size on computed longitudinal FWD deflection basins of a concrete pavement loaded at the center.

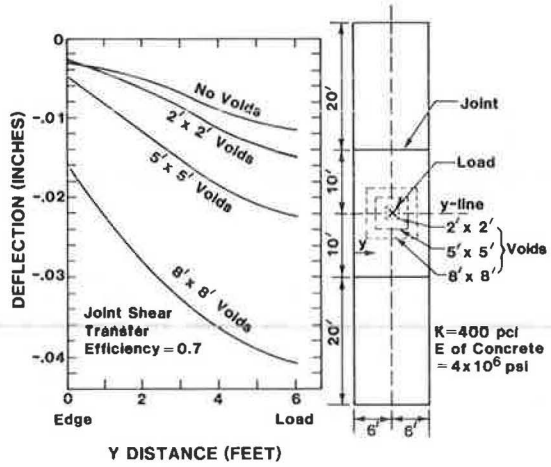

FIGURE 9 Effect of subgrade void size on computed transverse FWD deflection basins of a concrete pavement loaded at the center.

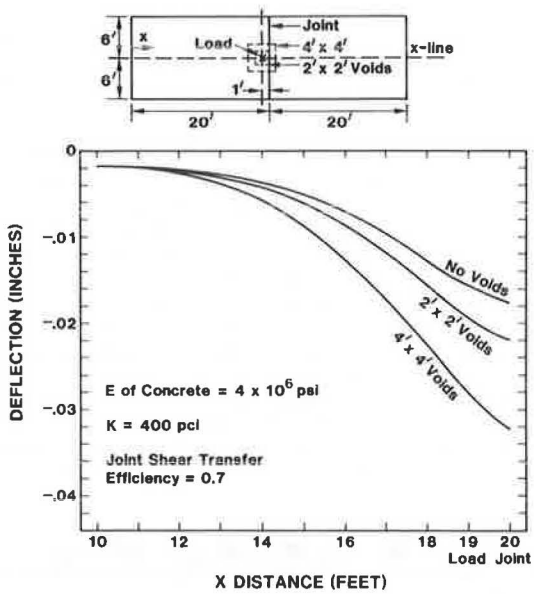

FIGURE 10 Effect of subgrade void size on computed longitudinal FWD deflection basins of a concrete pavement loaded at the joint.

of the joint. The same trend can be noted here. The more significant increase in deflection, when compared with the deflection basin of the reference pavement, occurs at and near the locations of the voids.

Effects of Elastic Modulus of Concrete

Pavements with deterioration in the concrete slab were modeled as having a reduced elastic modulus in the concrete material. The effects of reduced elastic modulus of concrete on the computed FWD deflection basins are presented in this section.

Figures 12 and 13 show the effects of elastic modulus of concrete on the computed longitudinal and transverse deflection basins of a concrete pavement loaded at the center of the slab. A subgrade stiffness of 400 pci (1.09 x 10^8 N/m^3) and a joint shear transfer efficiency of 0.7 were used to model pavement behavior. It can be noted that the magnitude of the maximum deflection increases as the elastic modulus of the concrete pavement material decreases. When compared with the deflection basin of the reference pavement, note that the more significant increase in pavement deflection (with the decrease in elastic modulus of concrete) occurs only at and near the applied load. At more than a certain distance [about 3 ft (0.9 m) in this case] away from the load, the change in elastic modulus of concrete has little effect on pavement deflection.

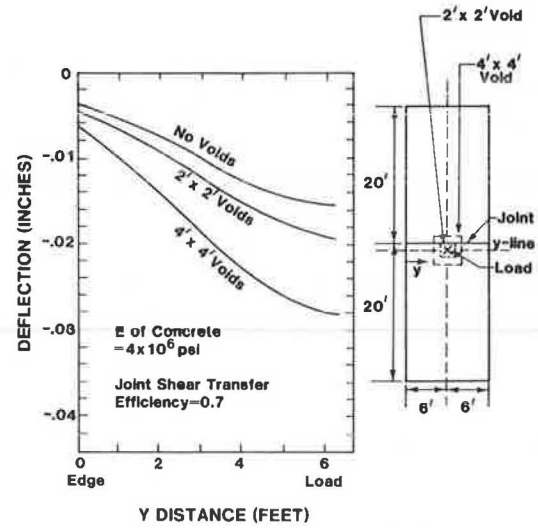

FIGURE 11 Effect of subgrade void size of computed transverse FWD deflection basins of a concrete pavement loaded at the joint.

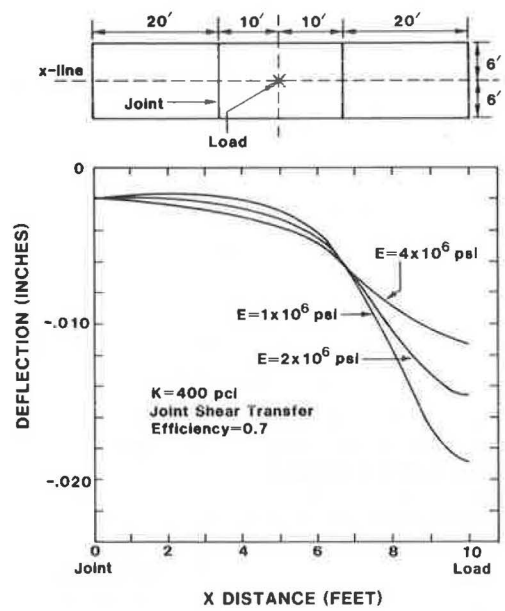

FIGURE 12 Effect of elastic modulus of concrete on computed longitudinal FWD deflection basins of a concrete pavement loaded at the center.

Use of FWD Deflection Basins

It is clear from the results presented in the previous section that the three different types of structural deficiency in concrete pavements give three distinctly different FWD deflection basin

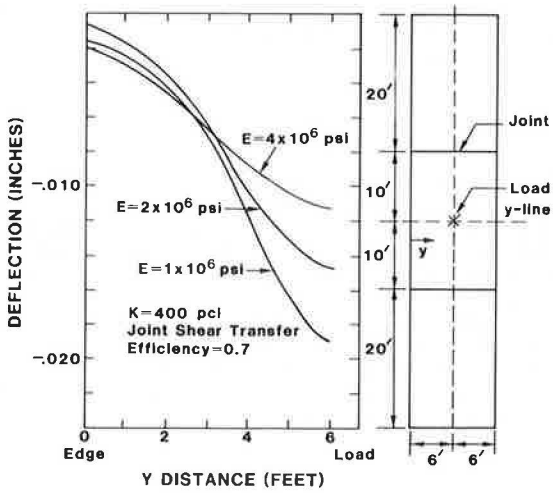

FIGURE 13 Effect of elastic modulus of concrete on computed transverse FWD deflection basins of a concrete pavement loaded at the center.

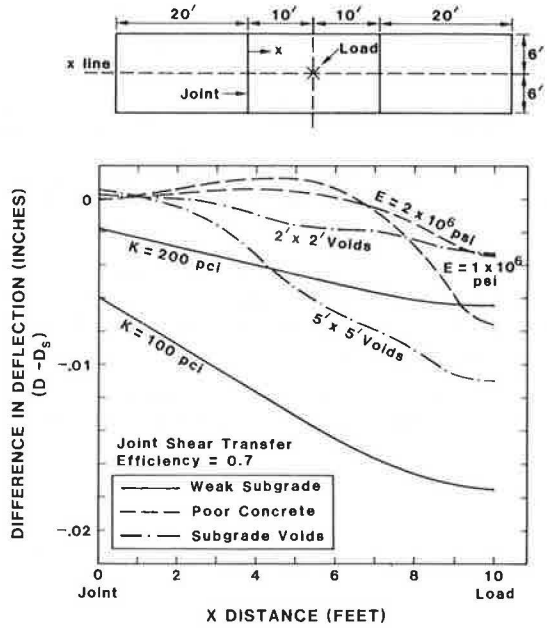

NOTE: D - Deflection of the pavement system considered
D_S - Deflection of the standard pavement system ($E = 4 \times 10^6$ psi, K = 400 pci)

FIGURE 14 Difference in computed longitudinal FWD deflection of a concrete pavement loaded at the center.

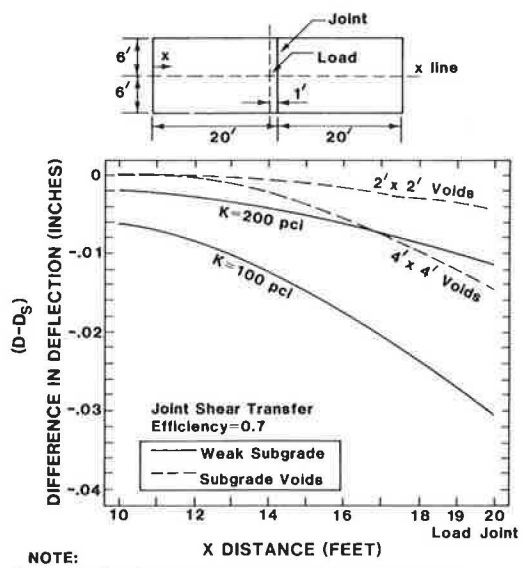

NOTE:
D —— Deflection of the Pavement System Considered
D_S —— Deflection of the Standard Pavement System ($E=4 \times 10$ psi, K=400 pci)

FIGURE 15 Difference in computed longitudinal FWD deflection of a concrete pavement loaded at the joint.

shapes. Although the shape of the FWD deflection basin appears to be related to the type of distress, the magnitude of the FWD deflection appears to be related to the severity of the distress conditions. When compared with the FWD deflection basin of a reference concrete pavement of good condition, the deflection basin of a concrete pavement with a weak subgrade is relatively higher in magnitude while having roughly the same shape. The FWD deflection basin of a concrete pavement with voids in the subgrade reveals relatively higher deflections at and near the location of the voids. The FWD deflection basin of a pavement with deterioration in the concrete slab reveals relatively higher deflections at and near the position of the FWD load.

The distinction among these three types of FWD deflection basins can be more easily seen by considering the differences between the FWD deflection of the pavement considered (D) and that of a standard pavement (D_S) of the same dimension, loaded at the same position. Figure 14 shows the plots of these differences in deflection ($D-D_S$) for the computed longitudinal FWD deflection of a concrete pavement loaded at the center. For the three types of concrete pavement deficiency, three distinctly different families of $D-D_S$ plots can be observed. The $D-D_S$ plot for the weak subgrade condition is nearly linear, and slopes downward toward the position of the FWD load. The $D-D_S$ plot for the pavement with subgrade voids is approximately equal to zero at some distance away from the location of the voids, and curves downward sharply at and near the location of the voids. The $D-D_S$ plot for the deteriorated concrete condition is approximately equal to zero at some distance away from the FWD load, turns slightly upward as it moves toward the load, and then curves downward sharply as it approaches the load. An increase in the deterioration condition is indicated by an increase in the magnitude of the $D-D_S$ plot.

Figure 15 shows the $D-D_S$ plots for the longitudinal FWD deflection of a concrete pavement loaded at the joint. The two pavement deficiency types shown in this figure are the weak subgrade condition and the subgrade voids condition. Similar trends are observed here. The $D-D_S$ plot for the weak subgrade condition slopes downward toward the position of the FWD load in a nearly linear fashion. The $D-D_S$ plot for the condition of the subgrade voids is approximately equal to zero at some distance away from the location of the voids, and curves downward sharply at and near the location of the voids.

In order to use the FWD deflection basins effectively for determining deteriorated areas in rigid pavement, the FWD deflection basin of a reference pavement of known properties must be obtained first. The type and the extent of the pavement distress can then be determined from the shape and magnitude of the $D-D_S$ plot.

CONCLUSIONS

The results of this analytical study indicate that the deflection basins measured by the FWD could be used to determine the type and severity of structural deficiency distress in a jointed rigid pavement. The effective use of these FWD deflection basins would require comparing them with the FWD deflection basin of a reference pavement of the same dimension and loaded at the same position. The results of the study also indicate that the effects of the joint are insignificant when the FWD load is applied at some distance away from the joint. The results of this study provide some guidelines for further field testing and verification of the FWD method.

The effects of temperature differentials between the top and bottom of the concrete slab were not considered in this study. The conclusions thus only apply to the condition when the temperature differential is zero.

REFERENCES

1. Y.T. Chou. Structural Analysis Computer Program for Rigid Multicomponent Pavement Structures with Discontinuities--WESLIQUID and WESLAYER. Tech. Report GL-80. U.S. Army Corps of Engineers Waterways Experiment Station, Vicksburg, Miss., Sept. 1980.
2. J.M. Lybas, M. Tia, and D.A. Twiddy. Response and Distress of Concrete Pavements. Structures and Materials Research Report 84-1. Department of Civil Engineering, University of Florida, Gainesville, April 1984.